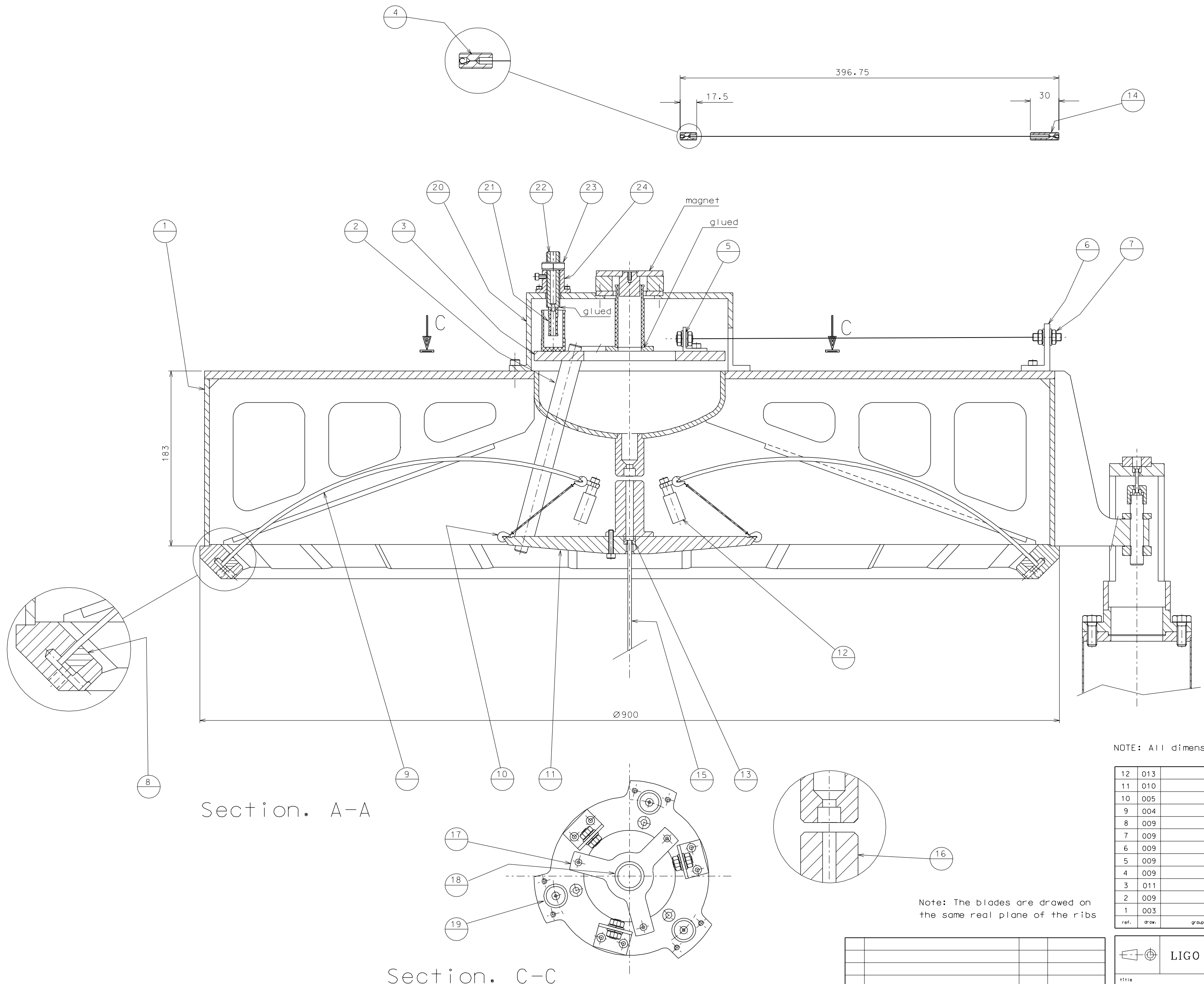

Note: The blades are drawed on the same real plane of the ribs

NOTE: All dimension in mm

ref.	draw.	group
12	013	
11	010	
10	005	
9	004	
8	009	
7	009	
6	009	
5	009	
4	009	
3	011	
2	009	
1	003	

ref.	draw.	group
24	016	
23	016	
22	016	
21	016	
20	016	
19	016	
18	016	
17	016	
16	011	
15	013	
14	009	
13	009	

ref.	note	date	signature

modifications

LIGO PROJECT	designed for R. De Salvo
	ass. numb. Filter_0.000
title PROTOTYPE FILTER_0 LATERAL SECTION	draw. PROMEC 30-1-99
	scale 1:2
	replaces dr. Numb.

LIGO-G000140-02-D
Part 2 of 2

Filter Prototype

Present Status of Development of GAS

- Resonance Frequency & Q Factor of the Blade Internal Modes
  - Result (3rd Mode)

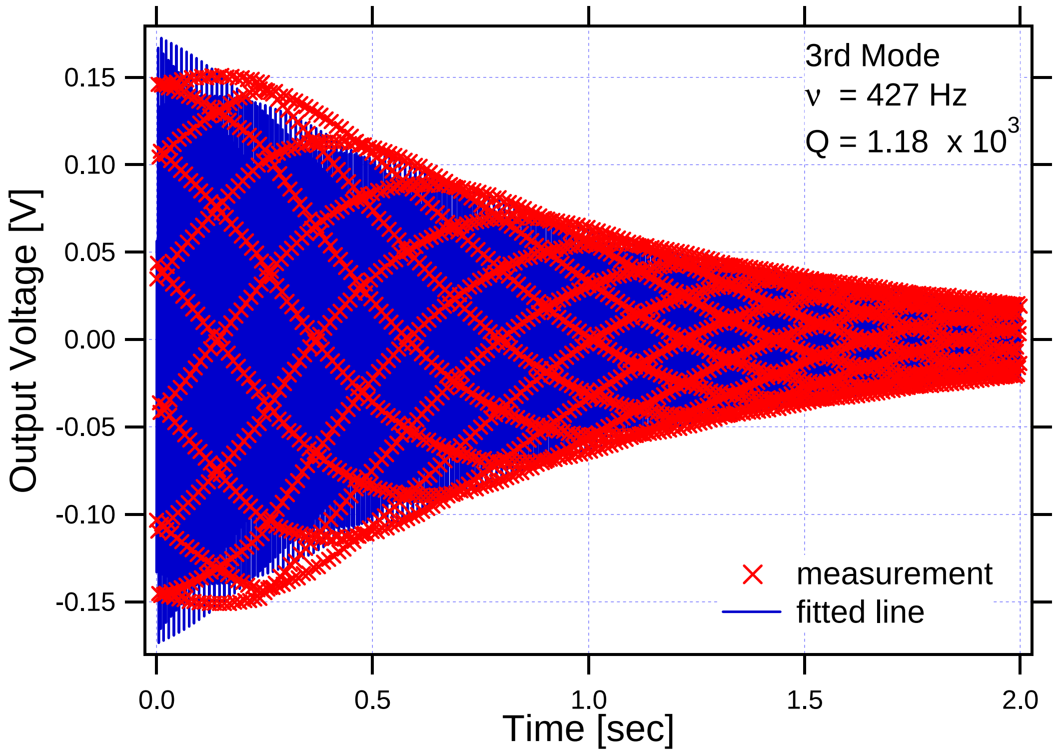

GAS Filter : Measurements

Vertical Isolation Performance

- Double GASF Chain

    - GASF Chain + Payload

    - Filter Zero is connected to a shaker.

    - Standard Filters are tuned to about 450mHz.

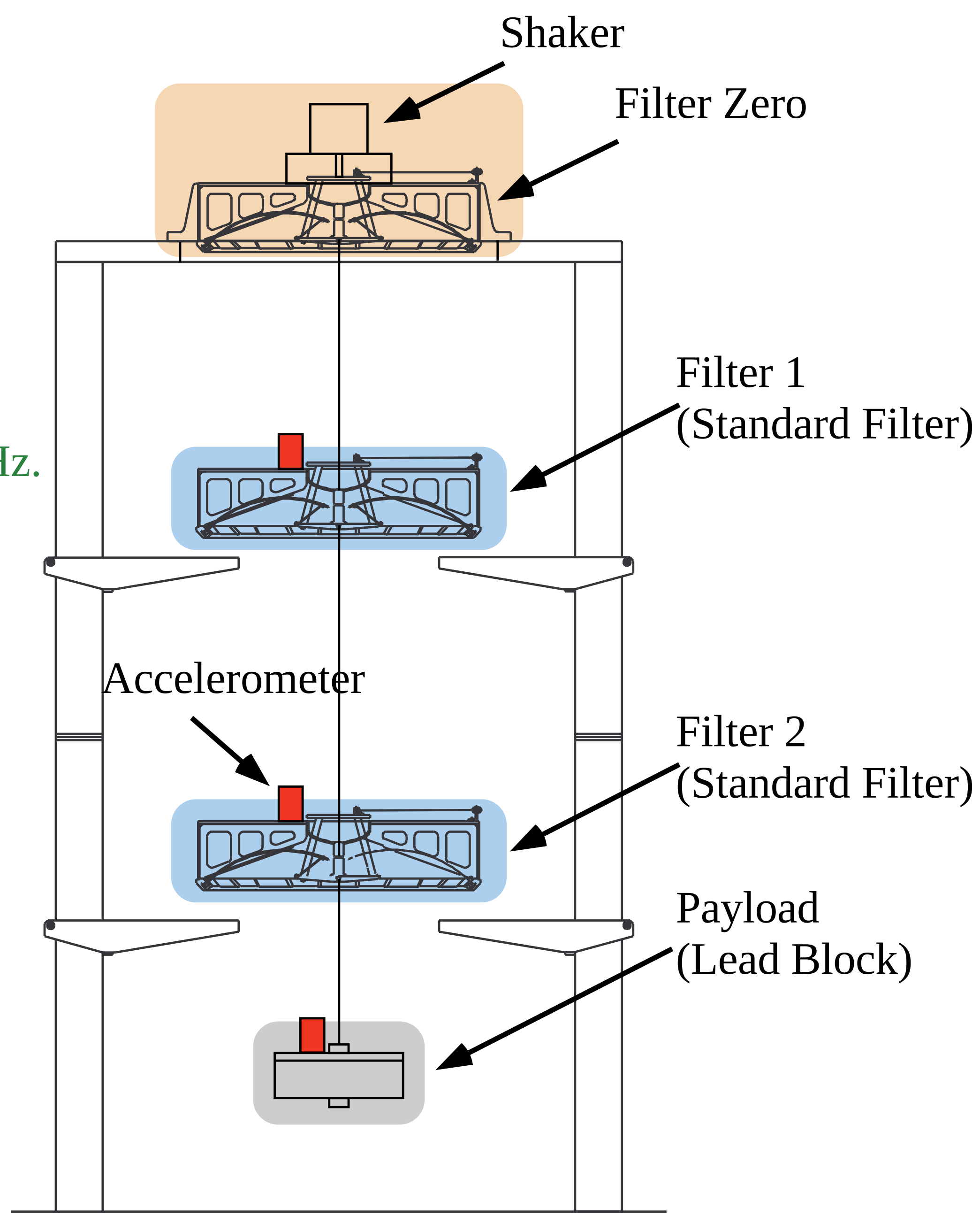


CAUTION DO NOT ENTER CAUTION DO NOT ENTER CAUTION DO NOT ENTER CAUTION DO

Test Tower

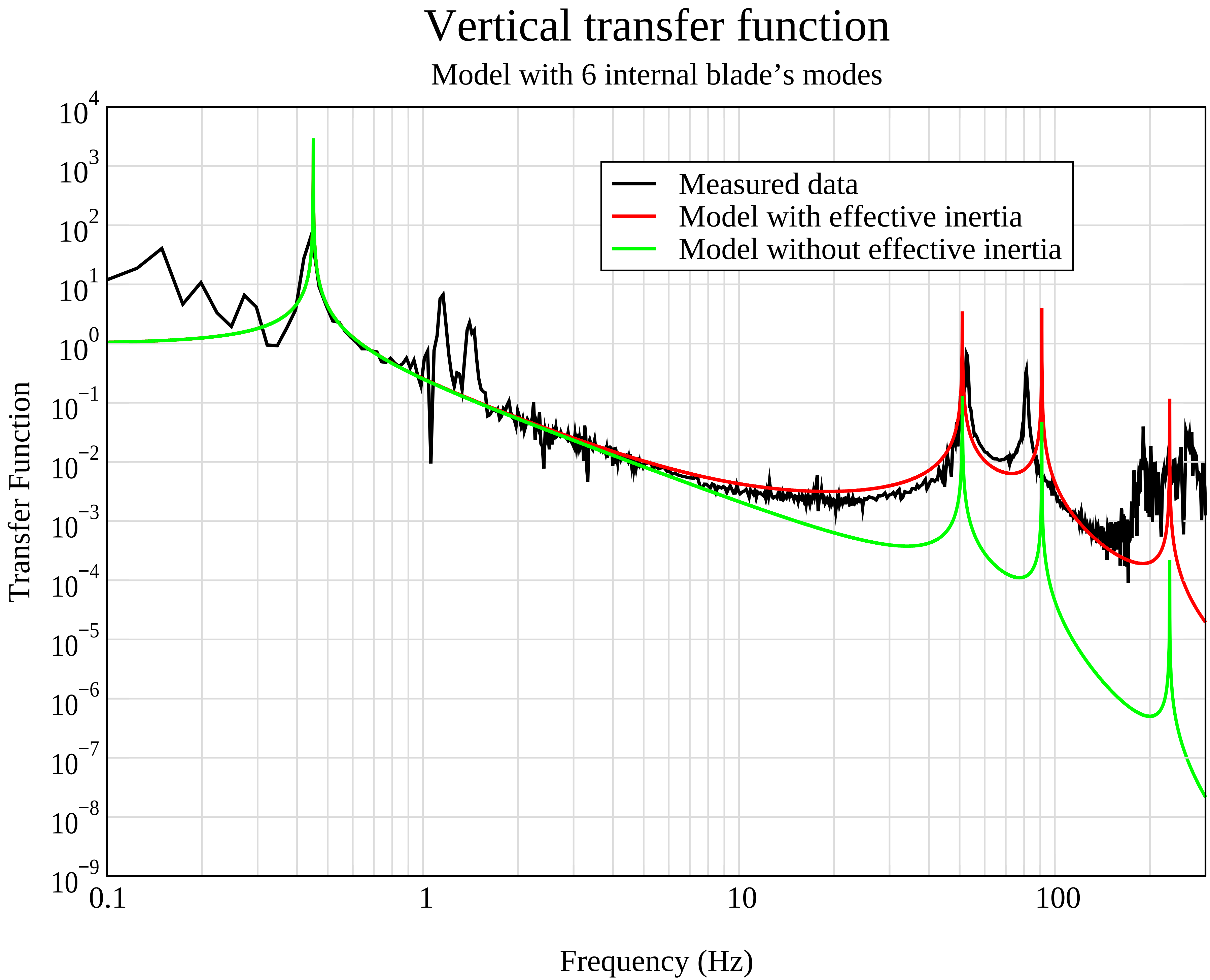
Vertical transfer function
Model with 6 internal blade's modes
Measured data
Model with effective inertia
Model without effective inertia
Transfer Function
Frequency (Hz)
10^4
10^3
10^2
10^1
10^0
10^−1
10^−2
10^−3
10^−4
10^−5
10^−6
10^−7
10^−8
10^−9
0.1
1
10
100

2 Standard Filter Chain,

Vertical Transfer Function (Good filters balance)

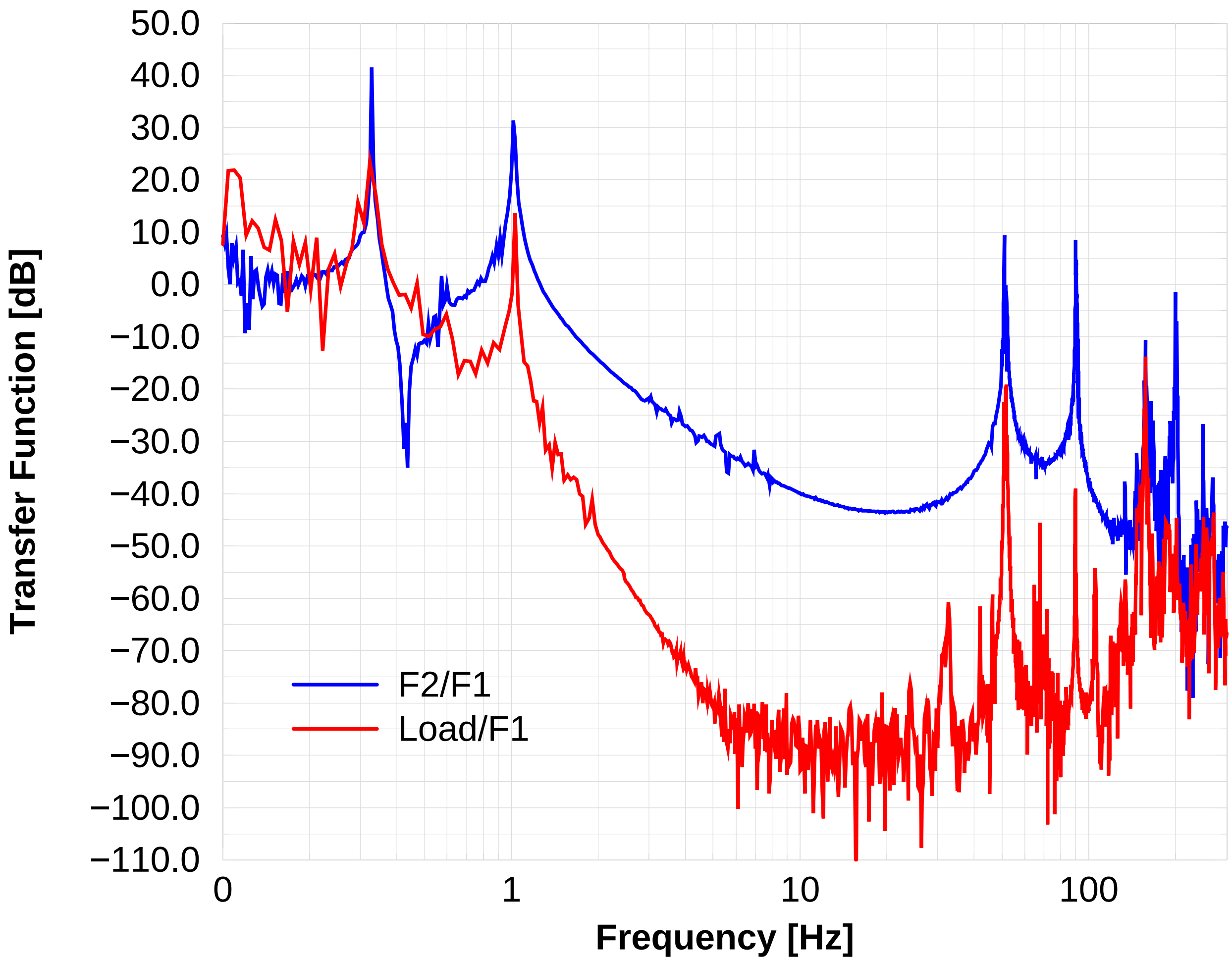

2 Standard Filter Chain, Vertical Transfer Function (Bad filters balance)

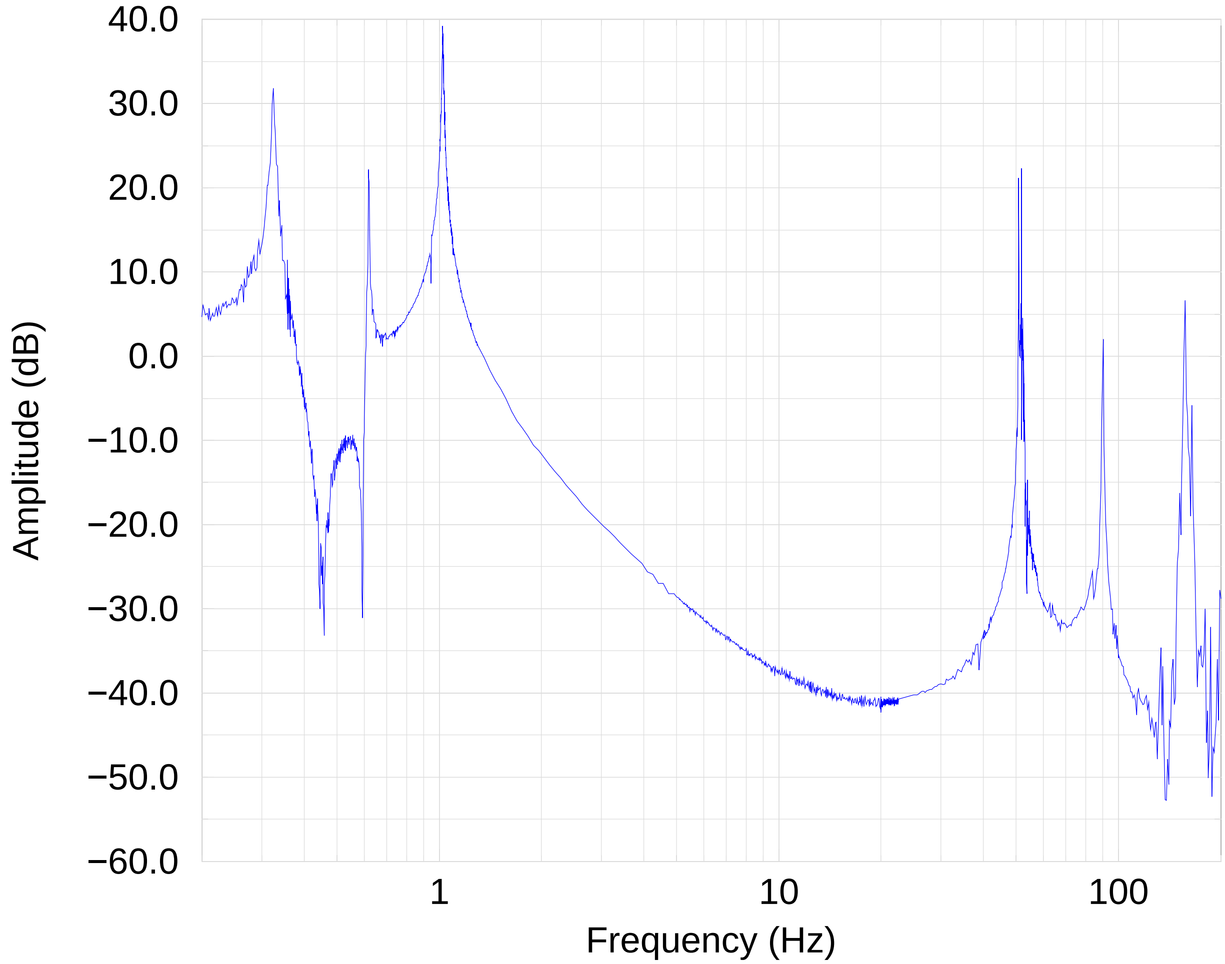

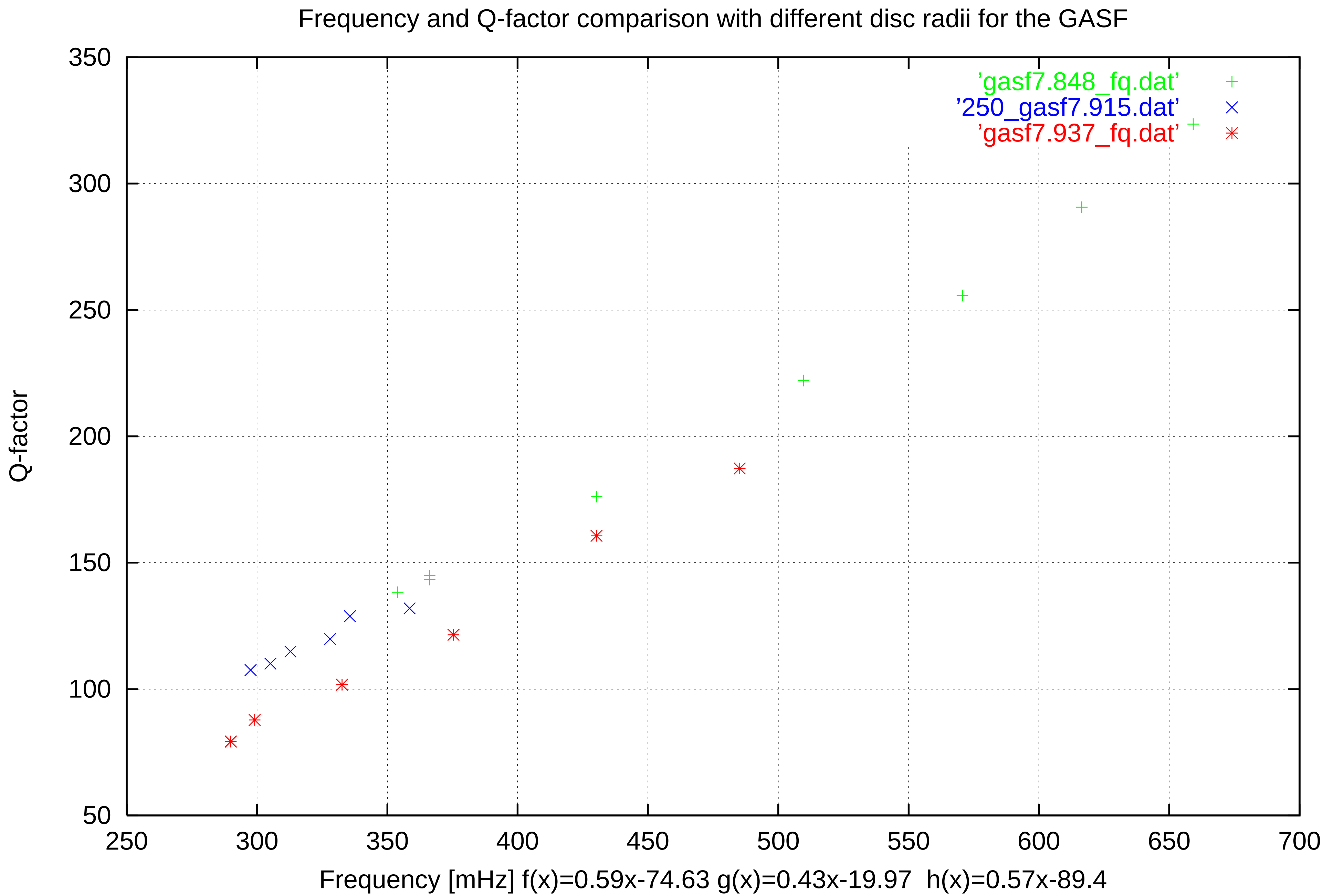
Frequency and Q-factor comparison with different disc radii for the GASF
'gasf7.848_fq.dat'
'250_gasf7.915.dat'
'gasf7.937_fq.dat'
Q-factor
350
300
250
200
150
100
50
250
300
350
400
450
500
550
600
650
700
Frequency [mHz] f(x)=0.59x-74.63 g(x)=0.43x-19.97 h(x)=0.57x-89.4

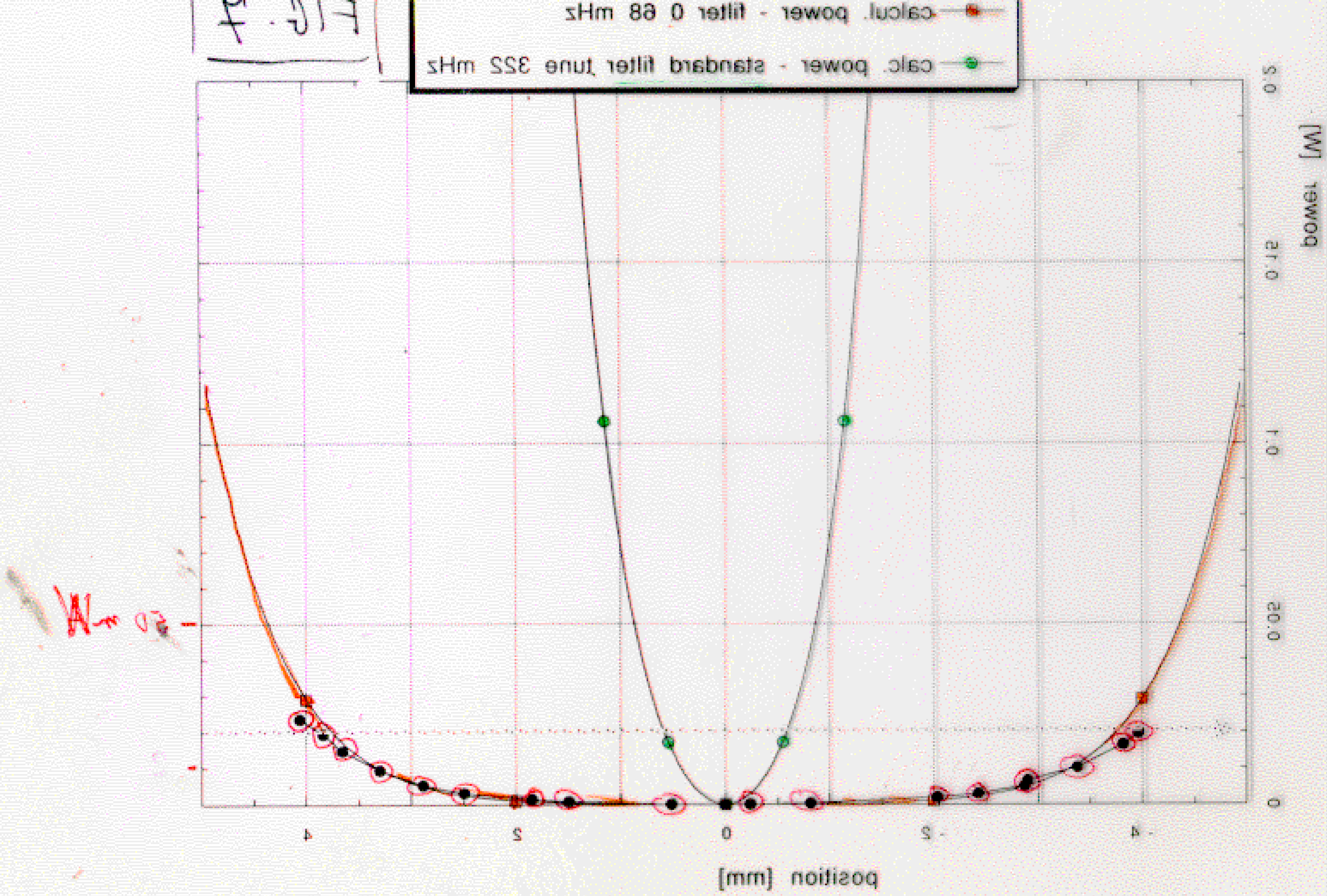

calc. power - standard filter june 322 mHz
calcul. power - filter 0 68 mHz
power [W]
position [mm]
0
0.05
0.1
0.15
0.2
-4
-2
0
2
4
-50 mW

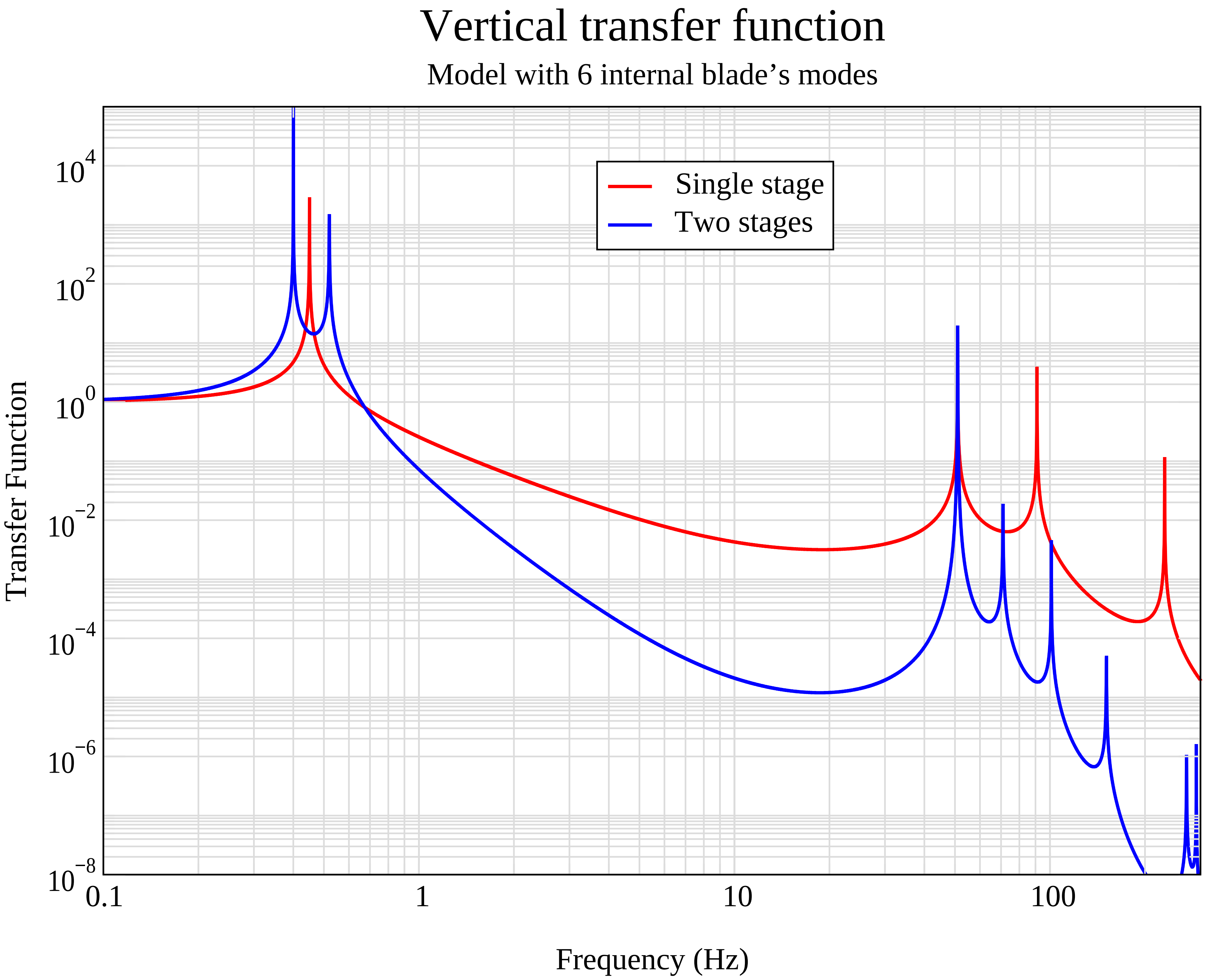

Vertical transfer function
Model with 6 internal blade’s modes
Single stage
Two stages
Transfer Function
Frequency (Hz)
10^4
10^2
10^0
10^−2
10^−4
10^−6
10^−8
0.1
1
10
100

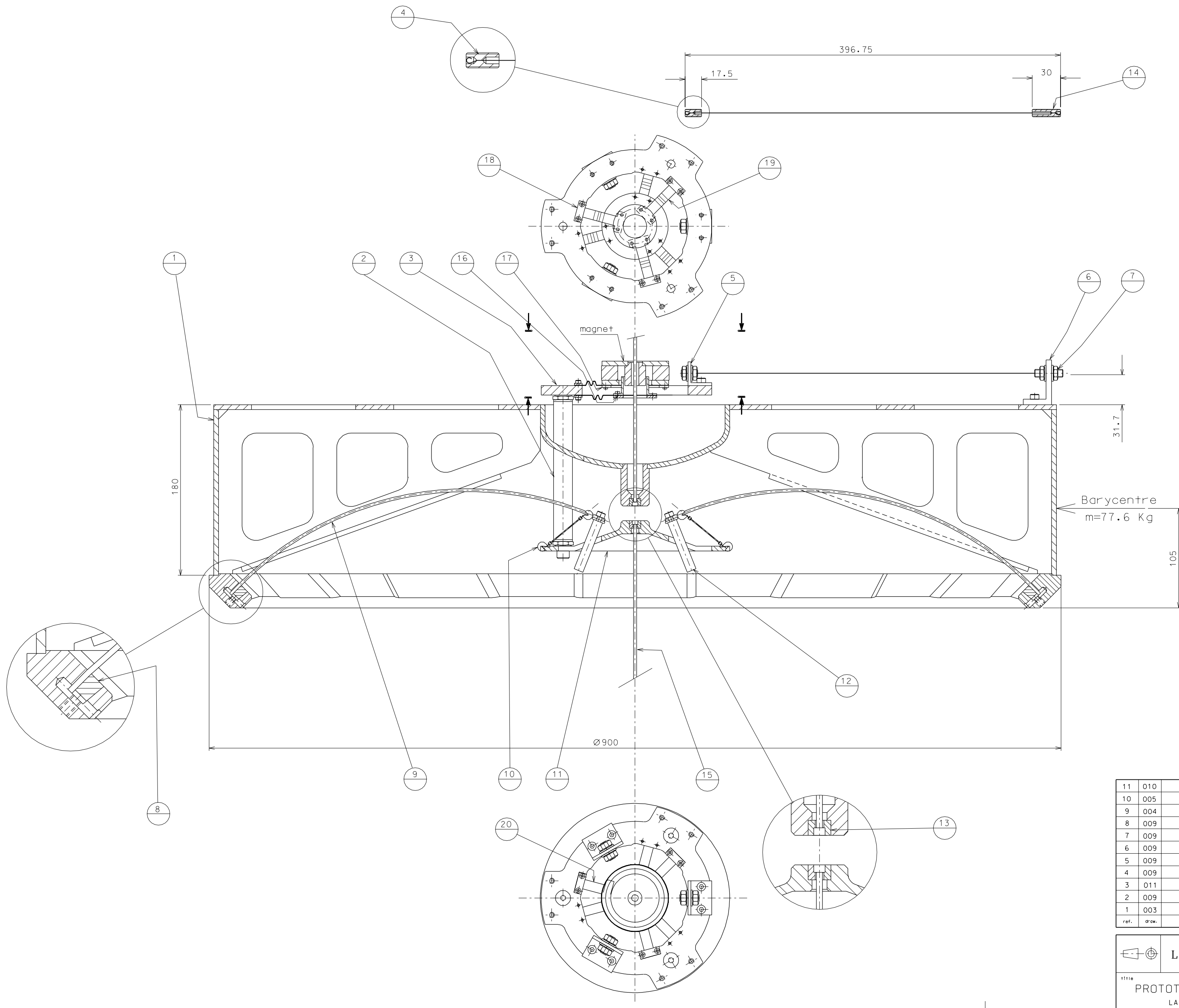

ref.	draw.	group
11	010	
10	005	
9	004	
8	009	
7	009	
6	009	
5	009	
4	009	
3	011	
2	009	
1	003	

ref.	draw.	group
20	016	
19	016	
18	016	
17	016	
16	016	
15	013	
14	009	
13	009	
12	013	

LIGO PROJECT	designed for R. De Salvo
	ass. numb. Filter.000
title PROTOTYPE FILTER LATERAL VIEW	draw. PROMEC 30-9-98
	scale 1:2
	replaces dr. numb.


SAFETY
FIRST

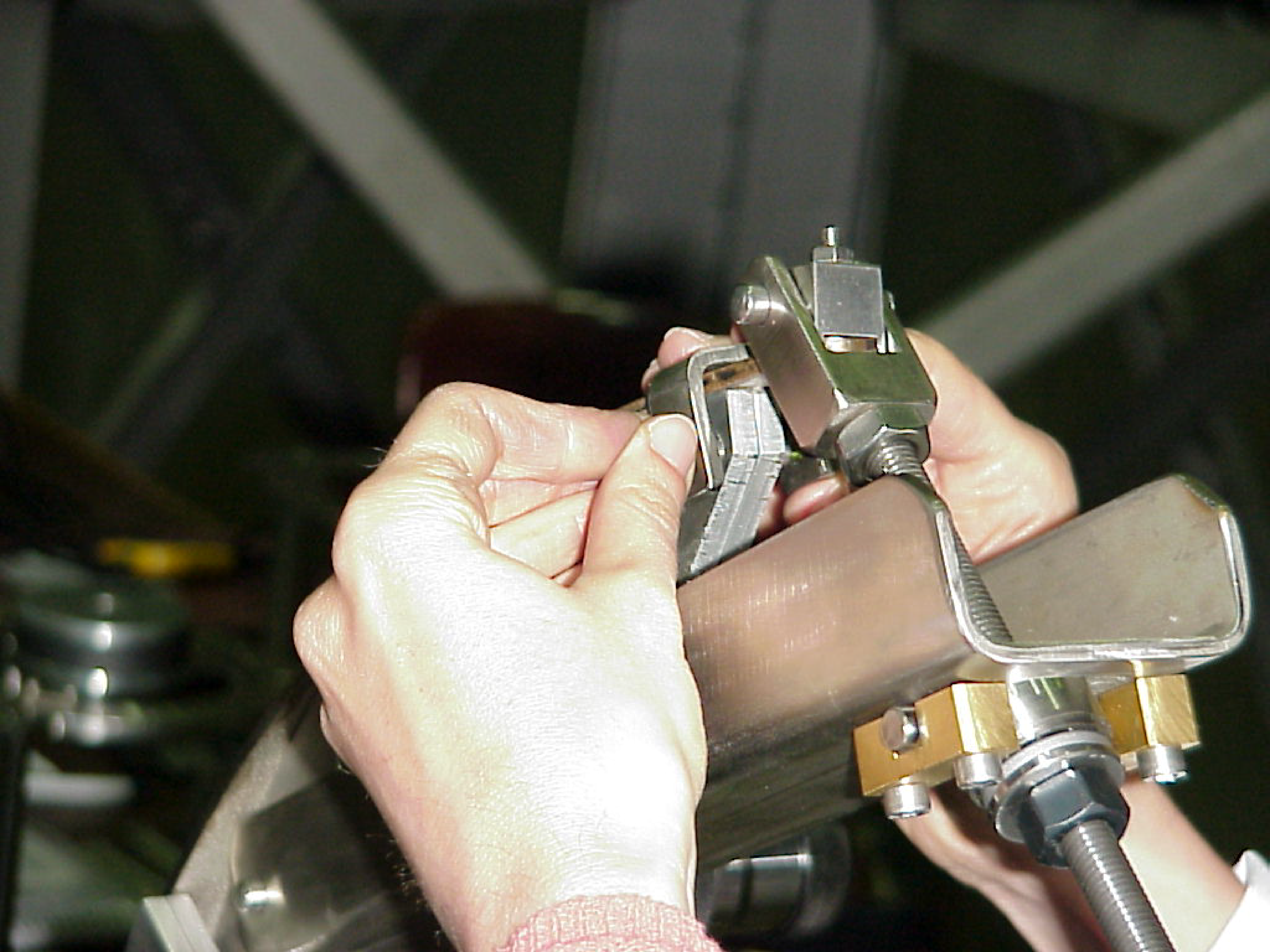

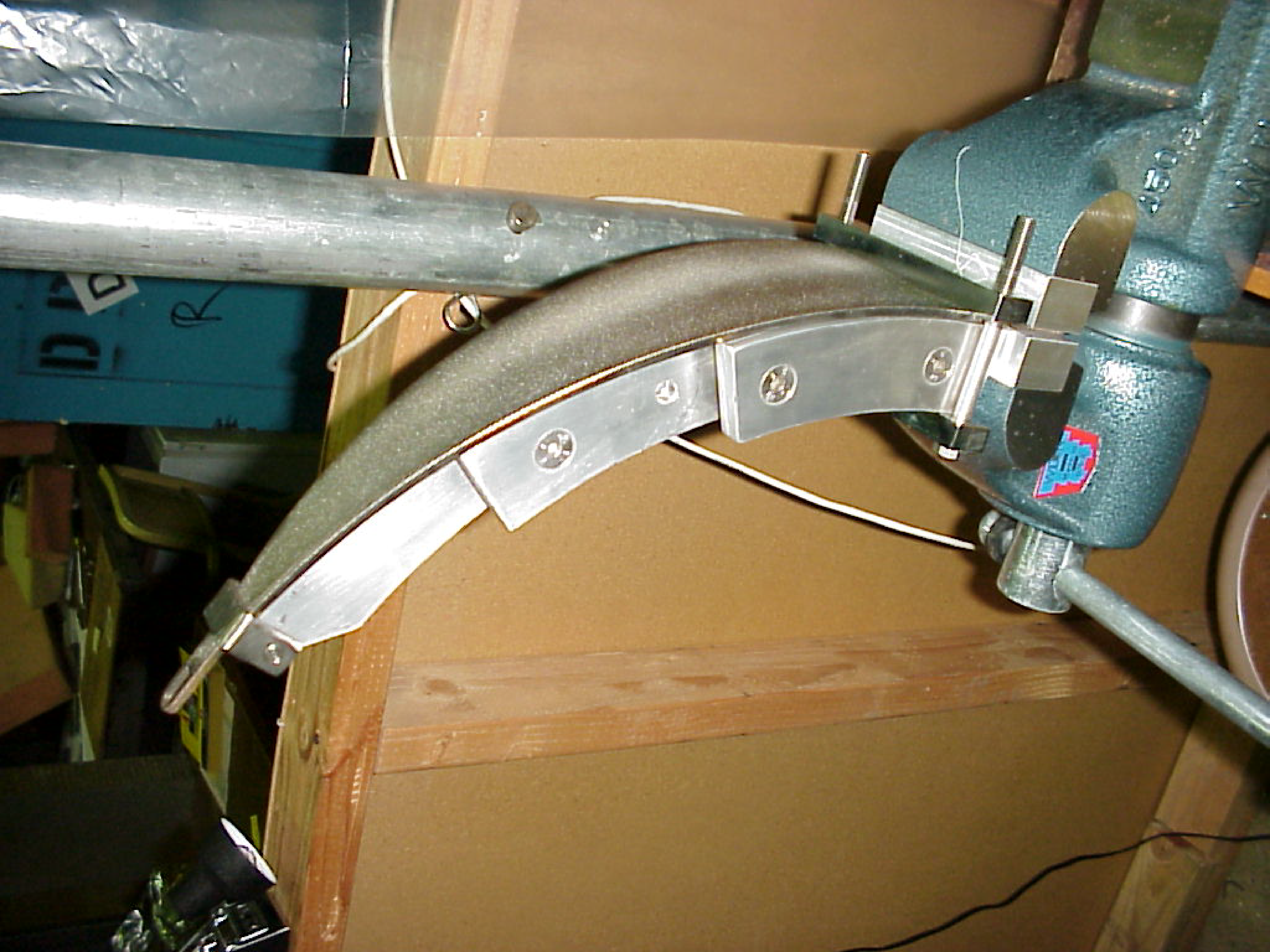

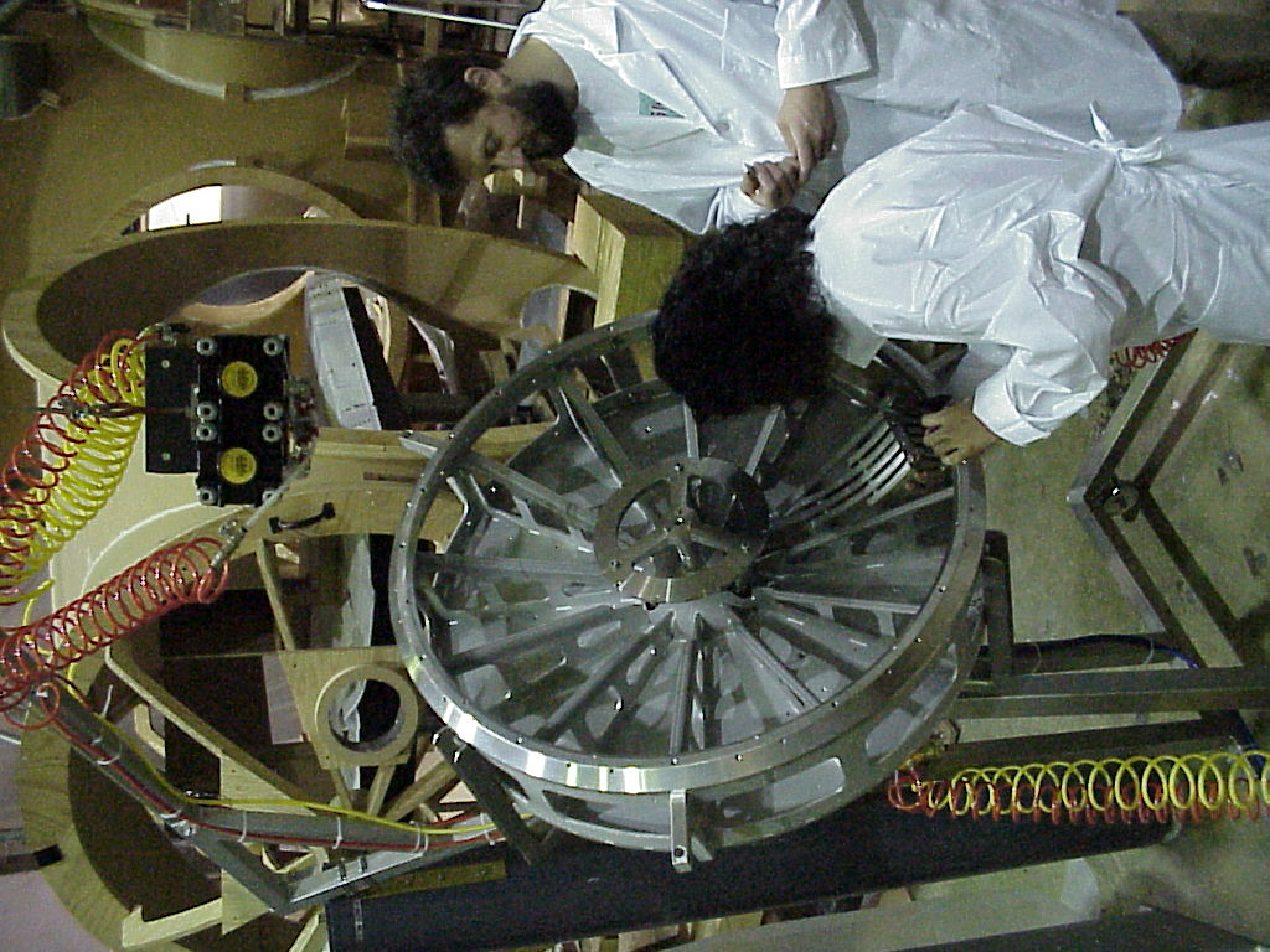

Blade Stress Simulation

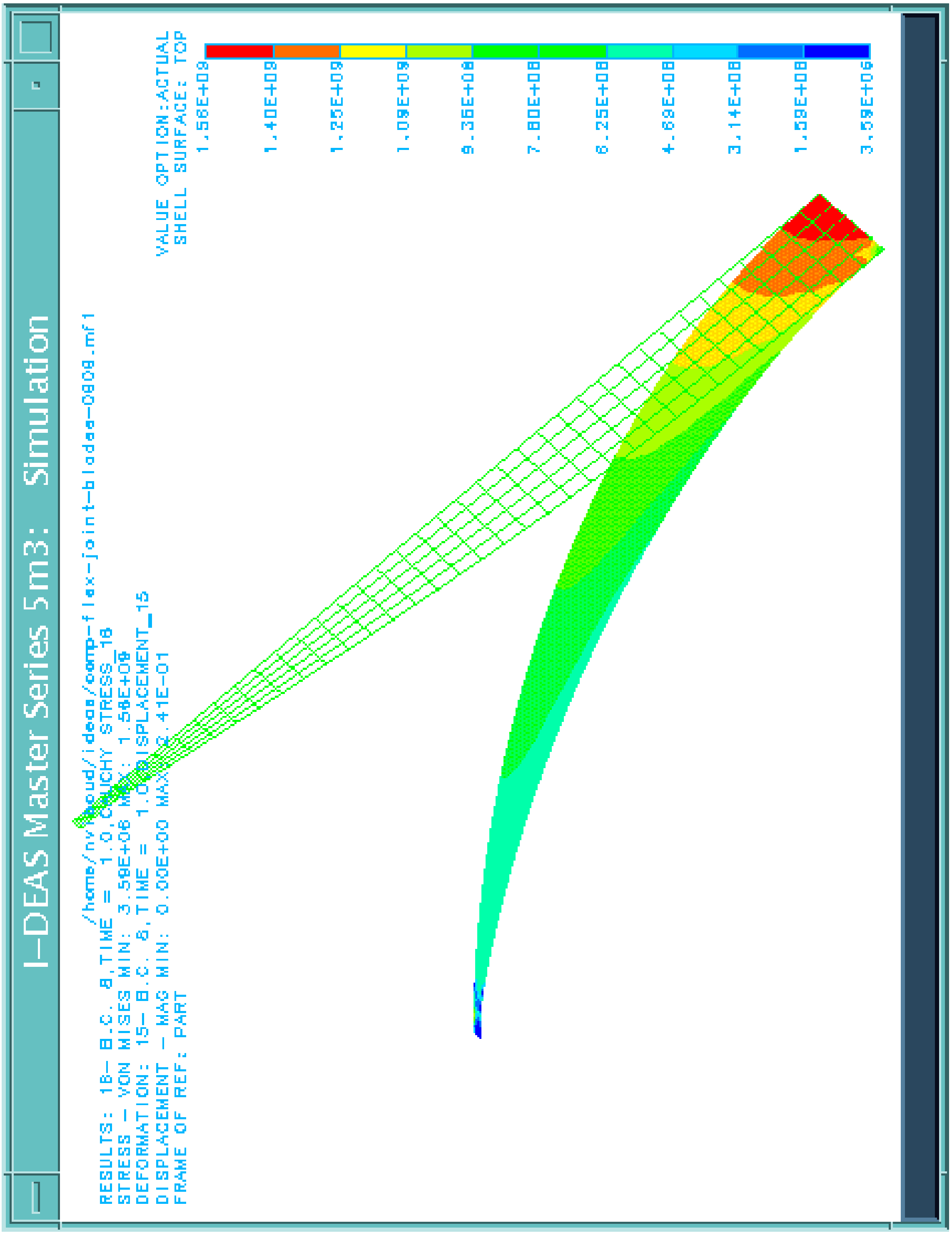

Present Status of Development of GAS

- Resonance Frequency & Q Factor of the Blade Internal Modes
  - Result (1st Mode)

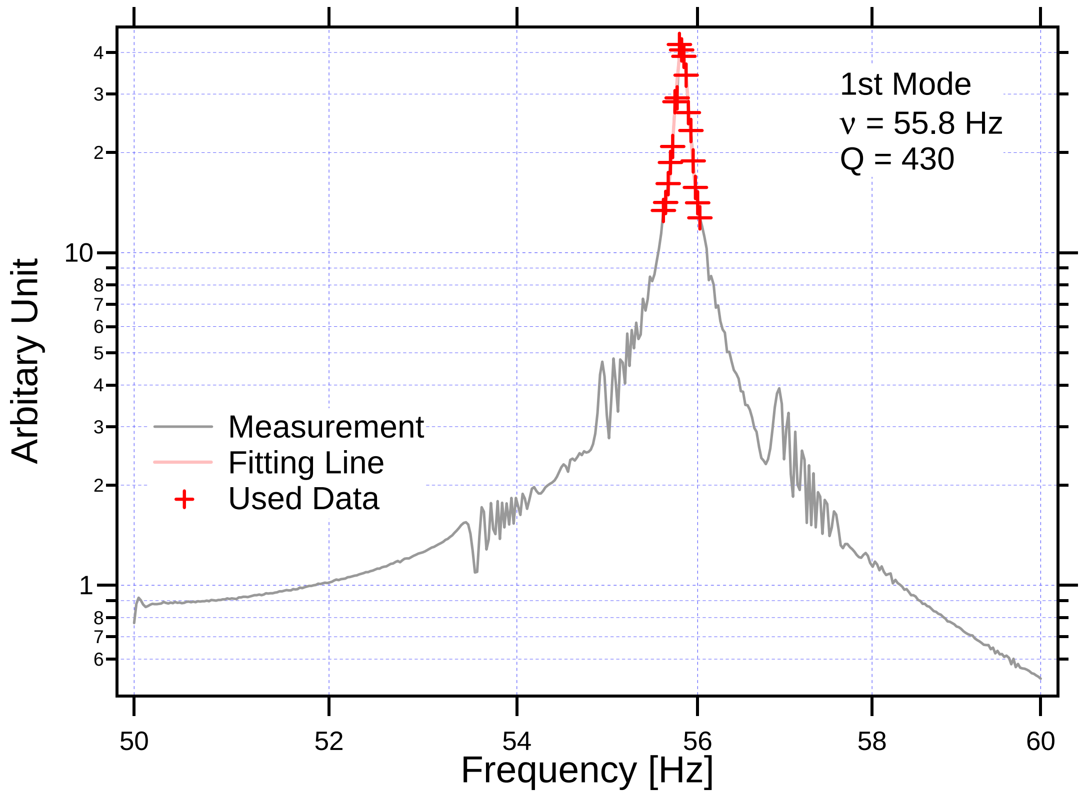

Internal Mode of GAS Blade

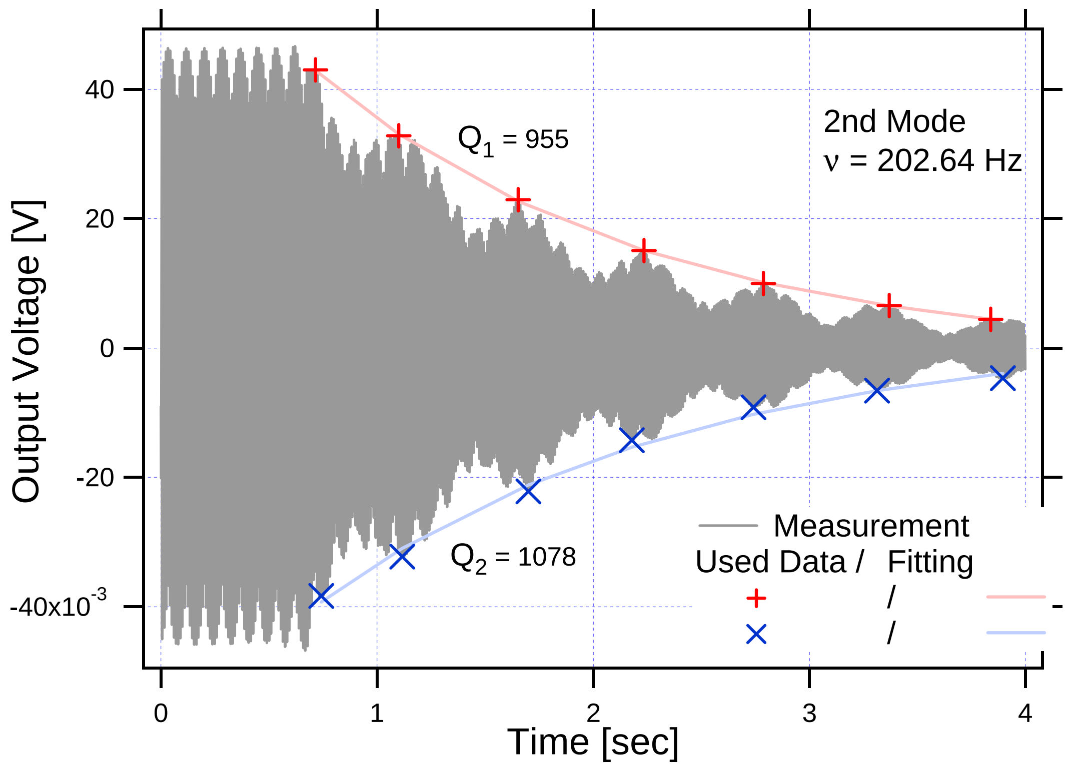

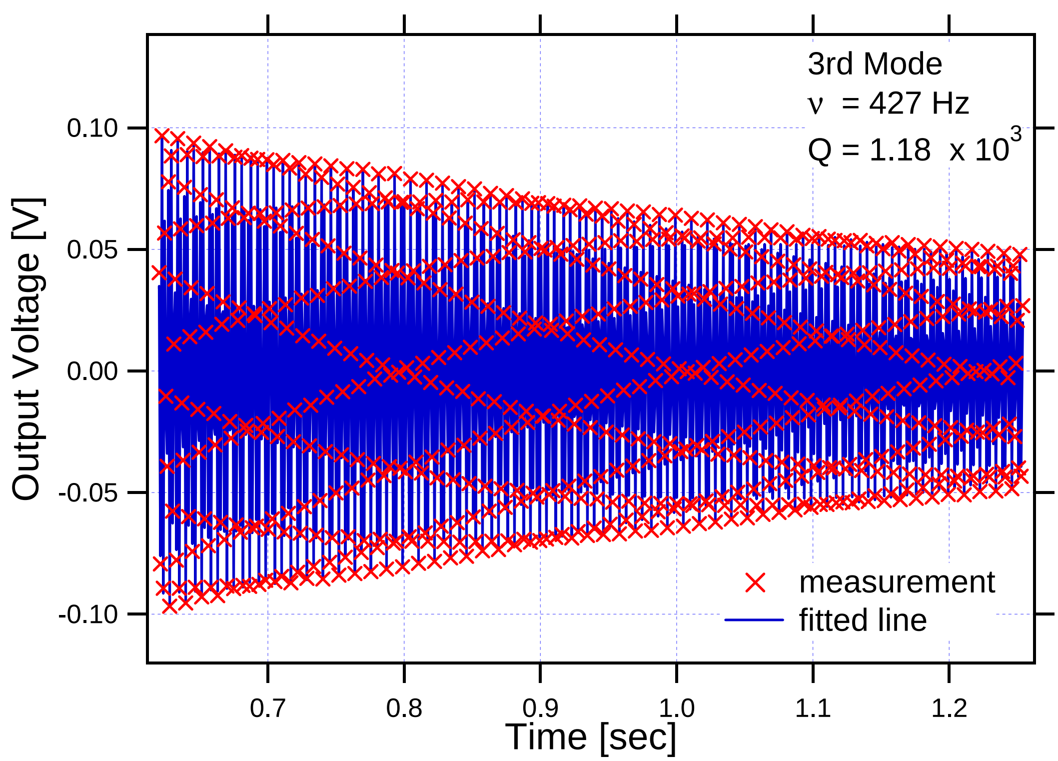

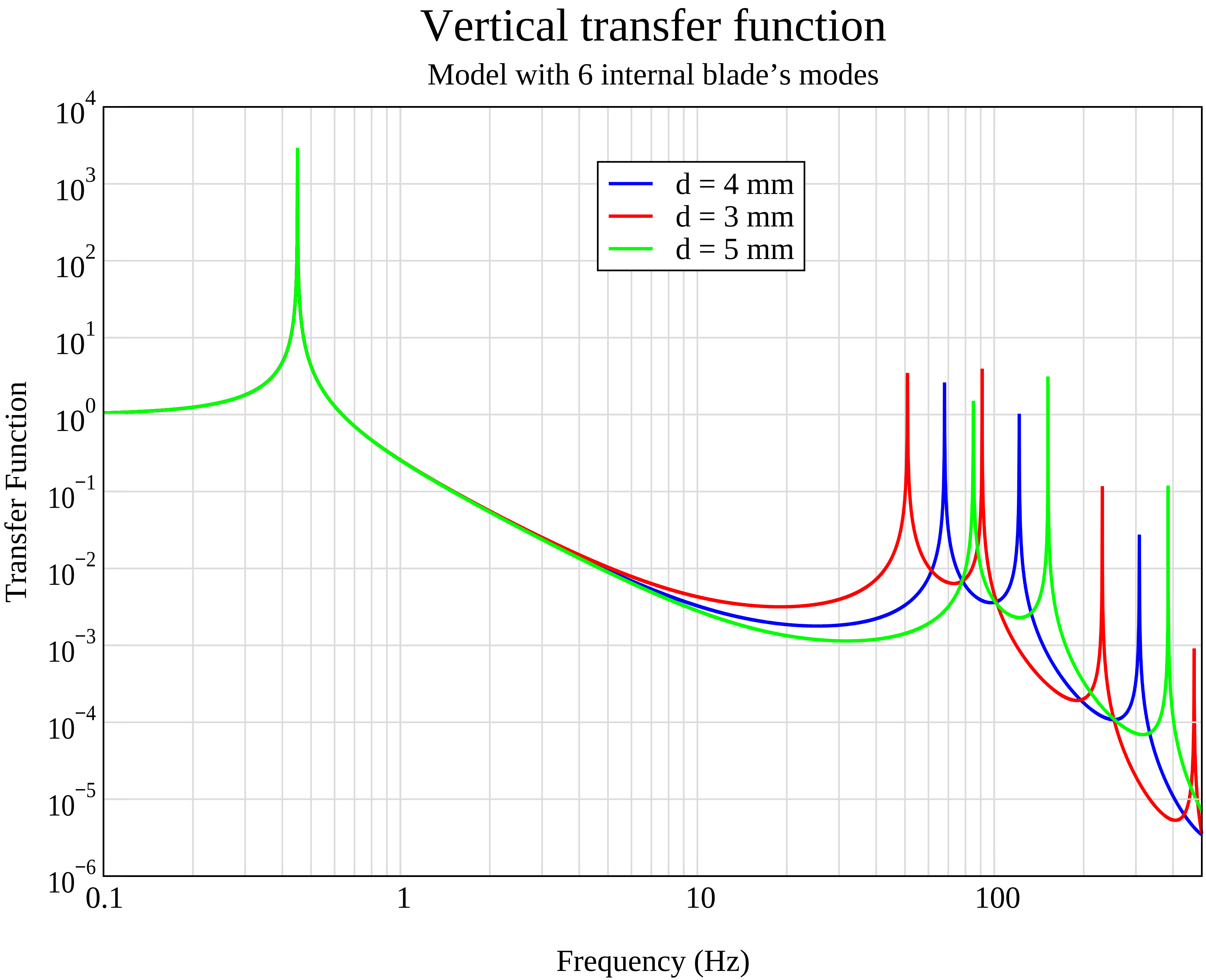

Vertical transfer function
Model with 6 internal blade's modes
d = 4 mm
d = 3 mm
d = 5 mm
Transfer Function
Frequency (Hz)
0.1
1
10
100

Blade Damper

- Passive Damper

- Small Oscillator on Blade
- Eddy Current Damping
- No Lossy Materials

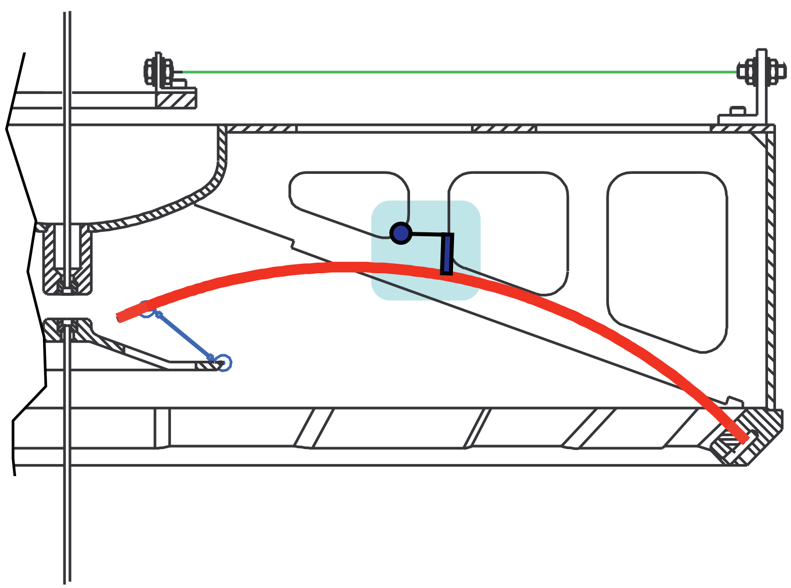

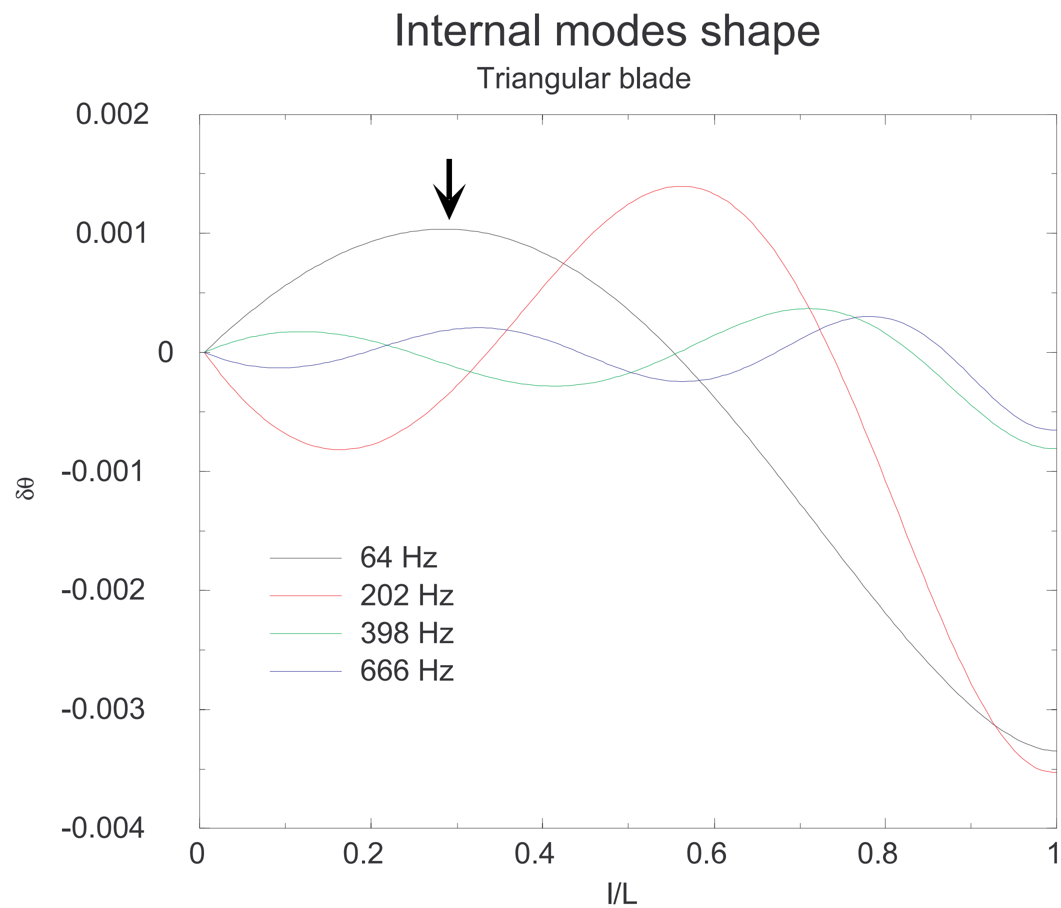

Blade Damper

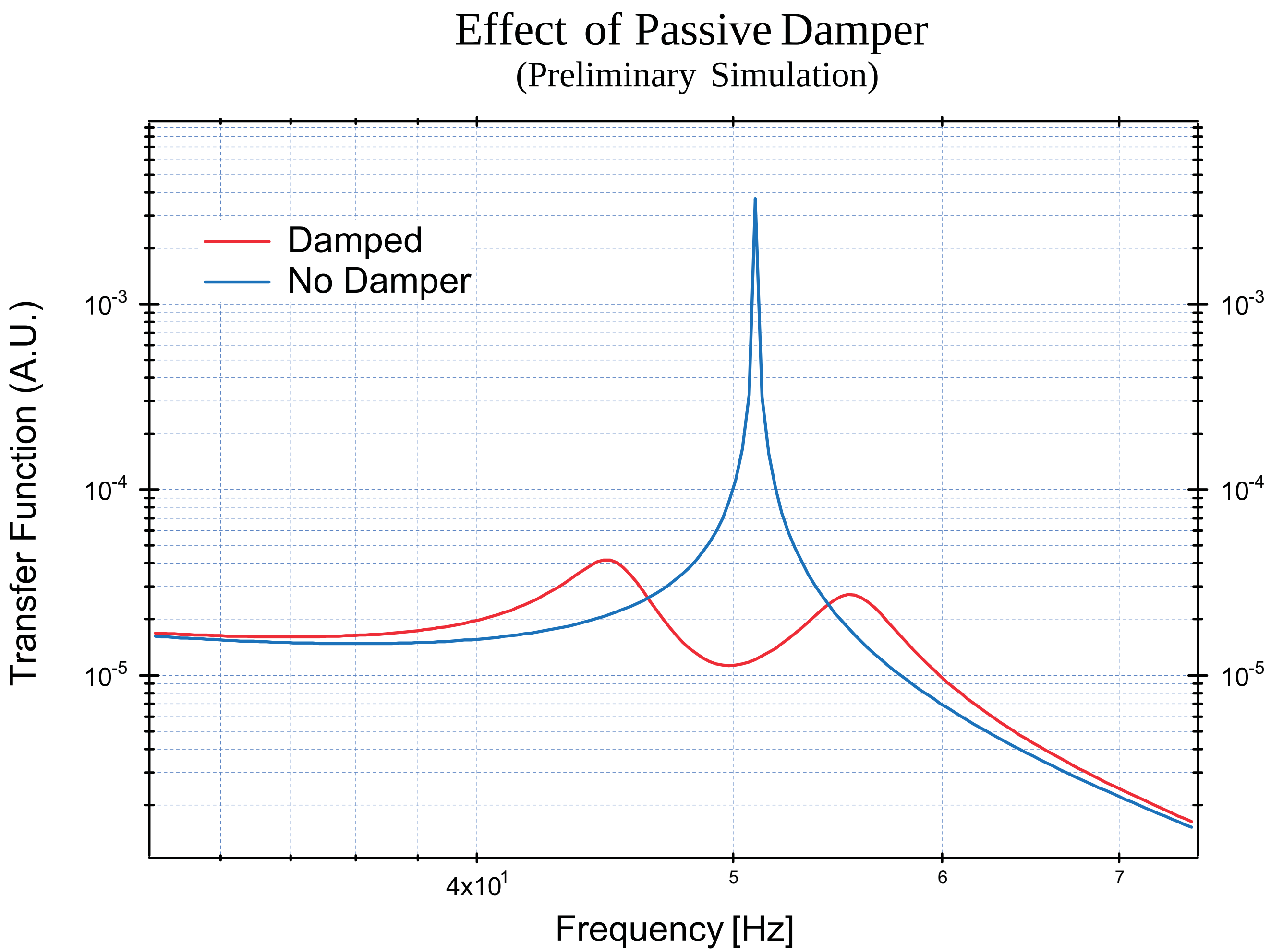

Akiteru Takamori

Blade Damper

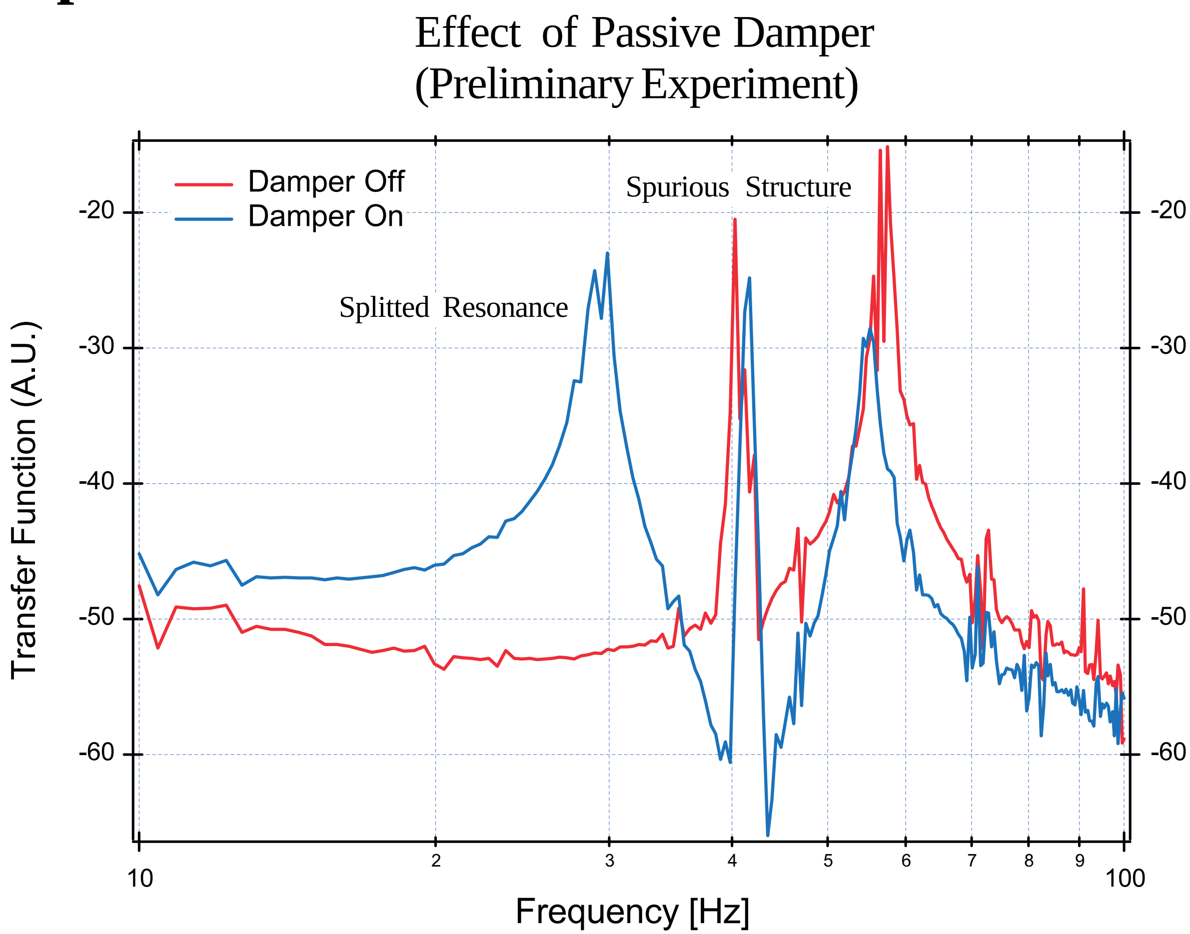

Next Steps:

More Damping Force

Lighter Oscillator

SAS Standard Filter Improvements

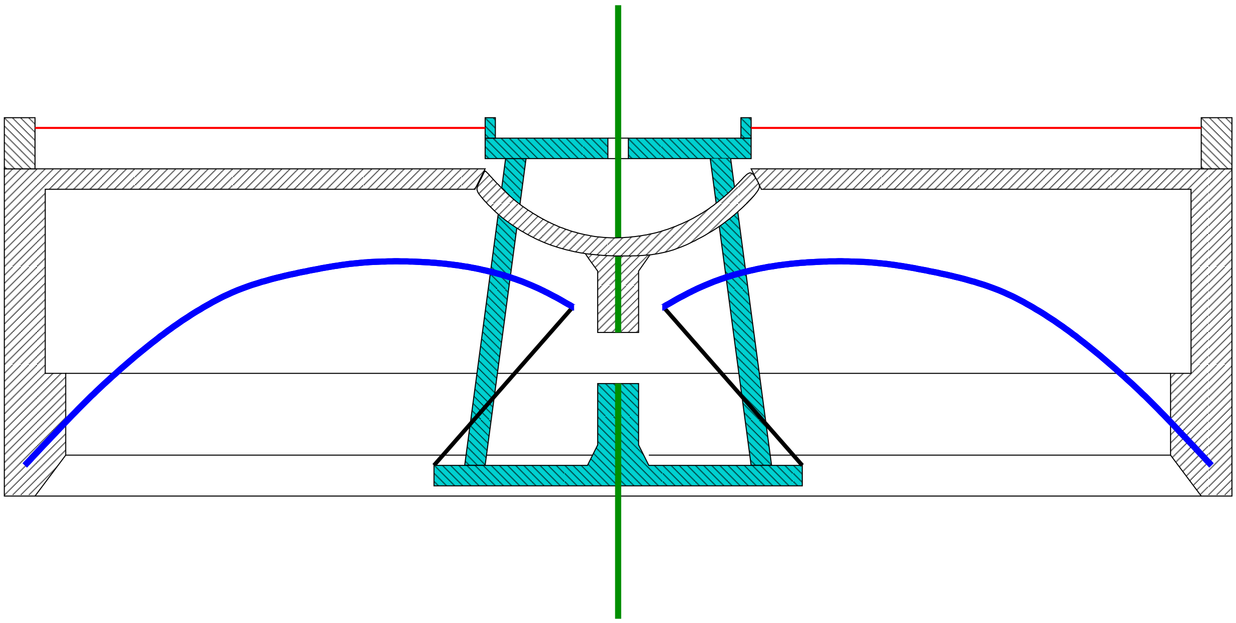

Standard Filter

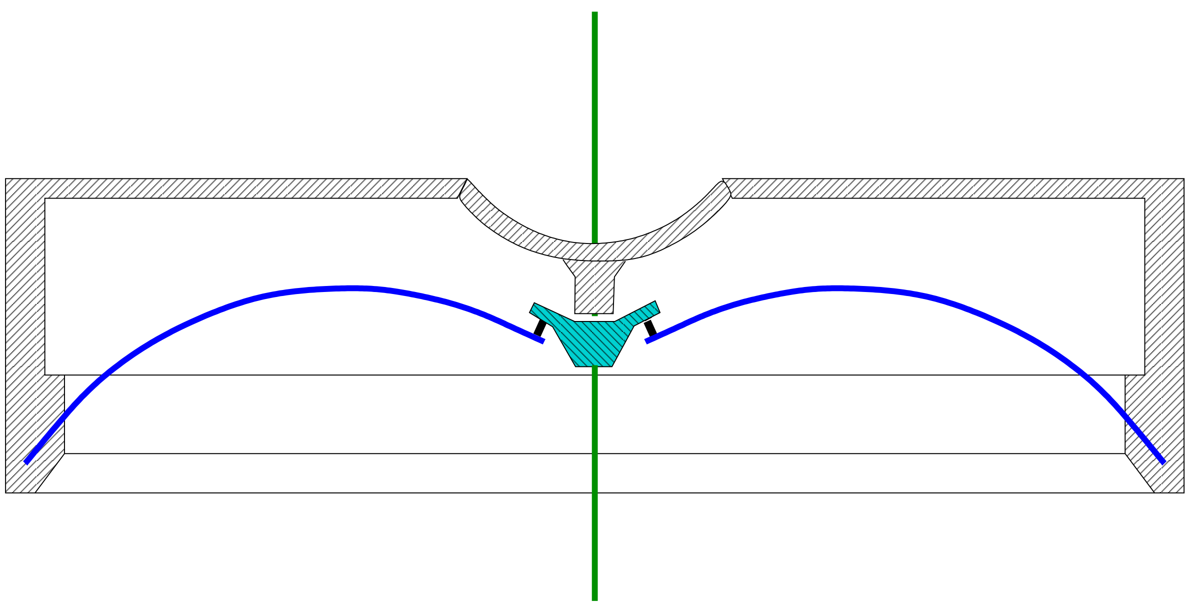

Enhanced Standard Filter

GAS Filter : Current Work

"Link-less" GASF

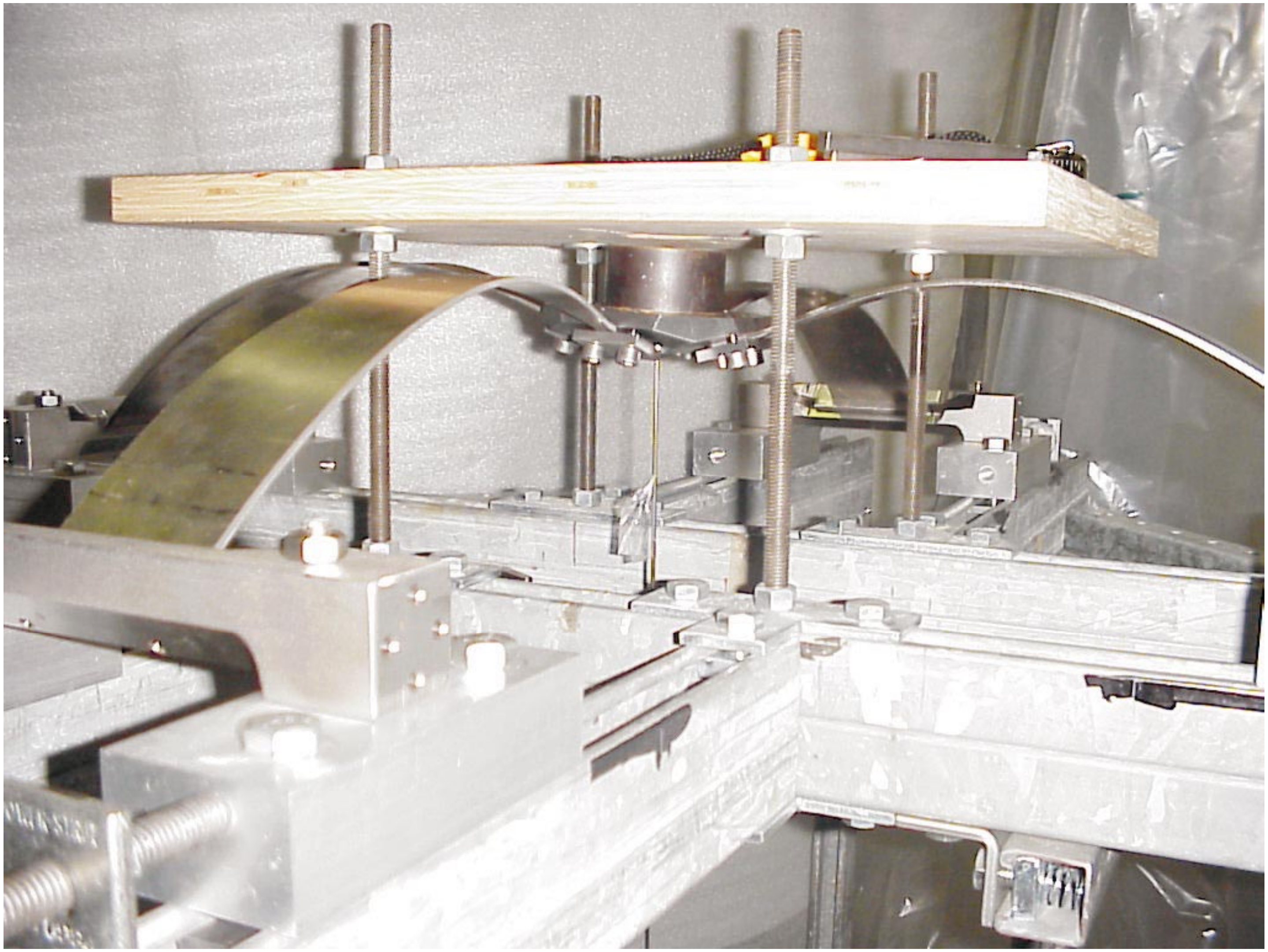

Pre-Prototype of "Link-less" GASF

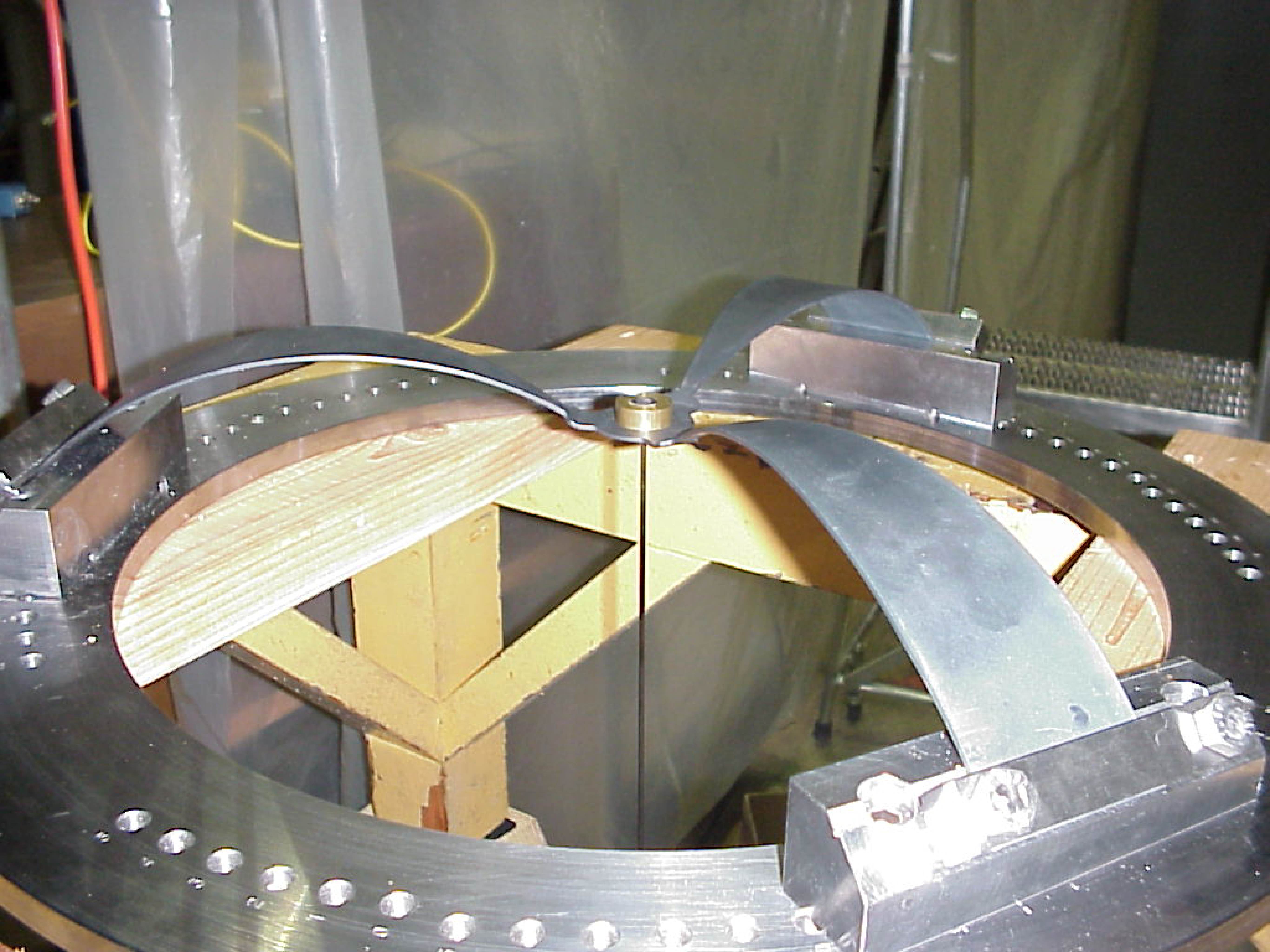

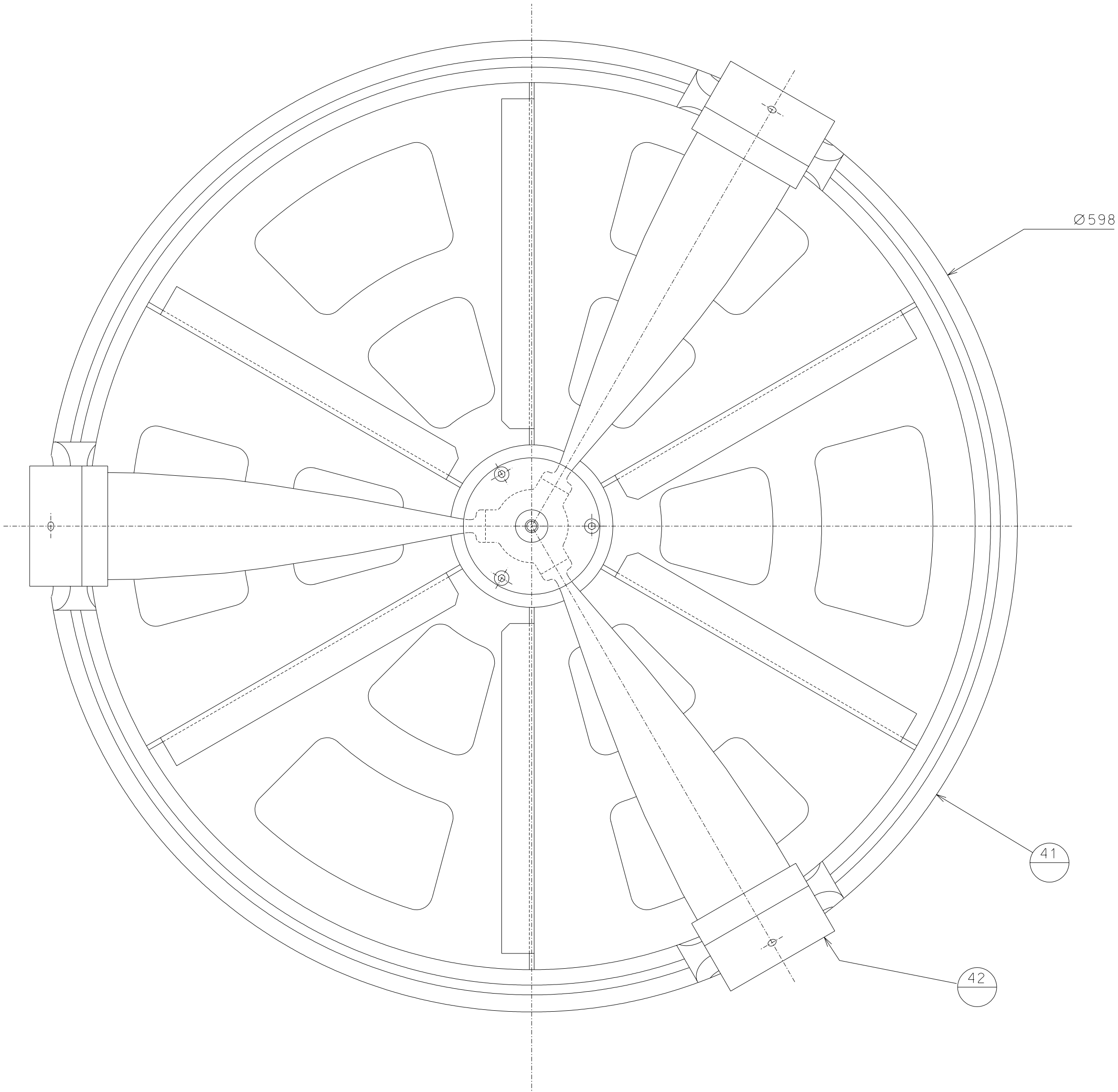

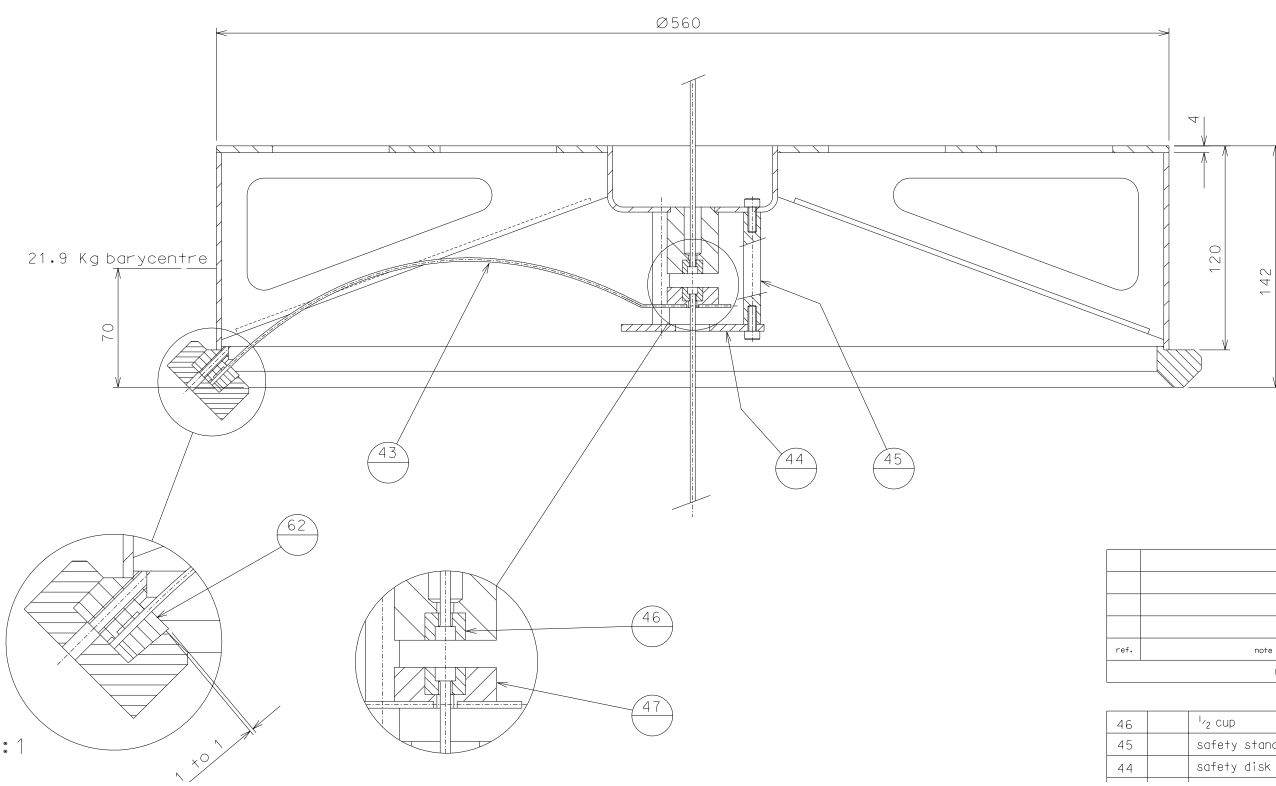

cale 1:1

ref.	note	date
modifications		

46		$^1/_2$ cup	
45		safety stand	
44		safety disk	

X	Y	
0	33.47	
67.67	32.67	
120.33	29	
146.67	25.67	
199.33	17.33	
265.13	4.67	
270.33	4	
272.33	4	
275.33	7	R -3
278.33	10	R 3
283	10	
309.5	0	center

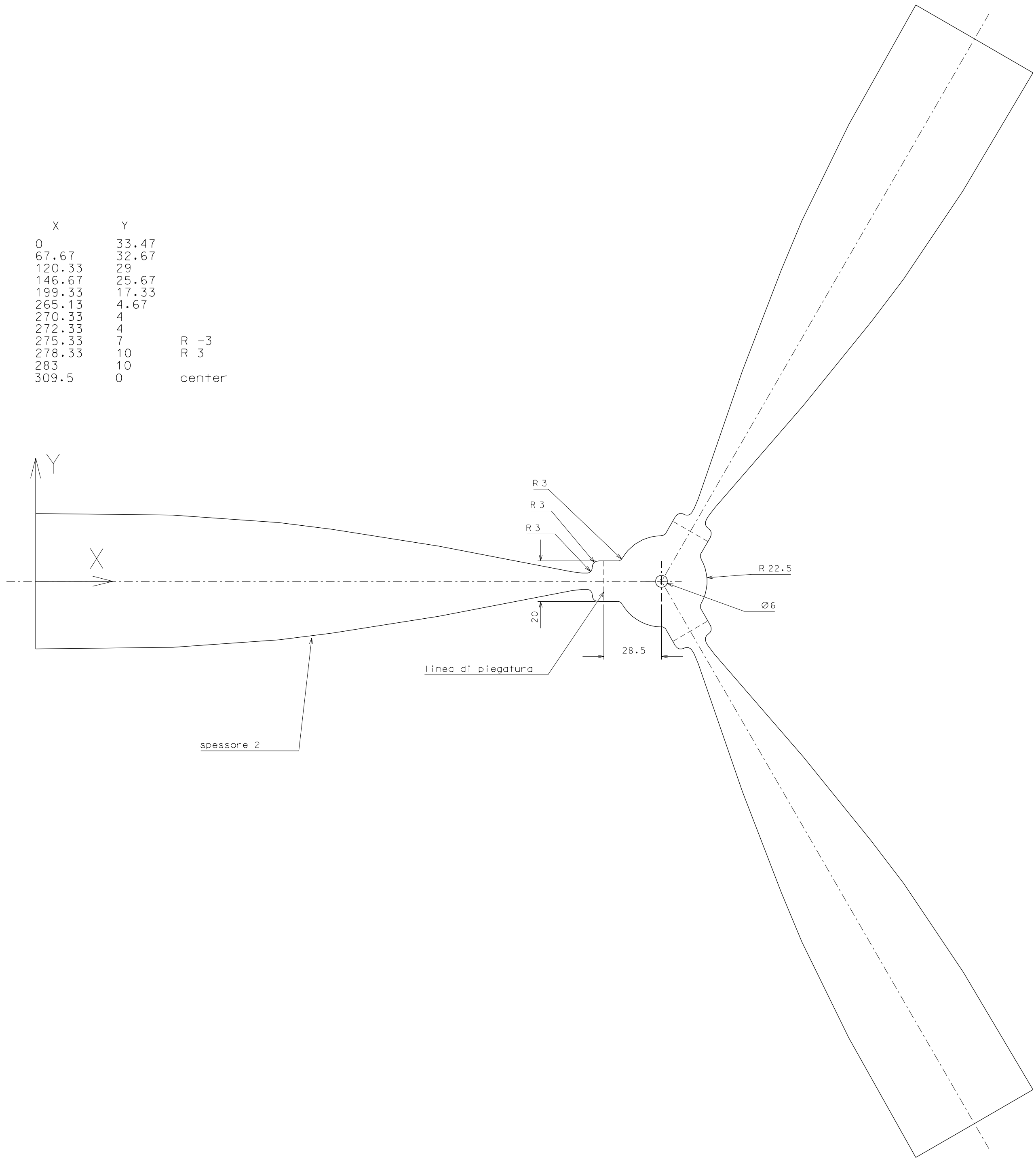

4	1	maraging	1:1
ref.	pieces	mat. and treatments	scale

ref.	pieces	mat. and treatments	scale

General machining tolerances UNI 5307-63

Dimensions	< 6	> 6-30	> 30-120	> 120-315	> 315-1000	>1000-2000	>2000-4000	> 4000
linear Toll.	± 0.1	± 0.2	± 0.3	± 0.5	± 0.8	± 1.2	± 2	± 3
angular Toll.	± 1	± 30′	± 20′	± 10′ refered to the shortest side				

LIGO PROJECT

designed for R. De Salvo

N.

draw. PROMEC 12-12-99

details from

replaces dr. Numb.

title

A1

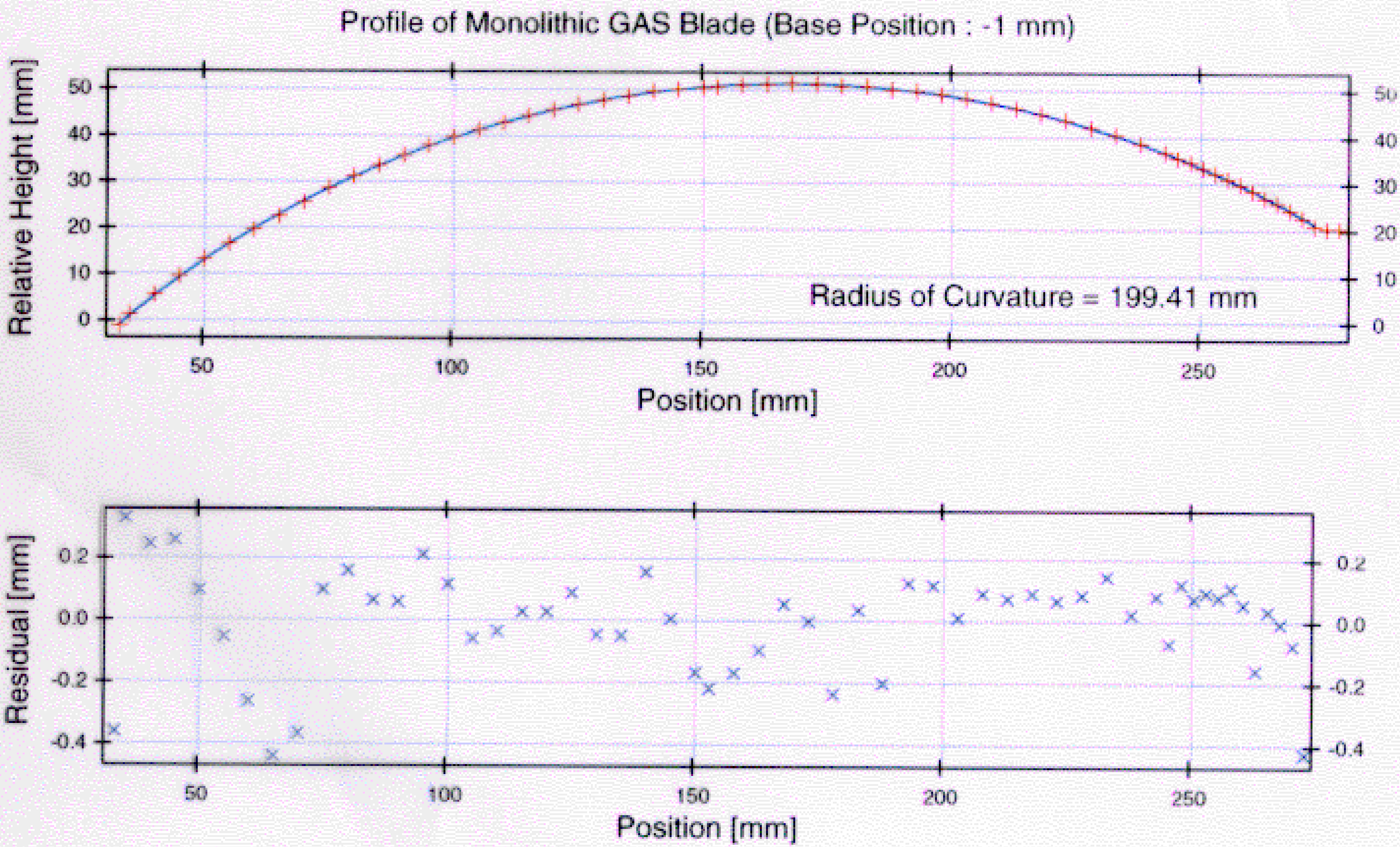

Profile of Monolithic GAS Blade (Base Position : -1 mm)
Relative Height [mm]
Radius of Curvature = 199.41 mm
Position [mm]
Residual [mm]
Position [mm]

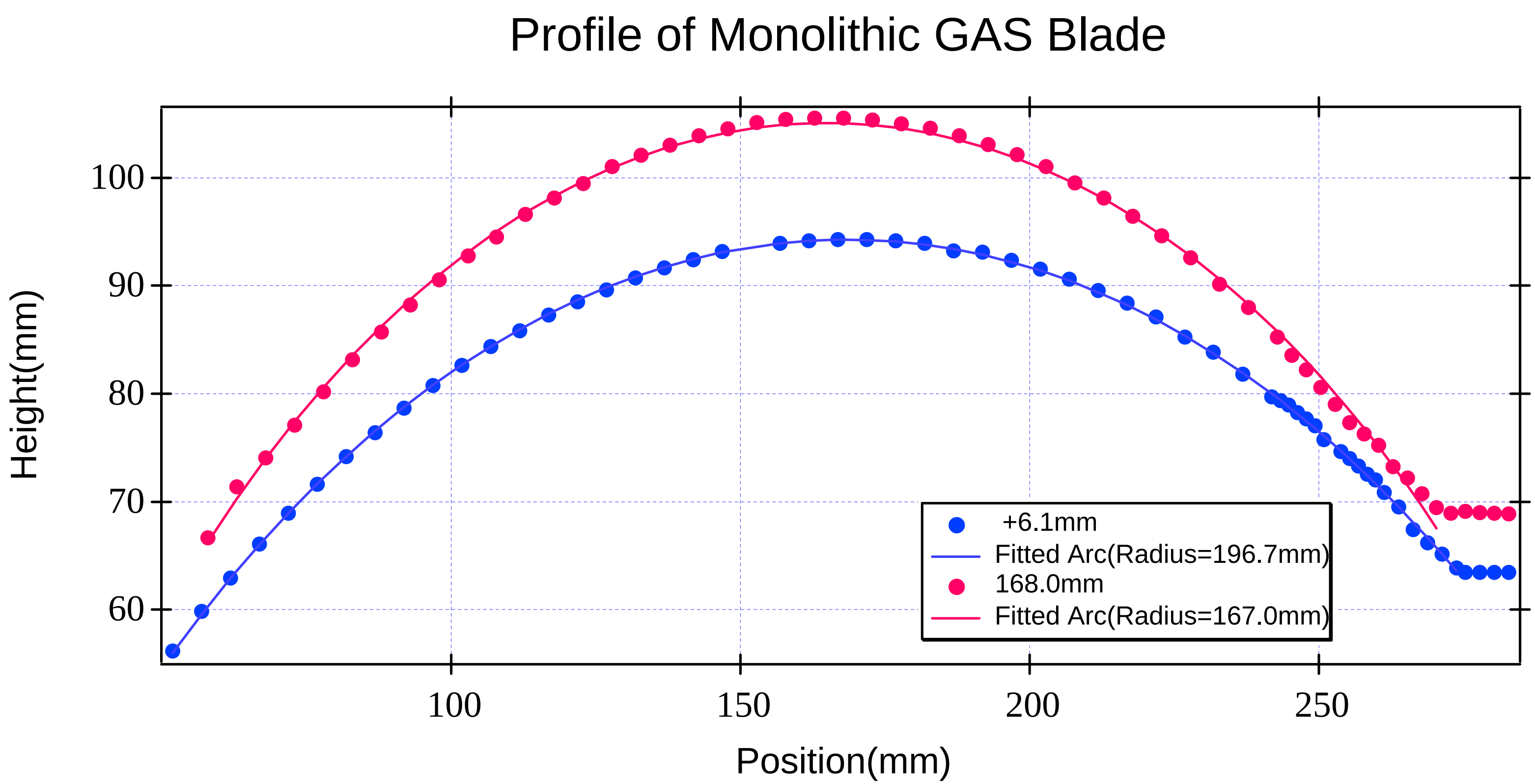
Profile of Monolithic GAS Blade
Height(mm)
Position(mm)
100
90
80
70
60
100
150
200
250
+6.1mm
Fitted Arc(Radius=196.7mm)
168.0mm
Fitted Arc(Radius=167.0mm)

Resonant Frequency vs Working Point

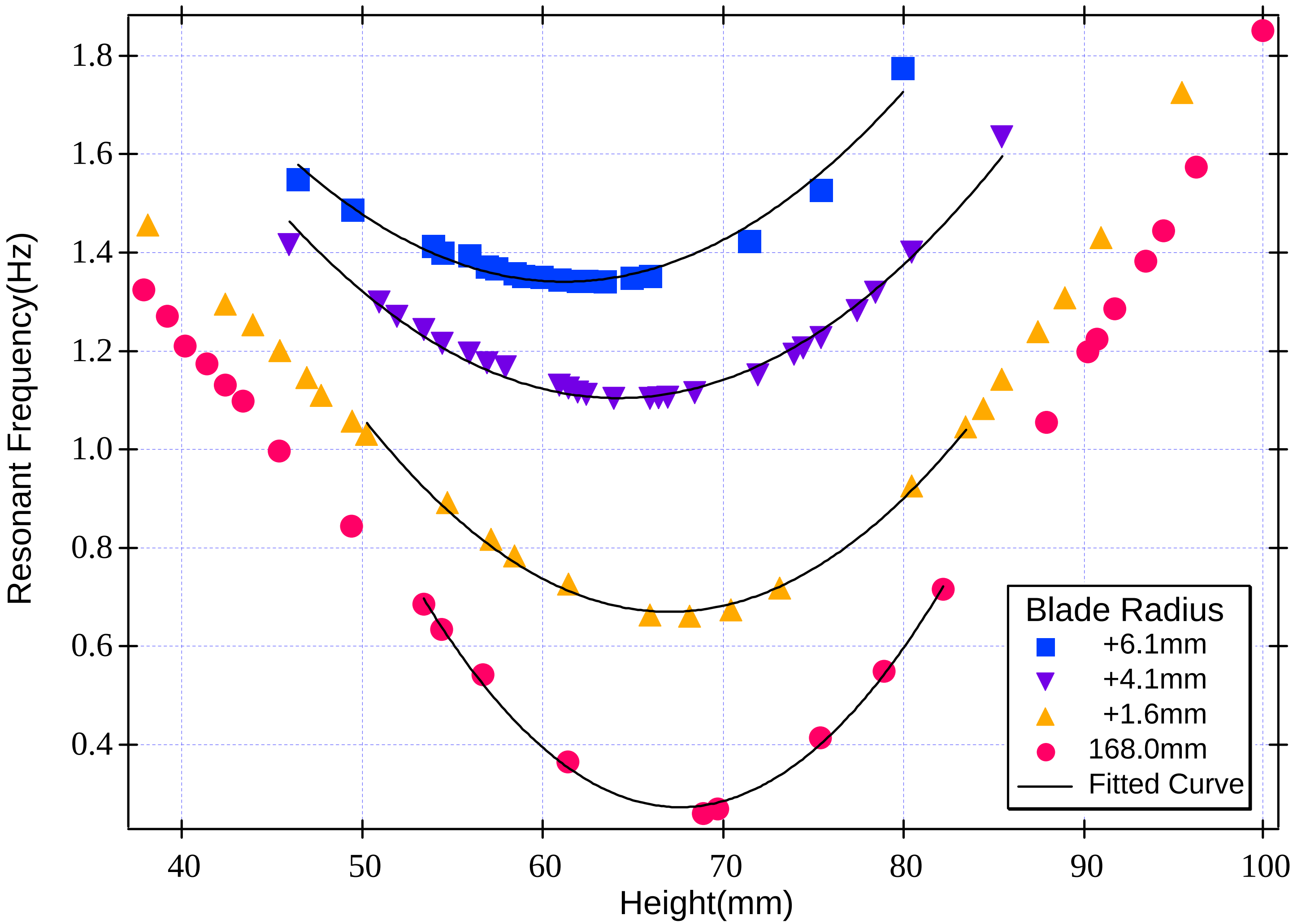

Minimum Vertical Resonant Frequency vs Blade Radius

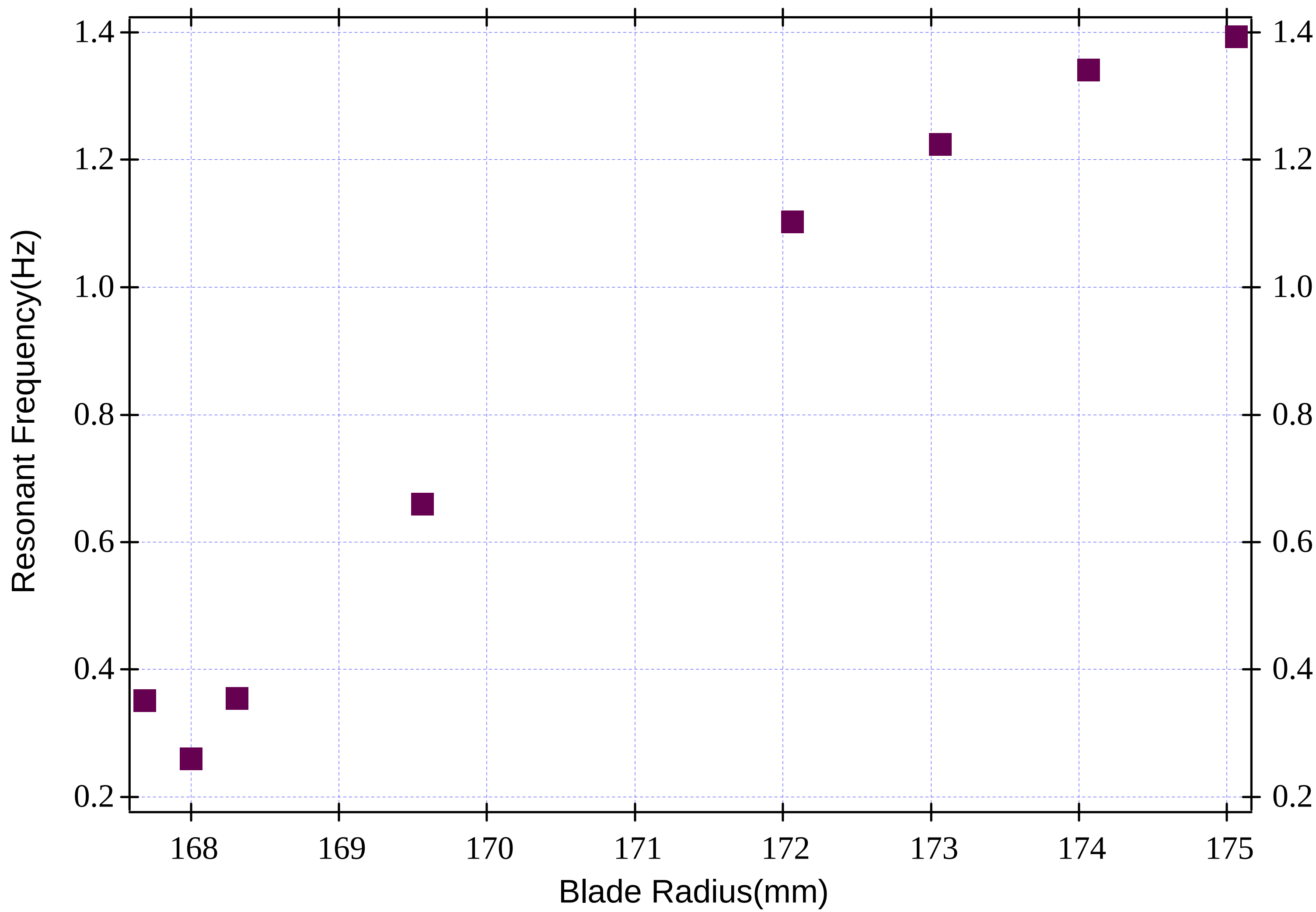

Kenji Numata

The Margin of Load for 10% Error of VRF

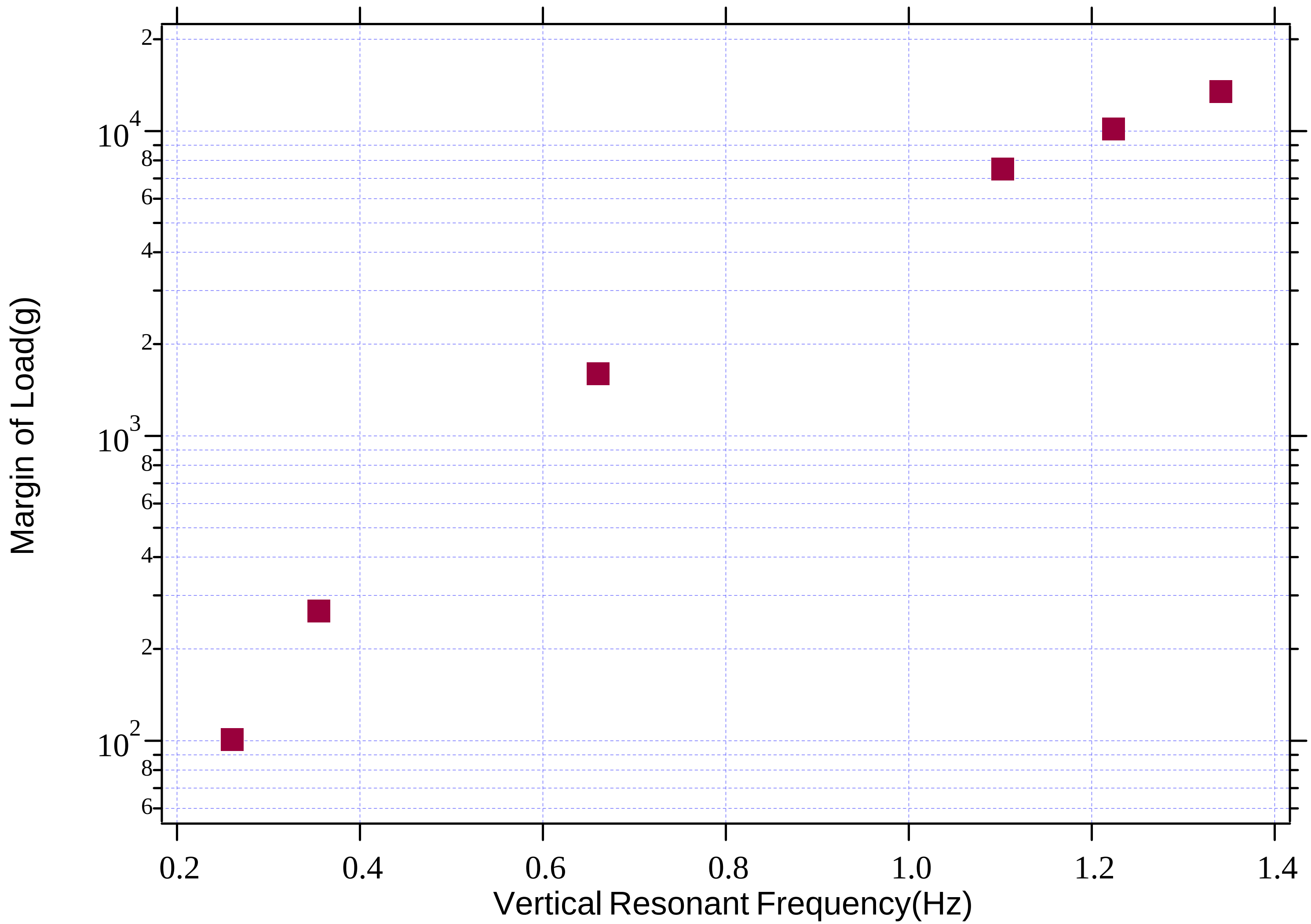

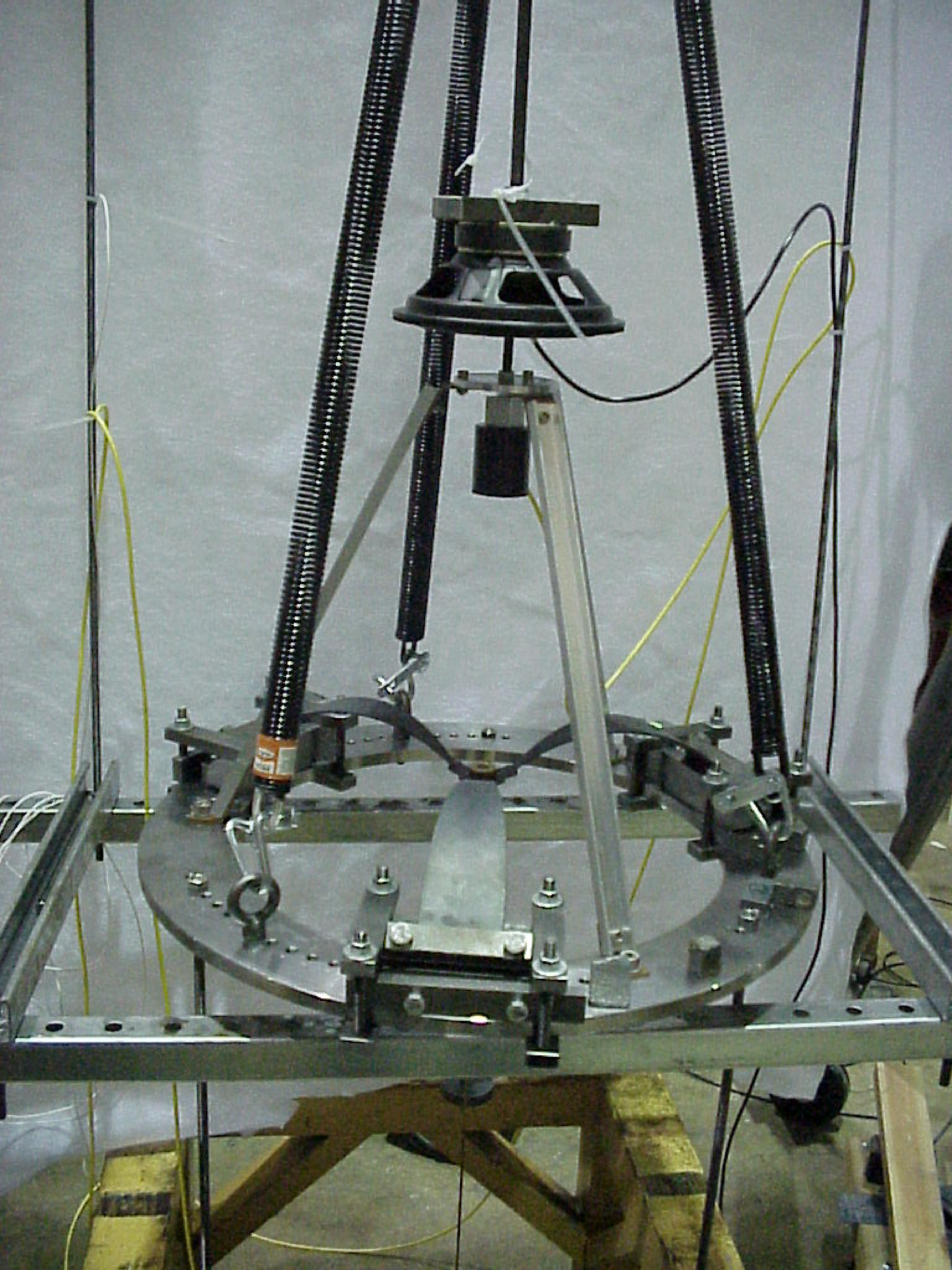

Transfer Function of Monolithic GAS Filter

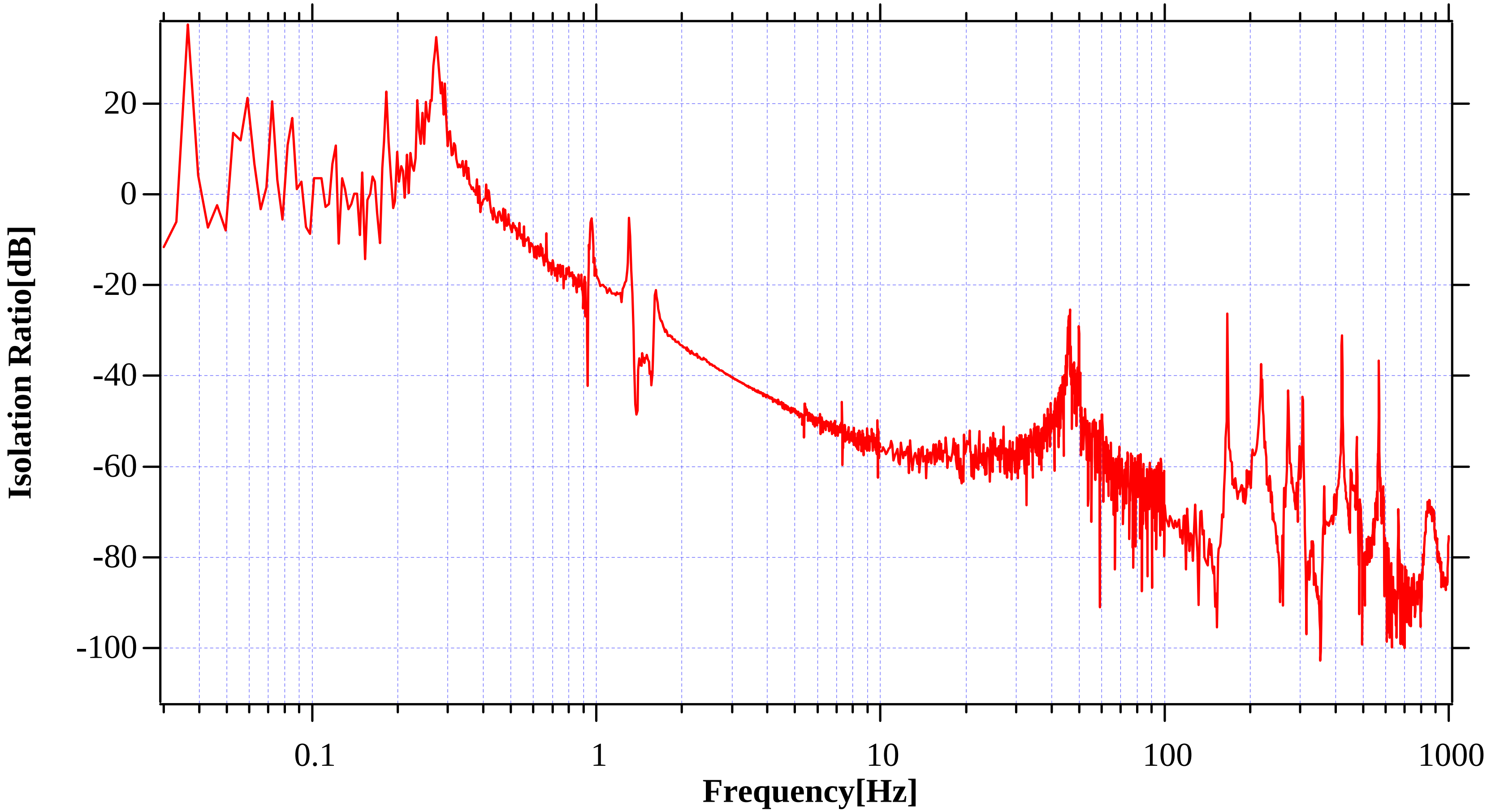

Kenji Numata

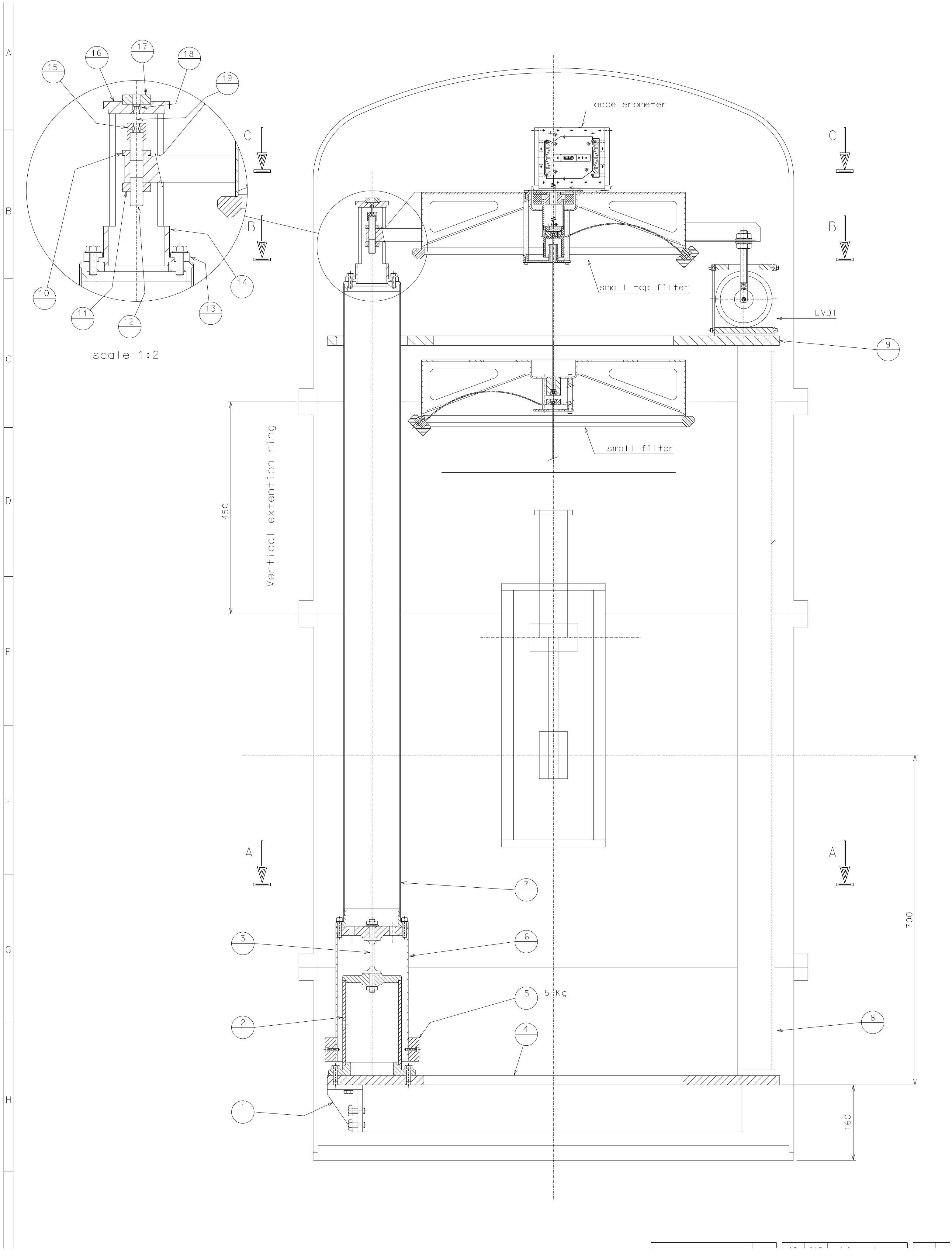

A
B
C
D
E
F
G
H
15
16
17
18
19
10
11
12
13
14
scale 1:2
accelerometer
C
C
B
B
small top filter
LVDT
9
small filter
450
Vertical extention ring
A
A
7
3
6
5
5 Kg
2
4
8
700
1
160

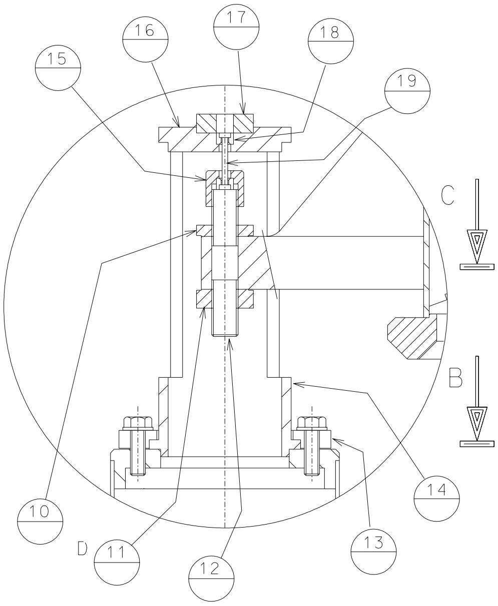

scale 1:2

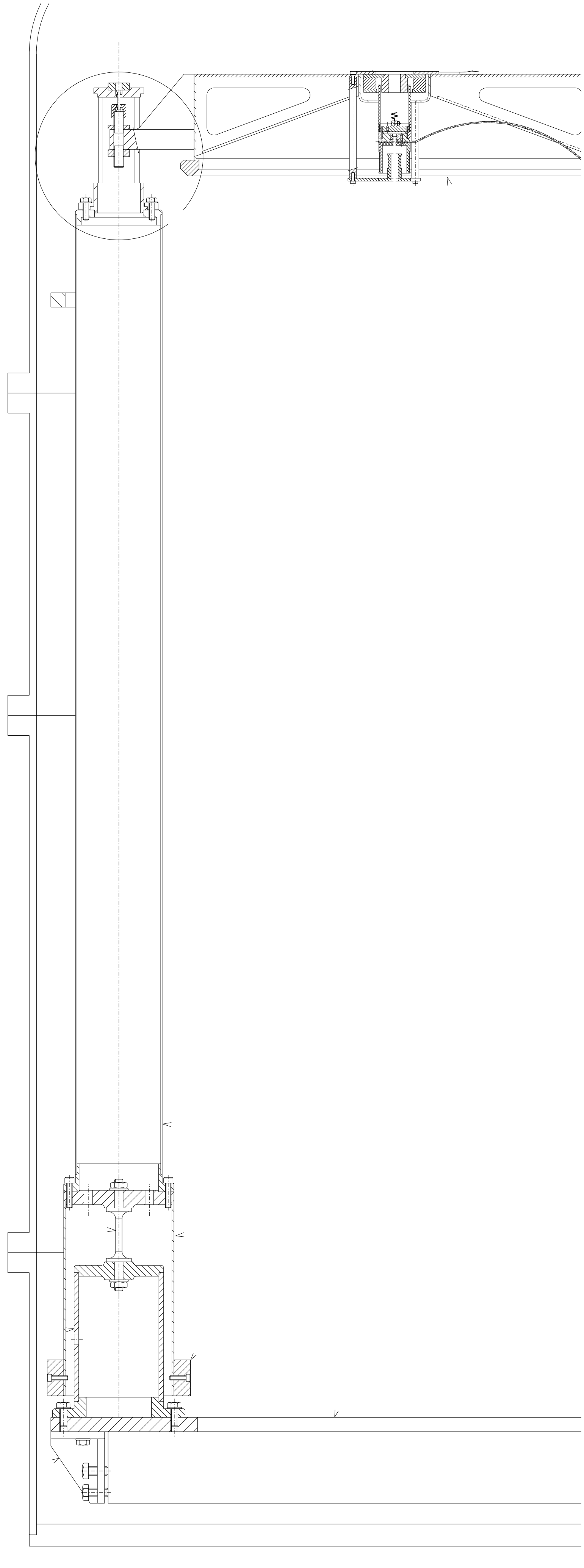

IP Assembly

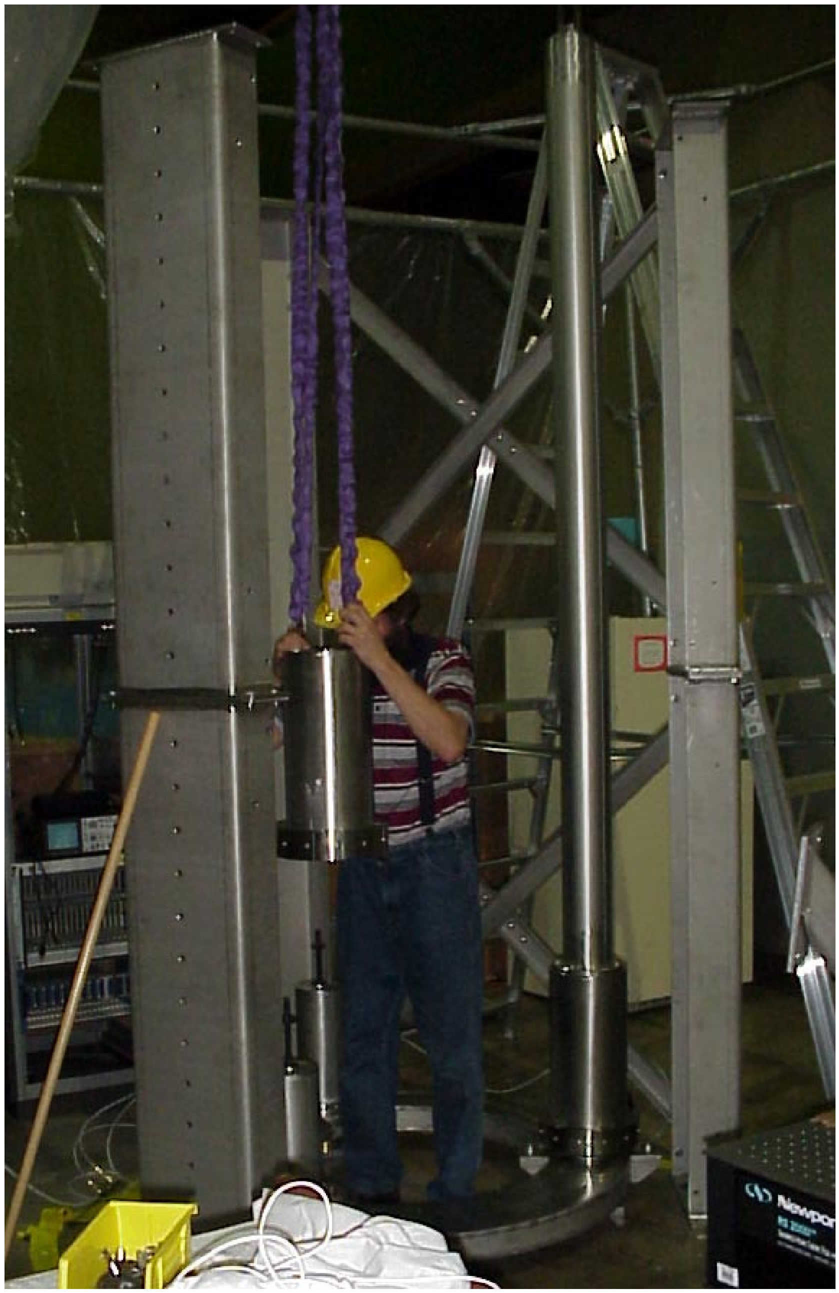

IP Leg

IP Assembly

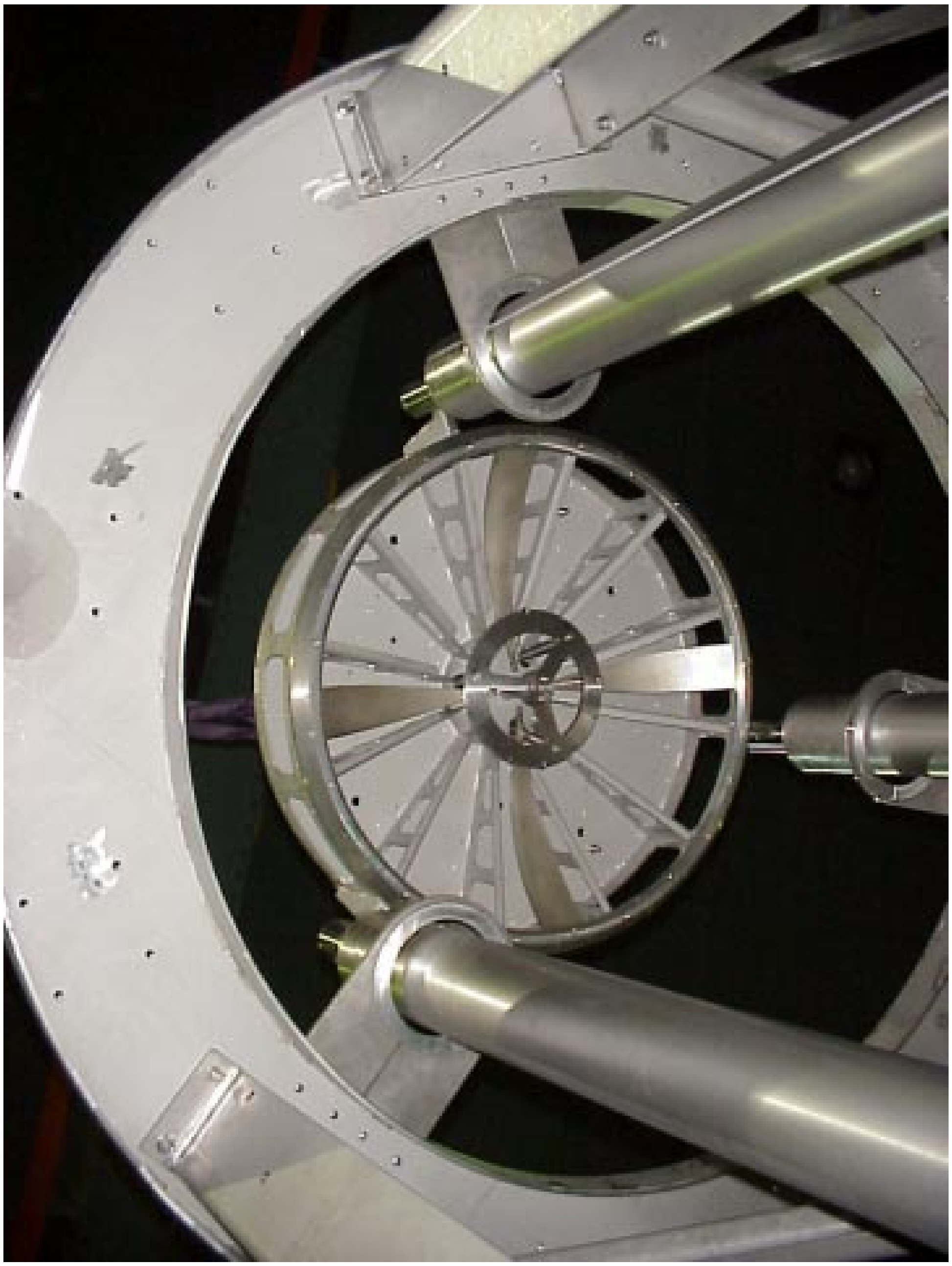

IP Assembly

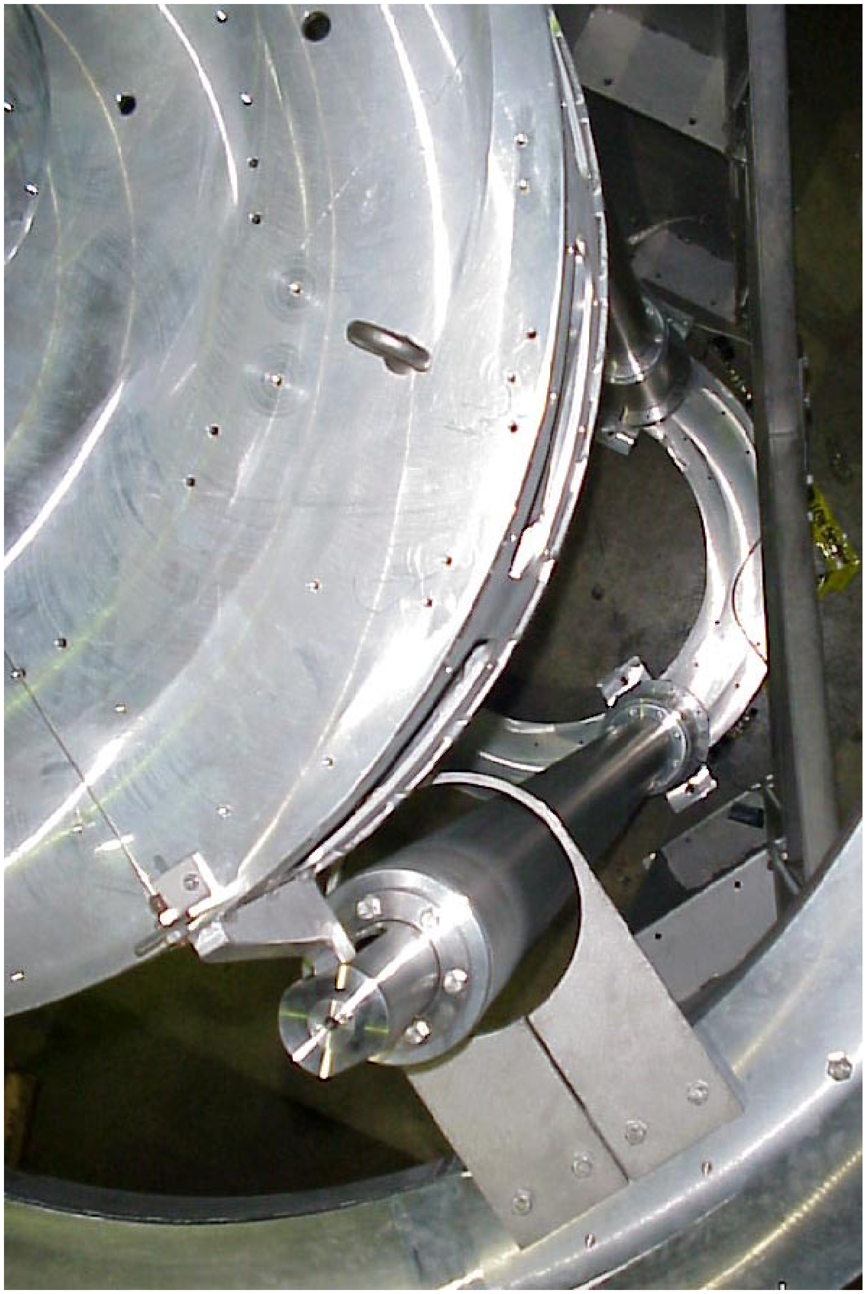

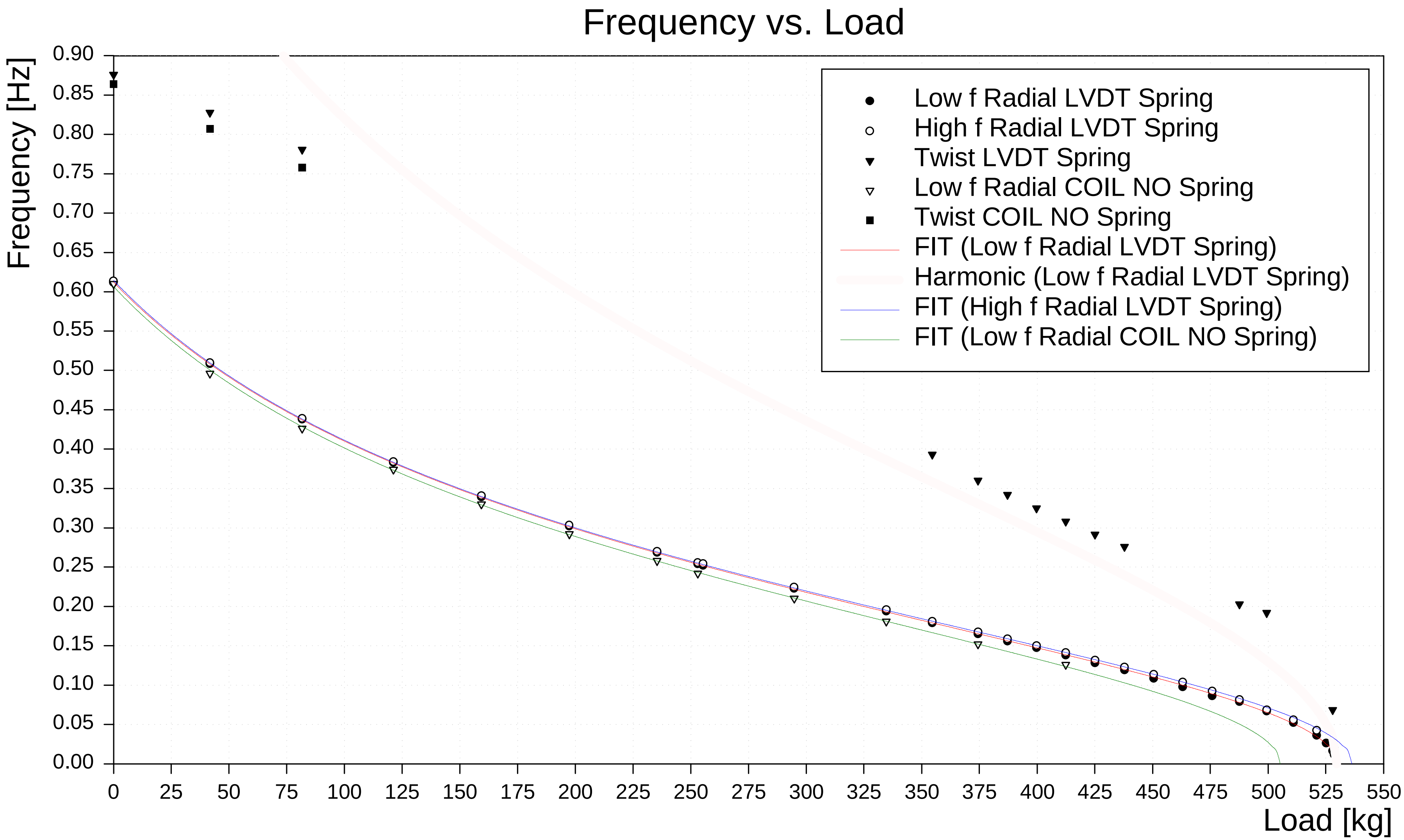
Frequency vs. Load
Frequency [Hz]
Load [kg]
0.90
0.85
0.80
0.75
0.70
0.65
0.60
0.55
0.50
0.45
0.40
0.35
0.30
0.25
0.20
0.15
0.10
0.05
0.00
0
25
50
75
100
125
150
175
200
225
250
275
300
325
350
375
400
425
450
475
500
525
550
Low f Radial LVDT Spring
High f Radial LVDT Spring
Twist LVDT Spring
Low f Radial COIL NO Spring
Twist COIL NO Spring
FIT (Low f Radial LVDT Spring)
Harmonic (Low f Radial LVDT Spring)
FIT (High f Radial LVDT Spring)
FIT (Low f Radial COIL NO Spring)

Inverted Pendulum: Radial Frequency vs. Load

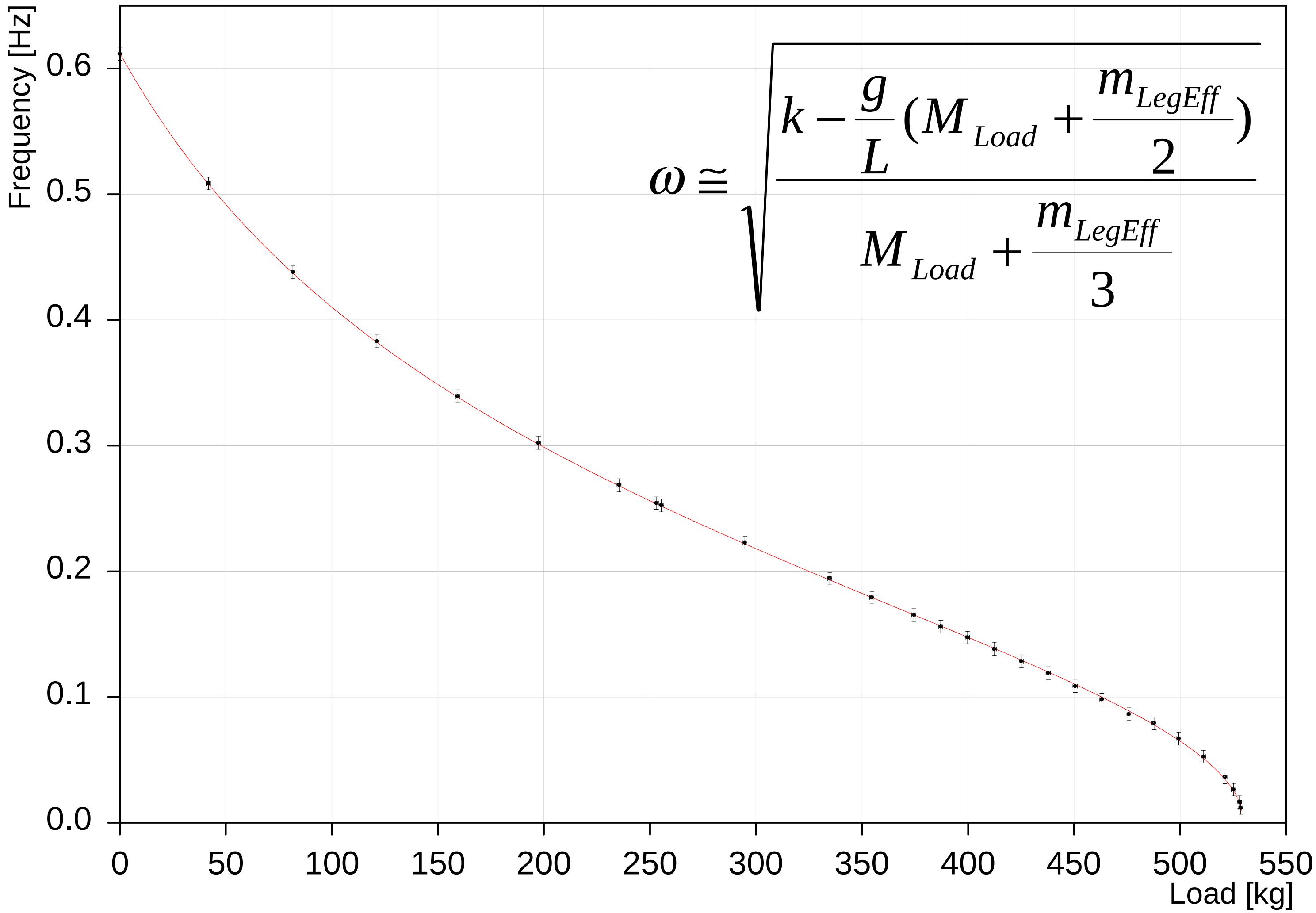

$$\omega \cong \sqrt{\frac{k - \frac{g}{L}\left(M_{Load} + \frac{m_{LegEff}}{2}\right)}{M_{Load} + \frac{m_{LegEff}}{3}}}$$

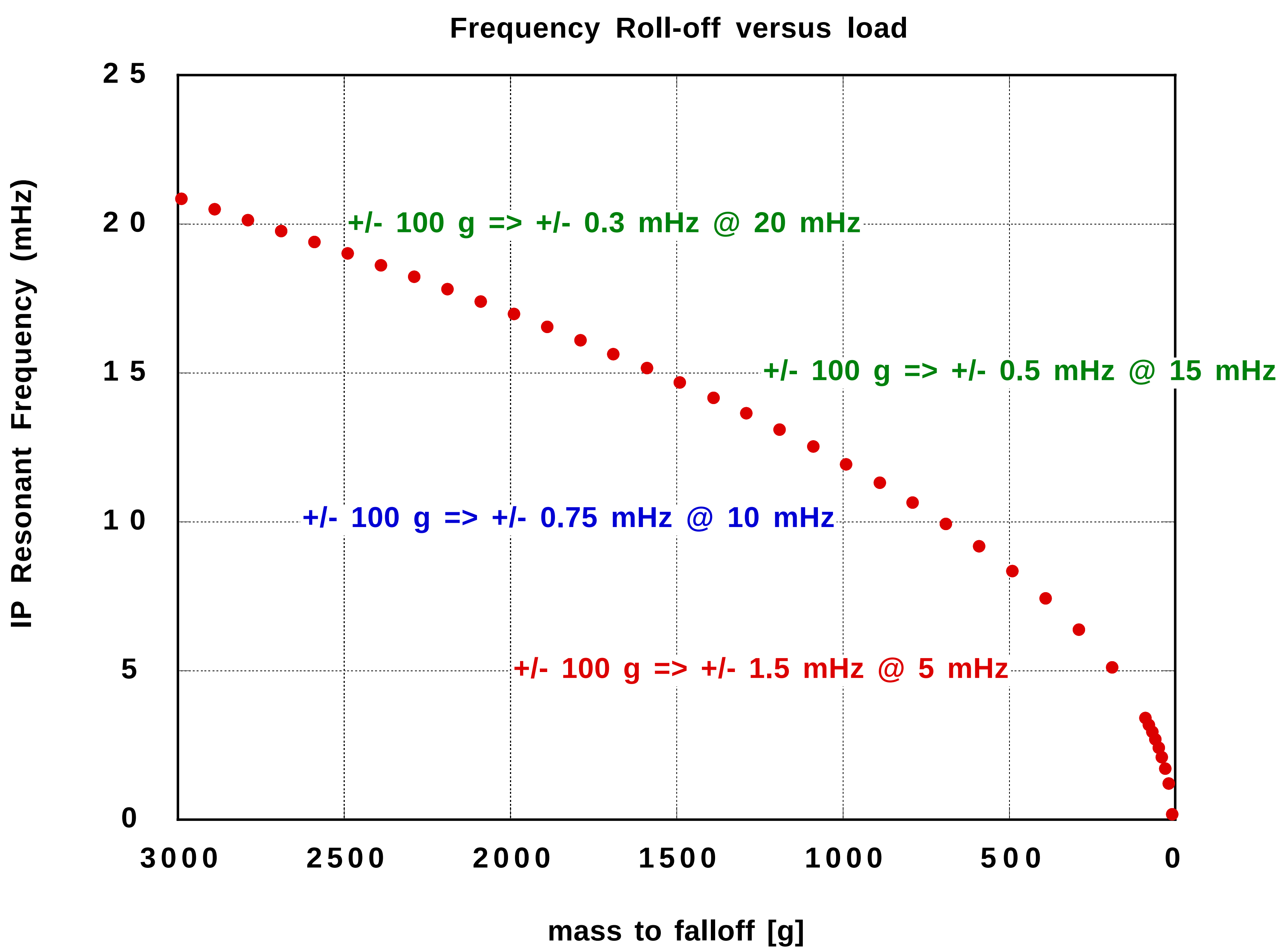

Frequency Roll-off versus load
IP Resonant Frequency (mHz)
mass to falloff [g]
25
20
15
10
5
0
3000
2500
2000
1500
1000
500
0
+/- 100 g => +/- 0.3 mHz @ 20 mHz
+/- 100 g => +/- 0.5 mHz @ 15 mHz
+/- 100 g => +/- 0.75 mHz @ 10 mHz
+/- 100 g => +/- 1.5 mHz @ 5 mHz

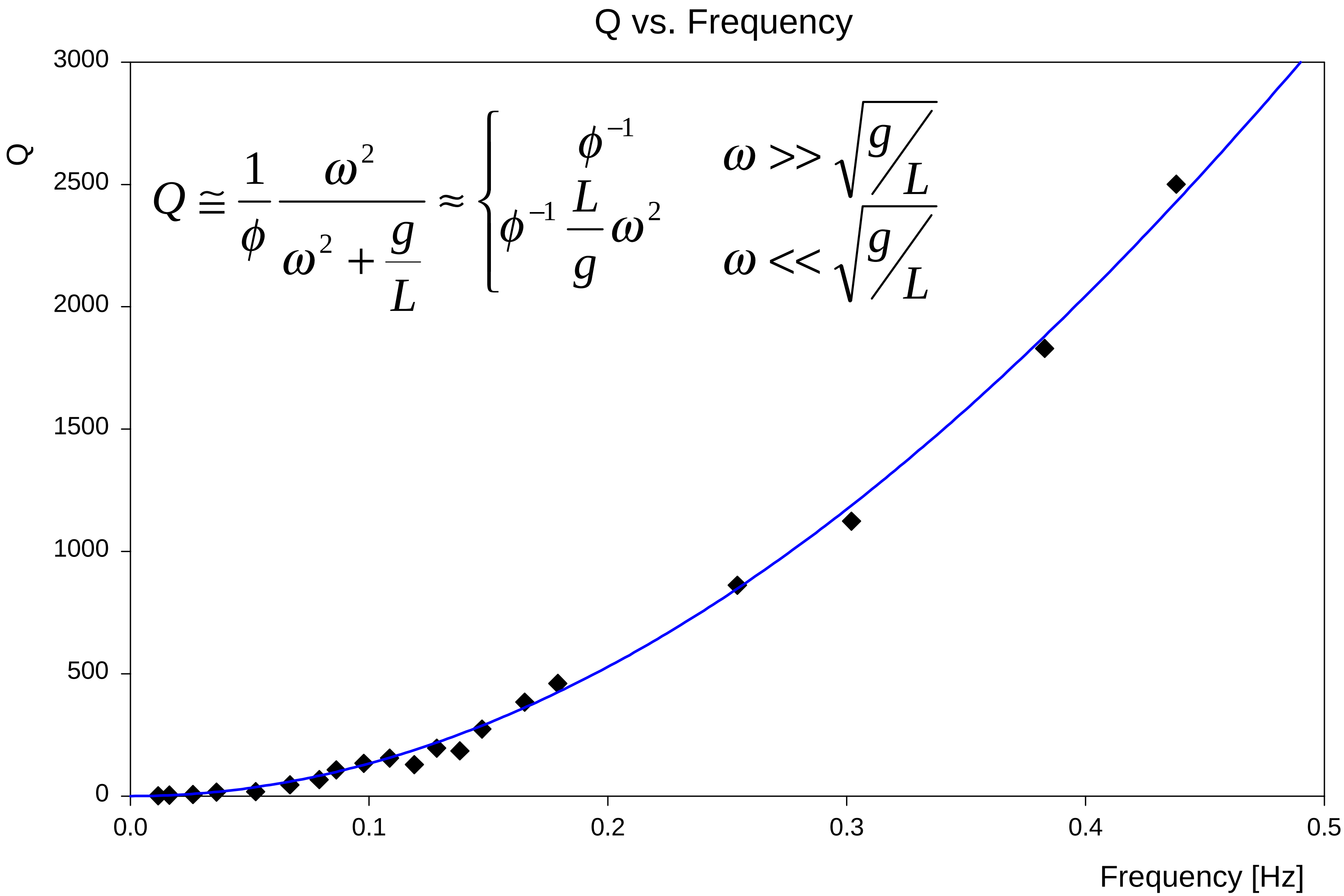
Q vs. Frequency
$Q \cong \frac{1}{\phi}\frac{\omega^2}{\omega^2+\frac{g}{L}} \approx \begin{cases}\phi^{-1} & \omega >> \sqrt{g/L} \\ \phi^{-1}\frac{L}{g}\omega^2 & \omega << \sqrt{g/L}\end{cases}$
Q
3000
2500
2000
1500
1000
500
0
0.0
0.1
0.2
0.3
0.4
0.5
Frequency [Hz]

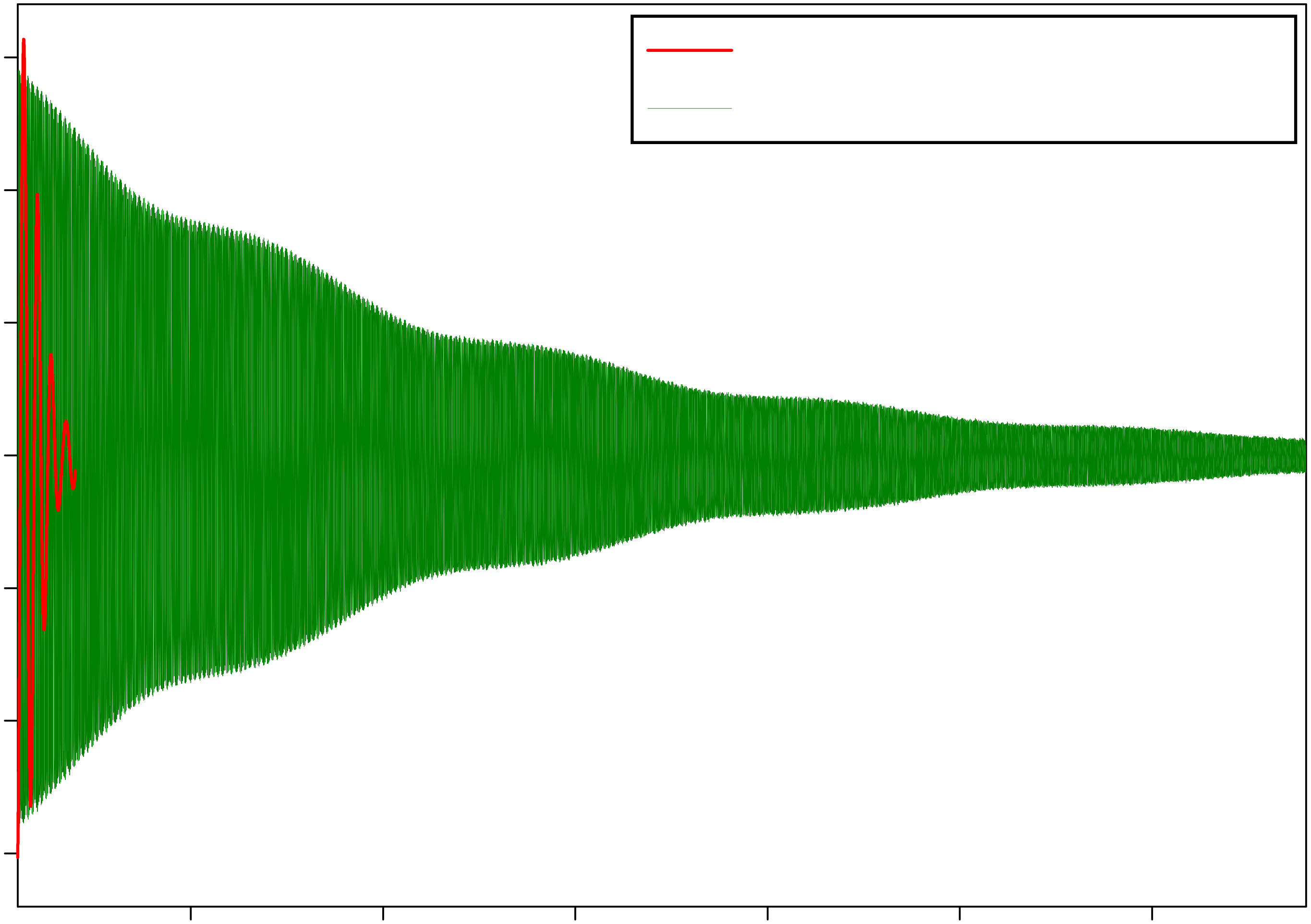

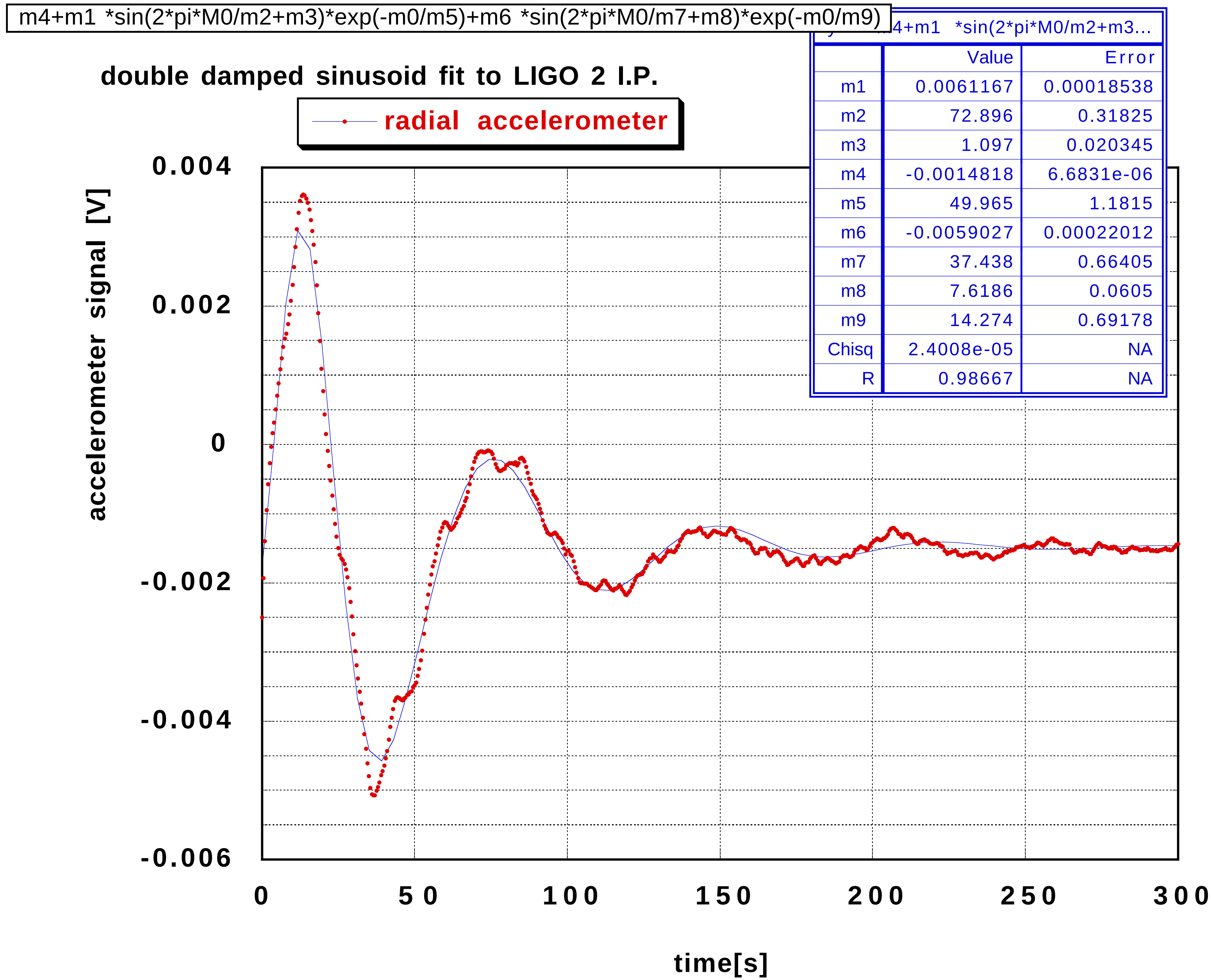
m4+m1 *sin(2*pi*M0/m2+m3)*exp(-m0/m5)+m6 *sin(2*pi*M0/m7+m8)*exp(-m0/m9)
double damped sinusoid fit to LIGO 2 I.P.
radial accelerometer
4+m1 *sin(2*pi*M0/m2+m3...
Value
Error
m1 0.0061167 0.00018538
m2 72.896 0.31825
m3 1.097 0.020345
m4 -0.0014818 6.6831e-06
m5 49.965 1.1815
m6 -0.0059027 0.00022012
m7 37.438 0.66405
m8 7.6186 0.0605
m9 14.274 0.69178
Chisq 2.4008e-05 NA
R 0.98667 NA
accelerometer signal [V]
0.004
0.002
0
-0.002
-0.004
-0.006
0
50
100
150
200
250
300
time[s]

Leg + C.W. Simulation (First Mode)

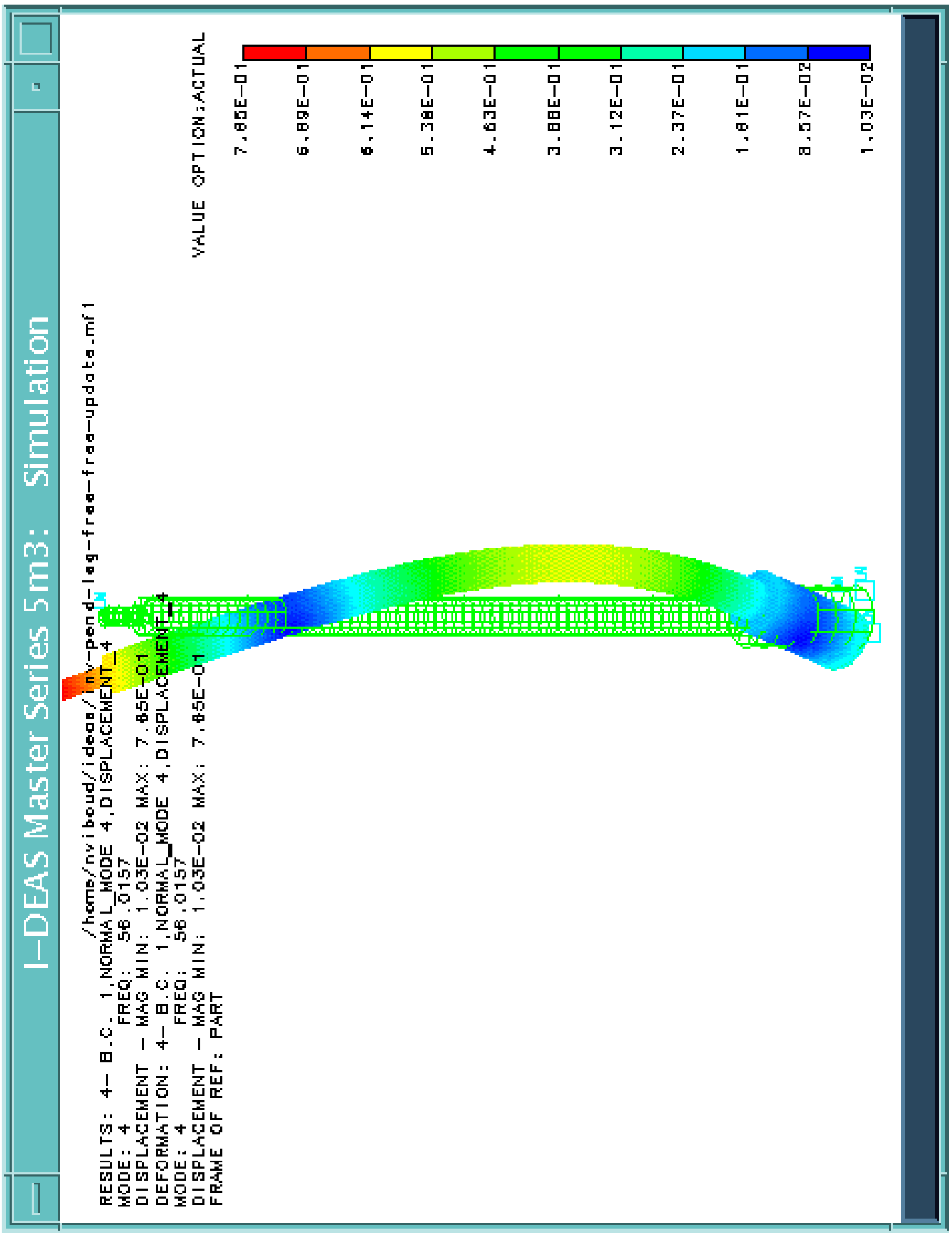

Leg + C.W. Simulation (Second Mode)

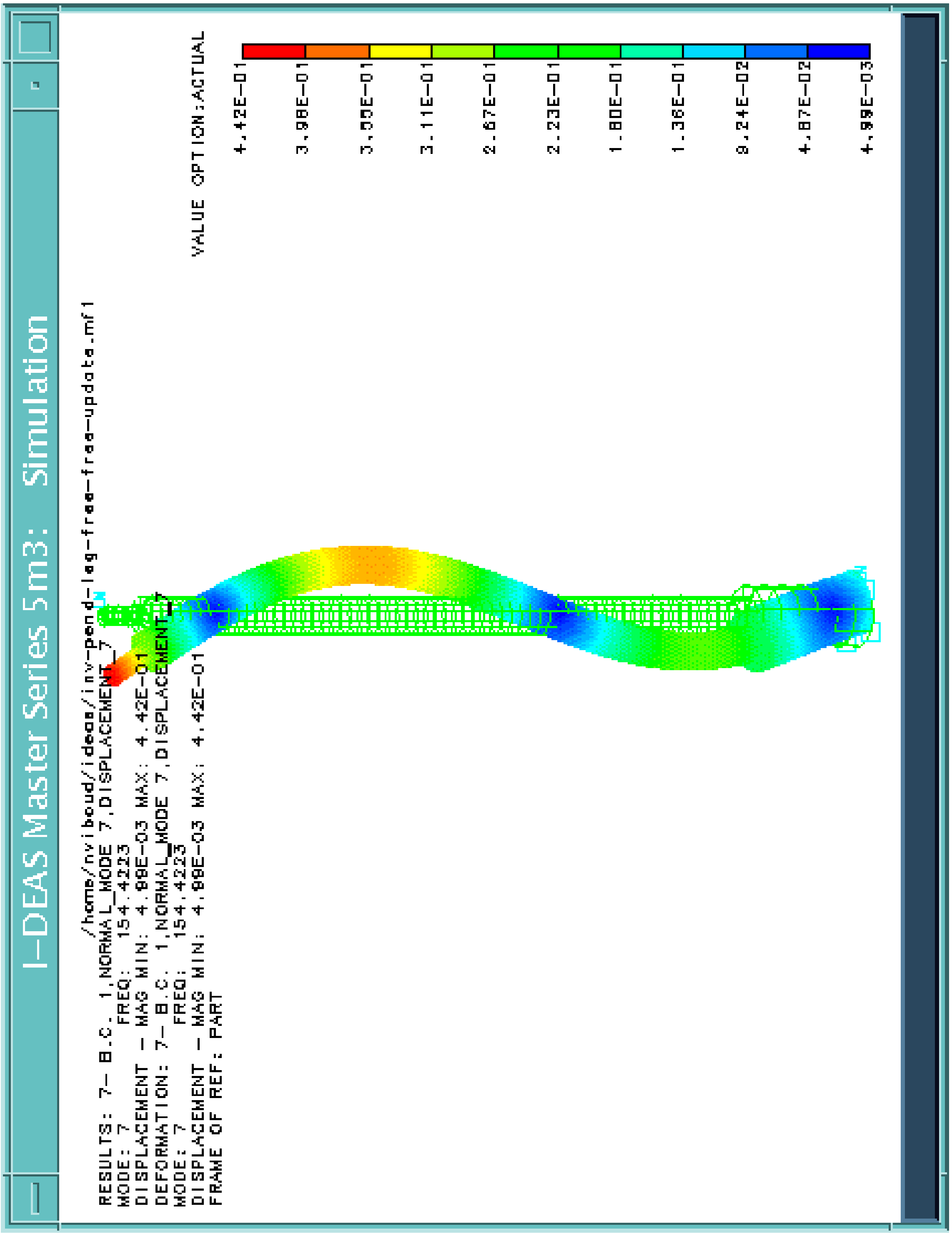

IP Leg + C.W Resonances

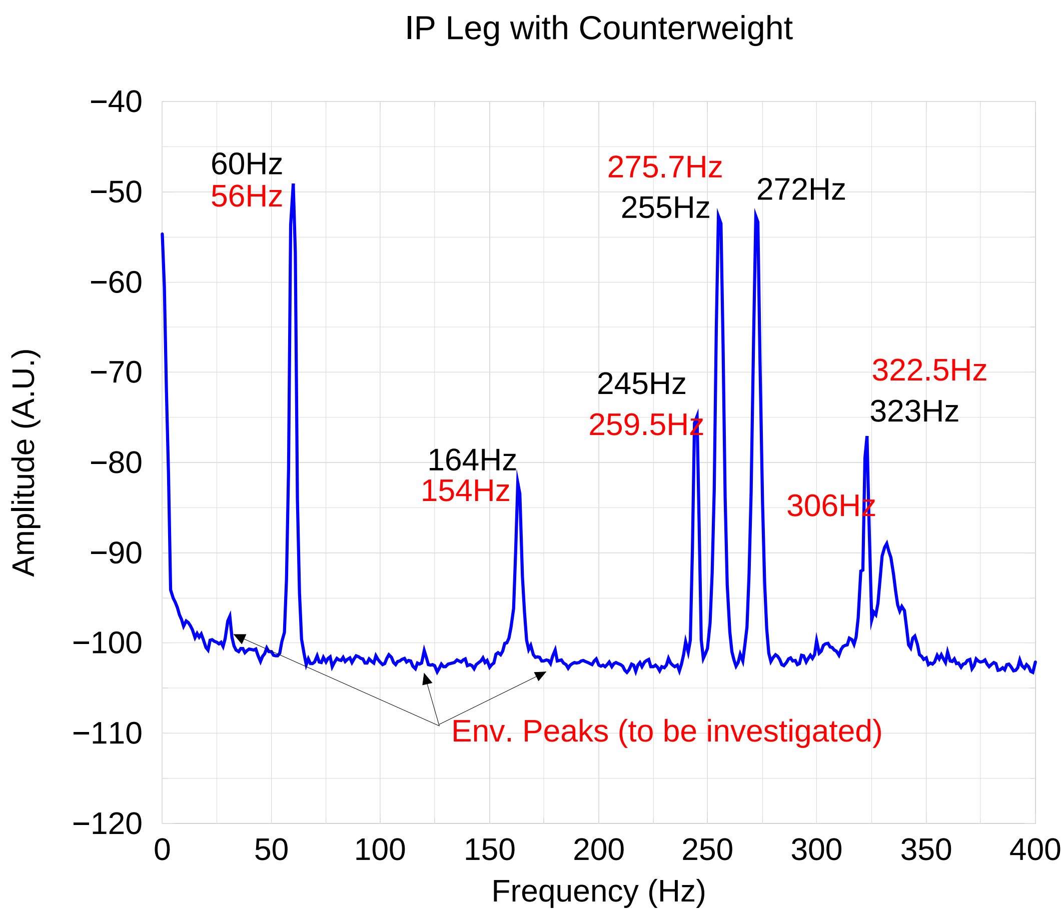

272Hz

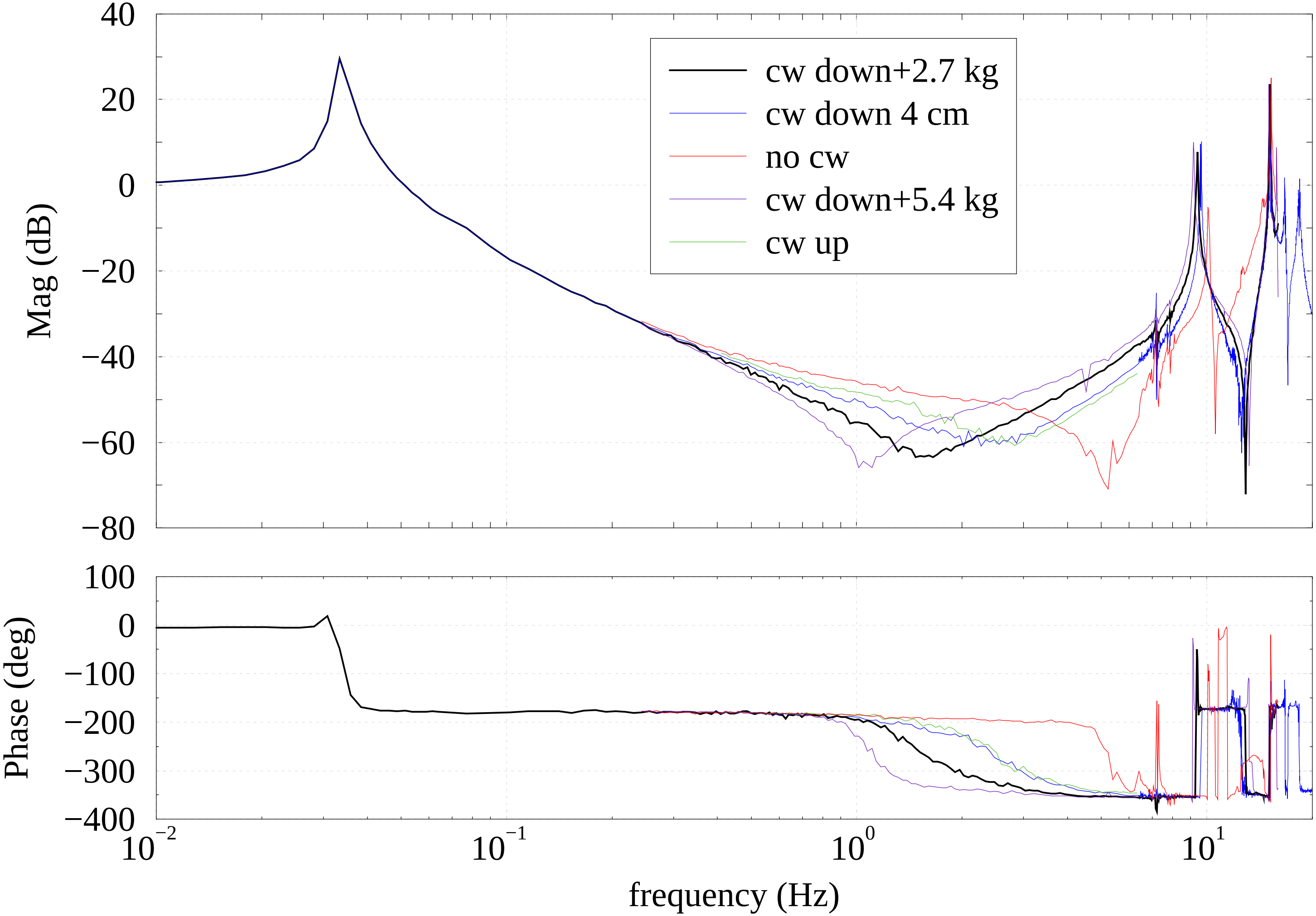

40
20
0
−20
−40
−60
−80
Mag (dB)
cw down+2.7 kg
cw down 4 cm
no cw
cw down+5.4 kg
cw up
100
0
−100
−200
−300
−400
Phase (deg)
10^{-2}
10^{-1}
10^{0}
10^{1}
frequency (Hz)

SAS-SUS Control
Sensors Actuator Map

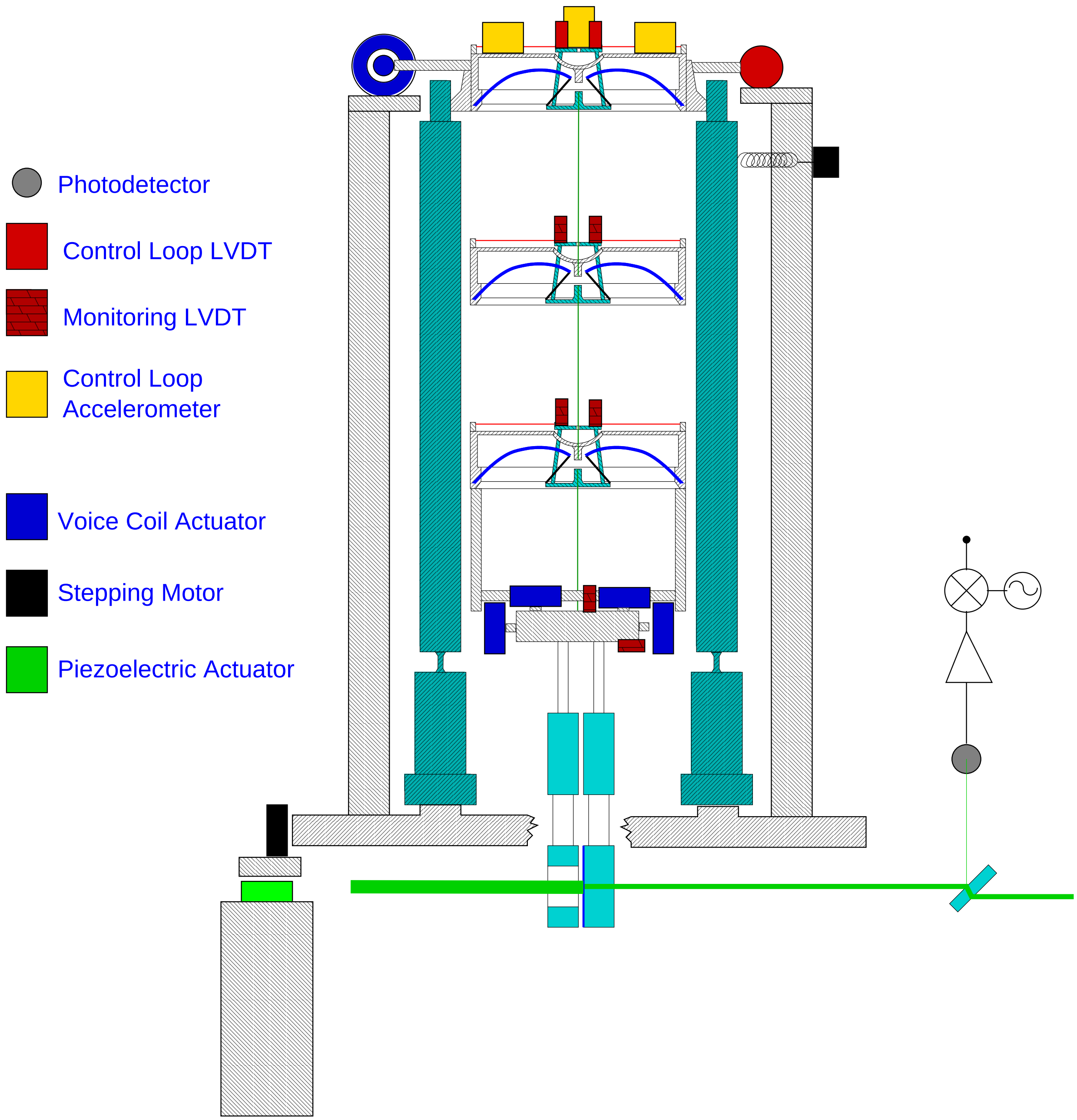

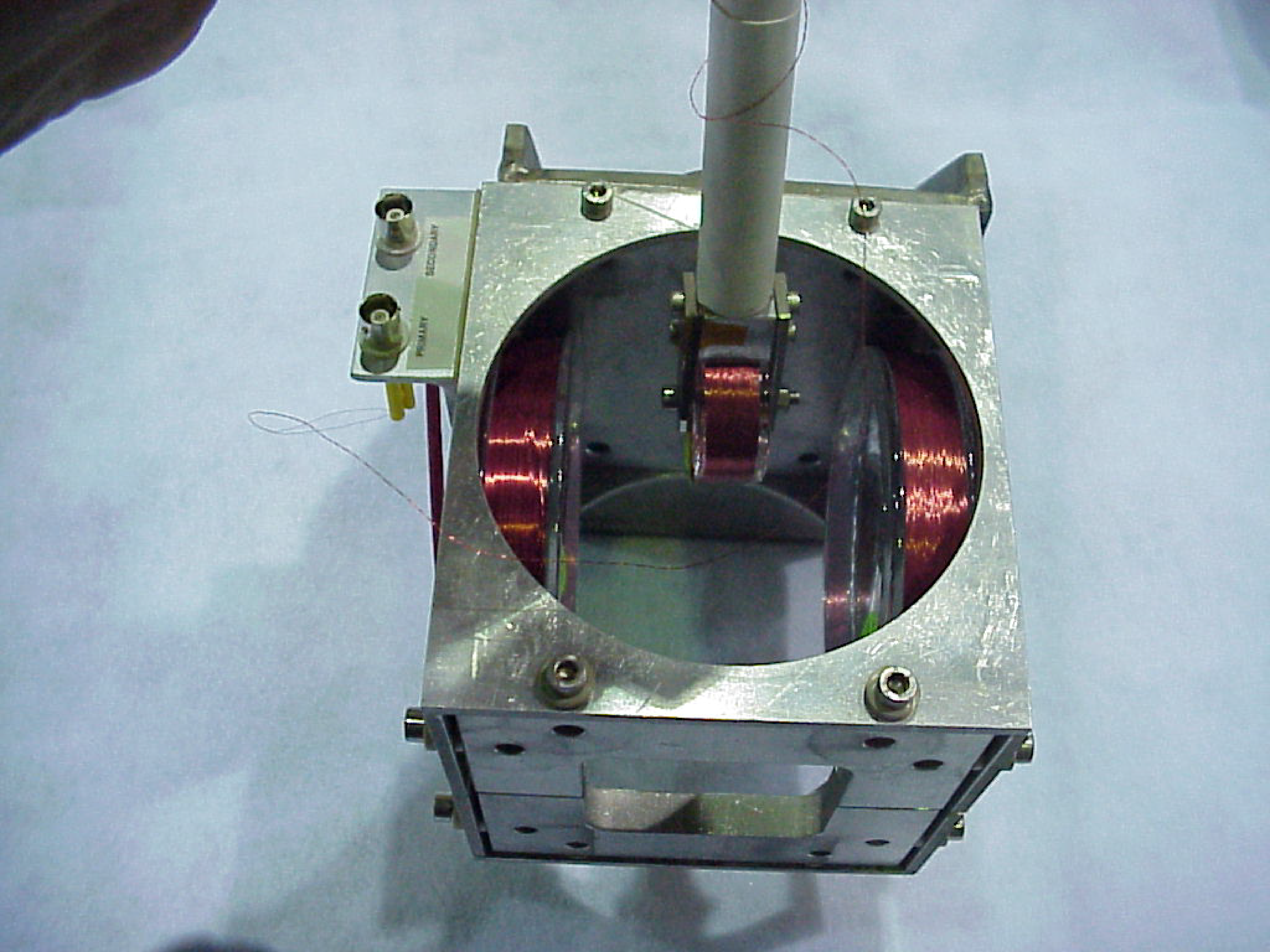
SECONDARY
PRIMARY

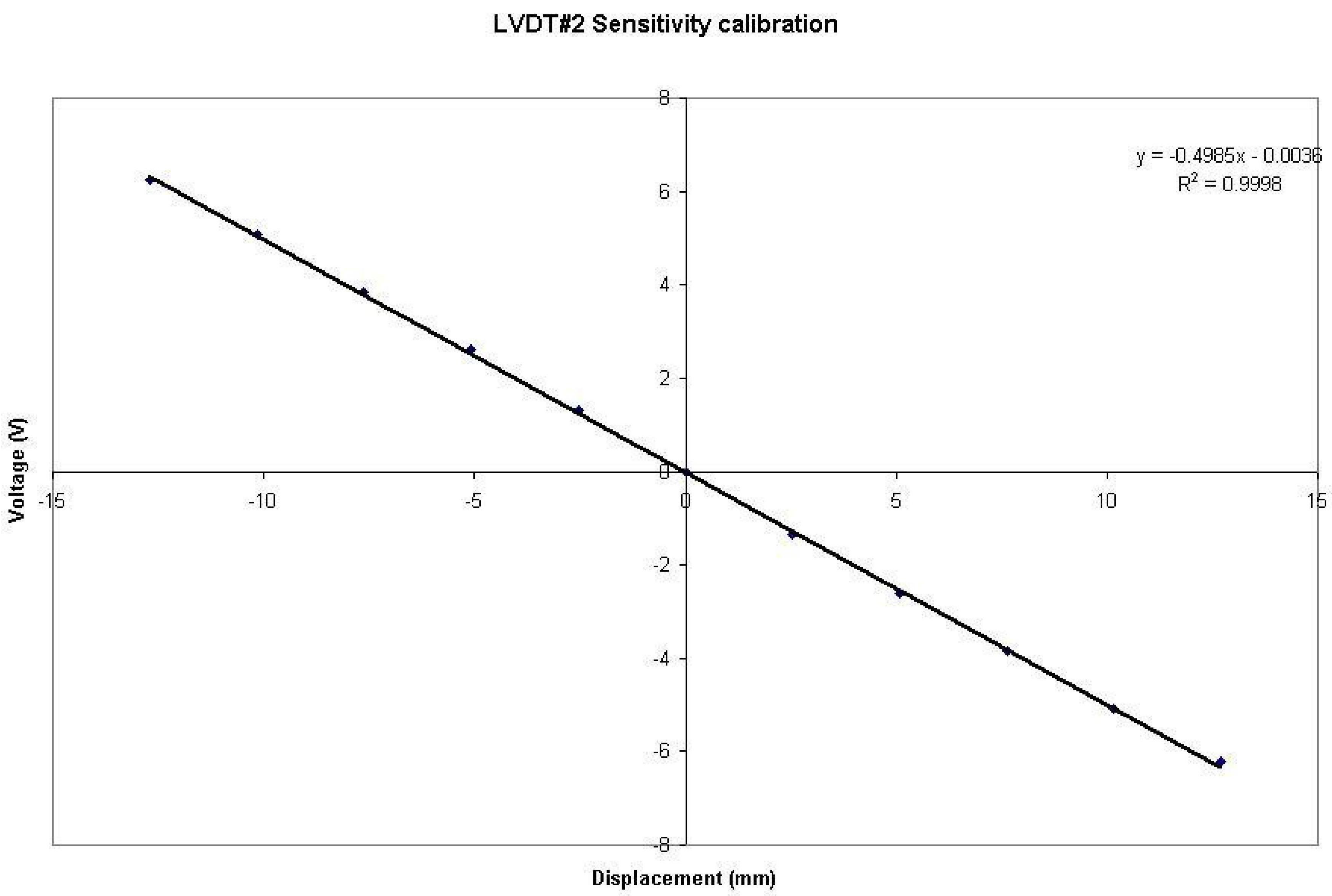
LVDT#2 Sensitivity calibration
y = -0.4985x - 0.0036
R2 = 0.9998
8
6
4
2
0
-2
-4
-6
-8
-15
-10
-5
0
5
10
15
Voltage (V)
Displacement (mm)

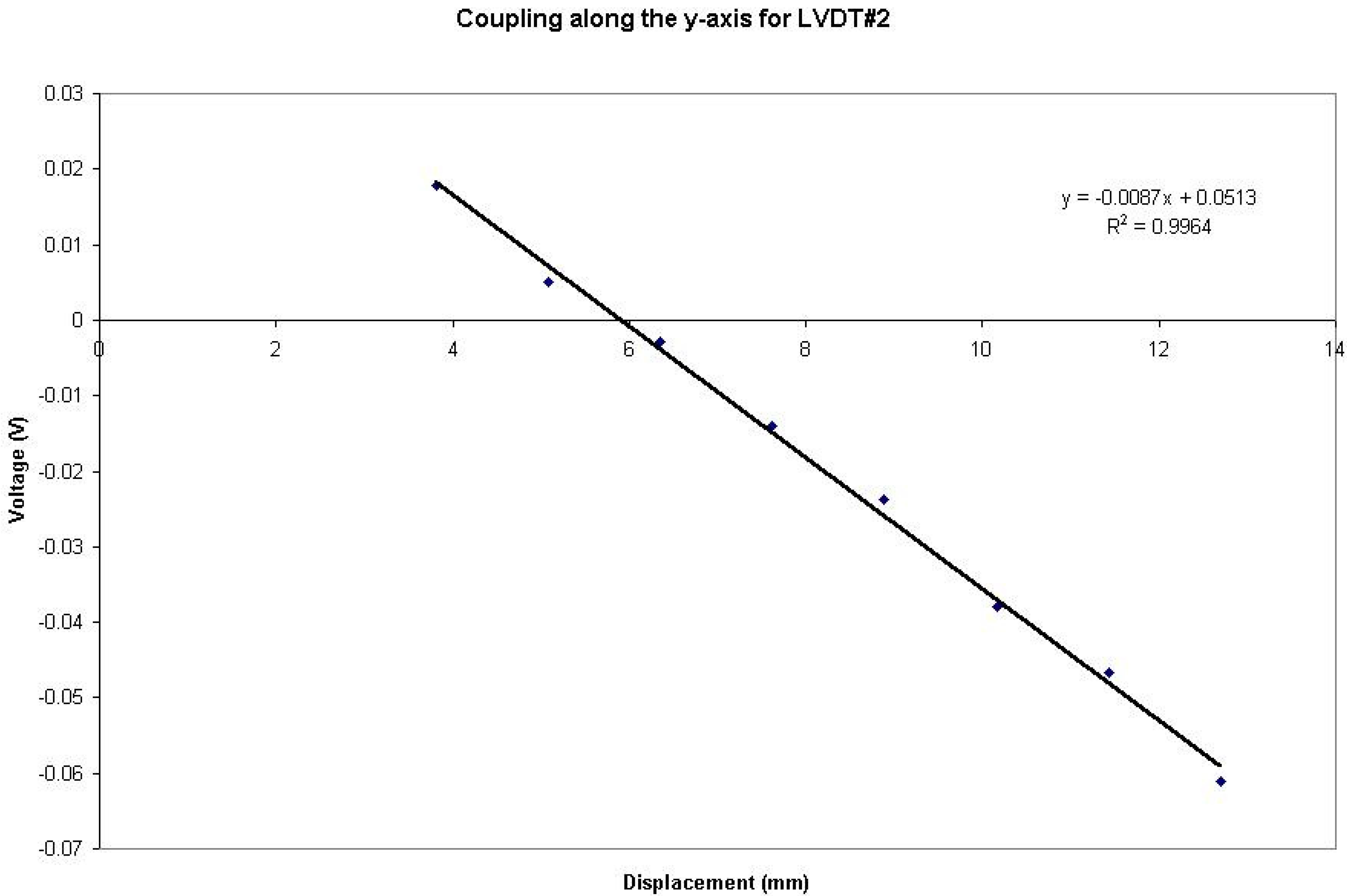
Coupling along the y-axis for LVDT#2
y = -0.0087x + 0.0513
R2 = 0.9964
Voltage (V)
Displacement (mm)
0.03
0.02
0.01
0
-0.01
-0.02
-0.03
-0.04
-0.05
-0.06
-0.07
0
2
4
6
8
10
12
14

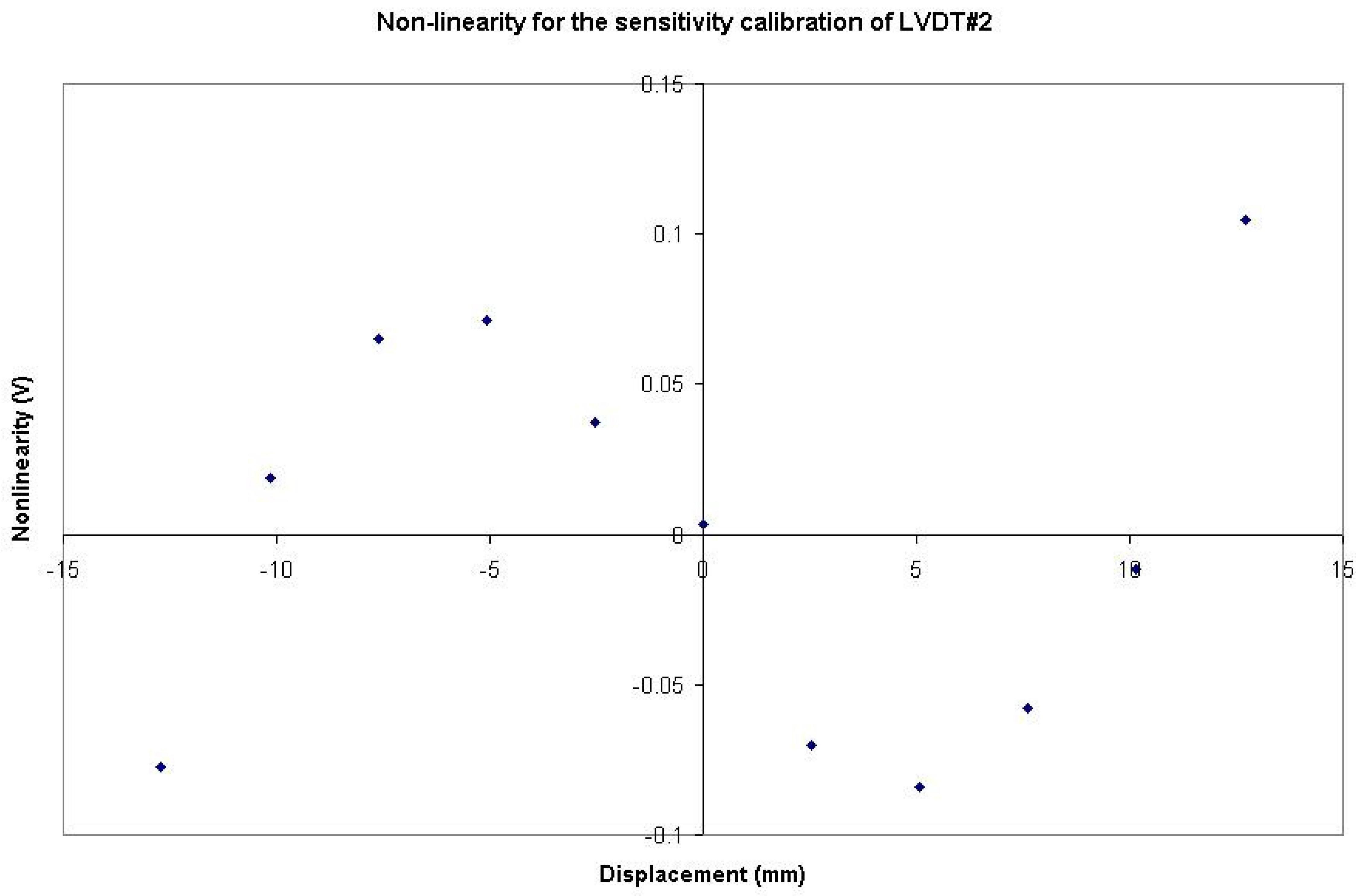
Non-linearity for the sensitivity calibration of LVDT#2
0.15
0.1
0.05
0
-0.05
-0.1
-15
-10
-5
0
5
10
15
Nonlinearity (V)
Displacement (mm)

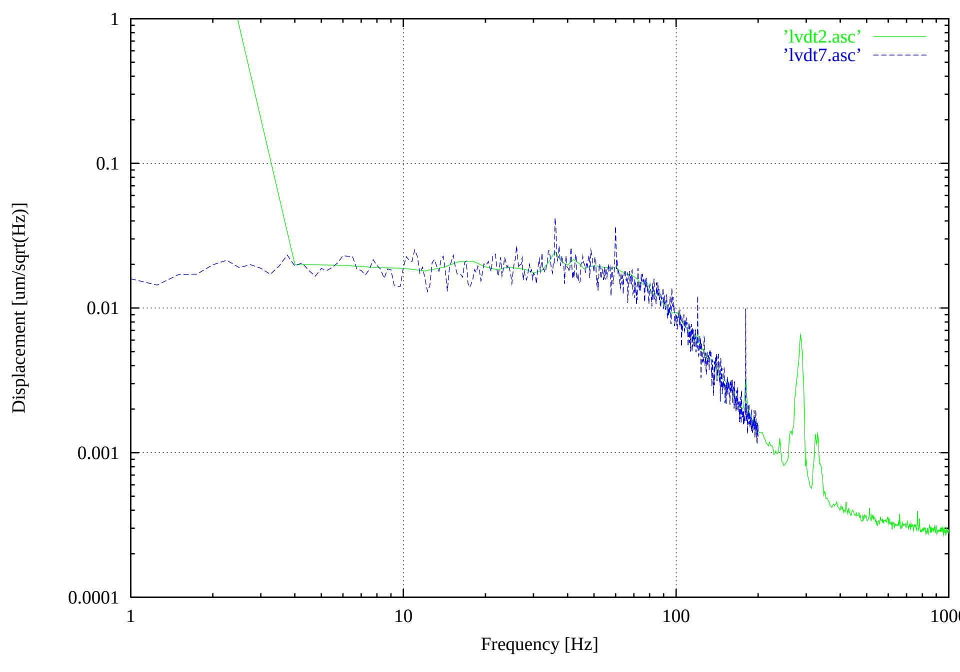

'lvdt2.asc'
'lvdt7.asc'
Displacement [um/sqrt(Hz)]
Frequency [Hz]
1
0.1
0.01
0.001
0.0001
1
10
100
1000

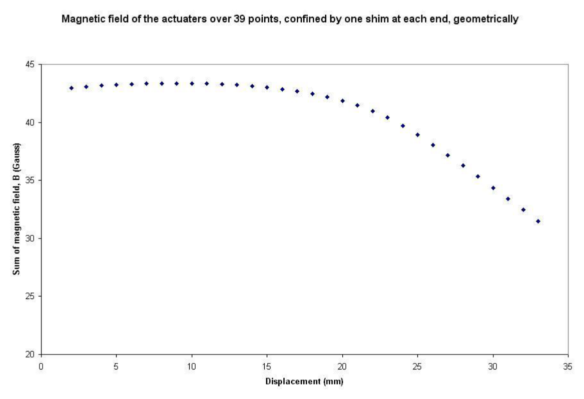

Magnetic field of the actuaters over 39 points, confined by one shim at each end, geometrically
Sum of magnetic field, B (Gauss)
45
40
35
30
25
20
0
5
10
15
20
25
30
35
Displacement (mm)

The folded pendulum

The folded pendulum dynamics:

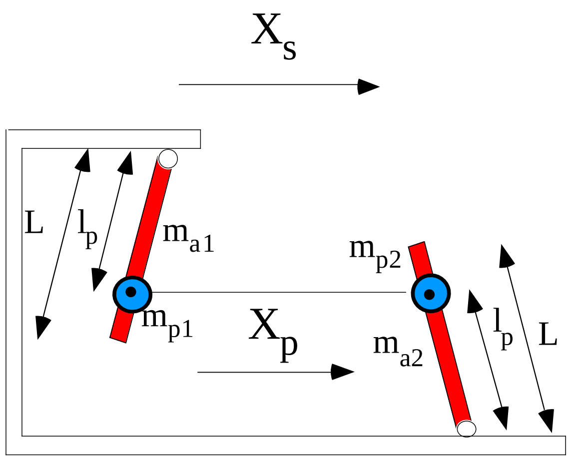

$$\omega_0^2 = \frac{\frac{L}{2l_p}\left(m_{a_1} - m_{a_2}\right) + \left(m_{p_1} - m_{p_2}\right)}{\frac{L^2}{3l_p^2}\left(m_{a_1} + m_{a_2}\right) + \left(m_{p_1} + m_{p_2}\right)} \cdot \frac{g}{l_p} + \gamma$$

Features:

- low resonant frequency: 0.1–1 Hz
- compactness: arm length less than 10 cm
- low dissipation: gravitational anti-spring effect

The VIRGO accelerometer

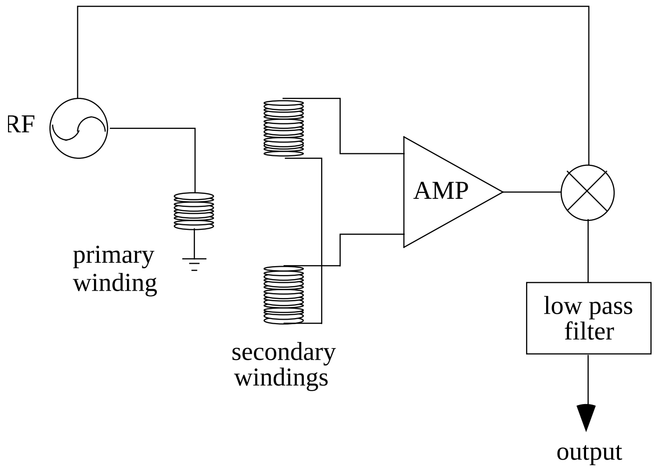

Schematic of an LVDT position sensor.

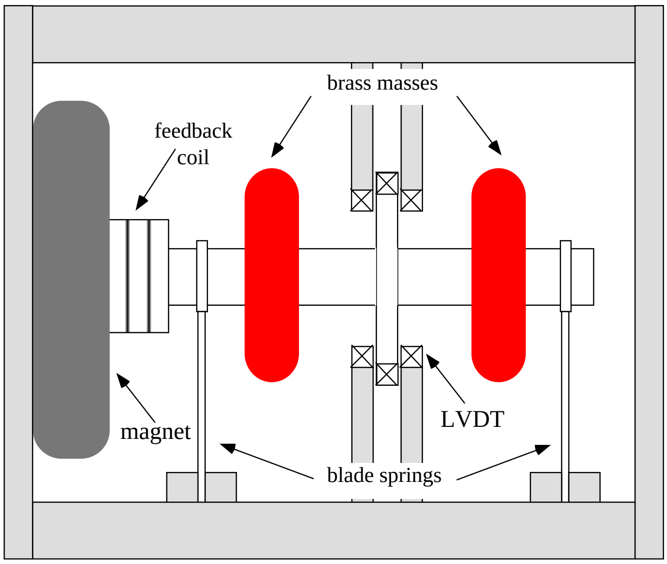

- force feedback accelerometer
- inverted pendulum
- Marval 18 blade springs
- ν_0=4 Hz, Q ~ 100, M=0.5 Kg
- full UHV compatible
- sensitivity: $< 10^{-9}$ m/s^2 / $\sqrt{\text{Hz}}$ @ 0.1 Hz

Resonant phase shift capacitance sensor

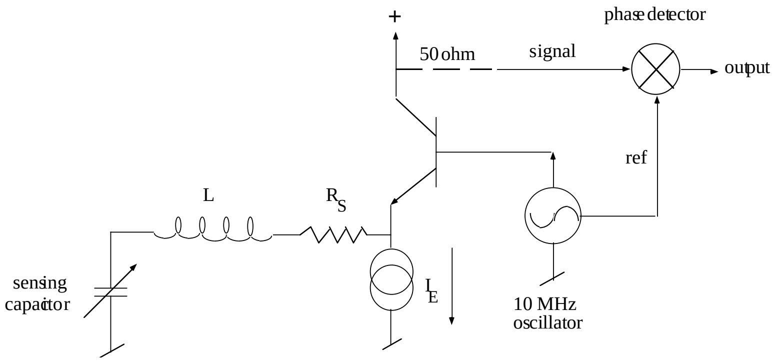

- low losses toroidal inductor: Q ~ 170
- high efficiency passive phase detector
- dynamic range ~ 3 µm
- output gain: 300 mV/ µm

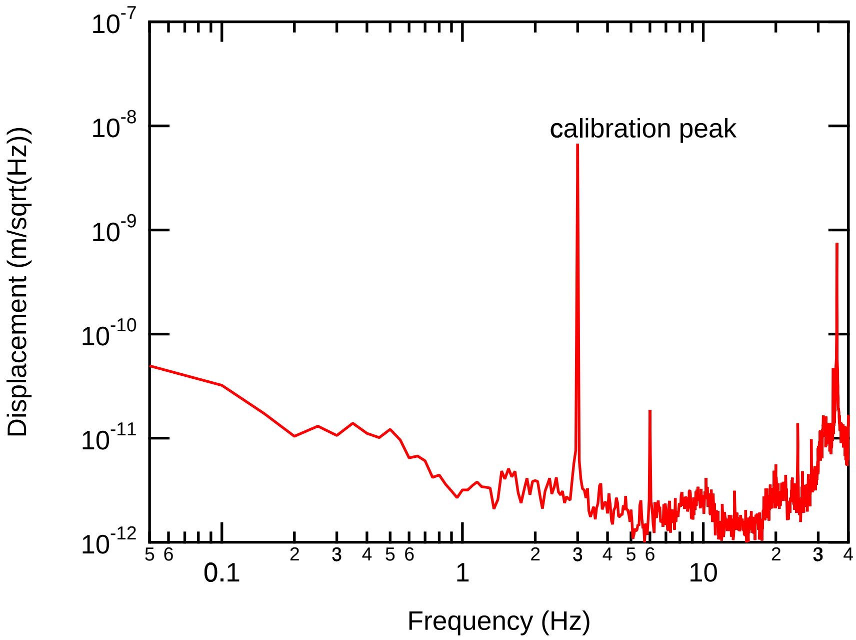

Sensor calibration

The FP transfer function

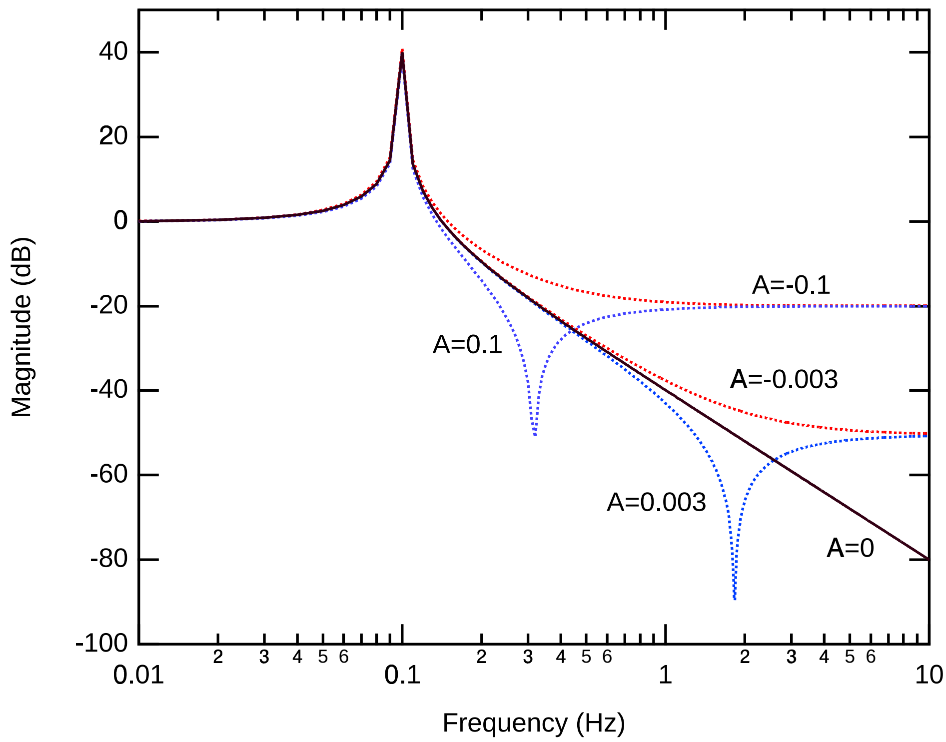

The center of percussion effect:

$$\frac{X_p}{X_s} = \frac{1 - A\dfrac{\omega^2}{\omega_0^2} + i\beta}{1 - \dfrac{\omega^2}{\omega_0^2} + i\beta}$$

where

$$A = \frac{\left(\dfrac{L}{3l_p} - \dfrac{1}{2}\right)\left(m_{a_1} + m_{a_2}\right)}{\dfrac{L}{3l_p}\left(m_{a_1} + m_{a_2}\right) + \left(m_{p_1} + m_{p_2}\right)}$$

The Q factor

– the mechanical dissipation is localized in the flexures

$$\phi_{eff} = \phi_{mat} \frac{\kappa_{flex}}{\kappa_{grav} + \kappa_{flex}}$$

where

$$\kappa_{grav} = g l_p \delta M$$

and

$$\kappa_{flex} = N\sqrt{EI\tau}\coth\left(l\sqrt{\frac{\tau}{EI}}\right)$$

acceleration thermal noise:

$$\tilde{a}_{tn}(\omega) = \frac{1}{M_e l_p}\sqrt{\frac{4K_B T \kappa_{flex}}{Q_{mat}\omega}}$$

Noise reduction:

– high strength, low dissipation, low creep materials
Cu–Be:
  - precipitation hardened alloy: yield stress 1.4 GPa
  - loss angle: $4.3 \cdot 10^{-5}$ below 100 mHz (Quinn *et al*.1995)

– 10-20 μm thick flexures allow dilution factors up to 10 also with a compact design: 10-cm long arms, 3 Kg of mass.

– stick-and-slip losses can be avoided by means of a monolithic design.

The capacitance actuator

$$F(V_s) = \frac{\varepsilon S}{2d^2} V_0^2 + \frac{\varepsilon S}{d^2} V_0 V_s + \frac{\varepsilon S}{2d^2} V_s^2 + \frac{\varepsilon S V_0^2}{d^3} \Delta x$$

– capacitance gap: 250 μm
– gain: 10 μN/Volt
– non–linearity ~ 1% with $V_0 = 100$ V
the actuator driver:

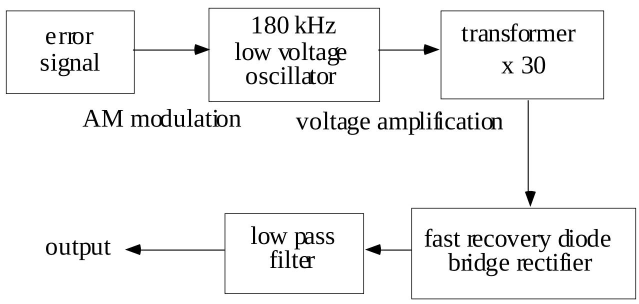

– noise: 5 μV$_{p\text{-}p}$ between 0.1 and 1 Hz.

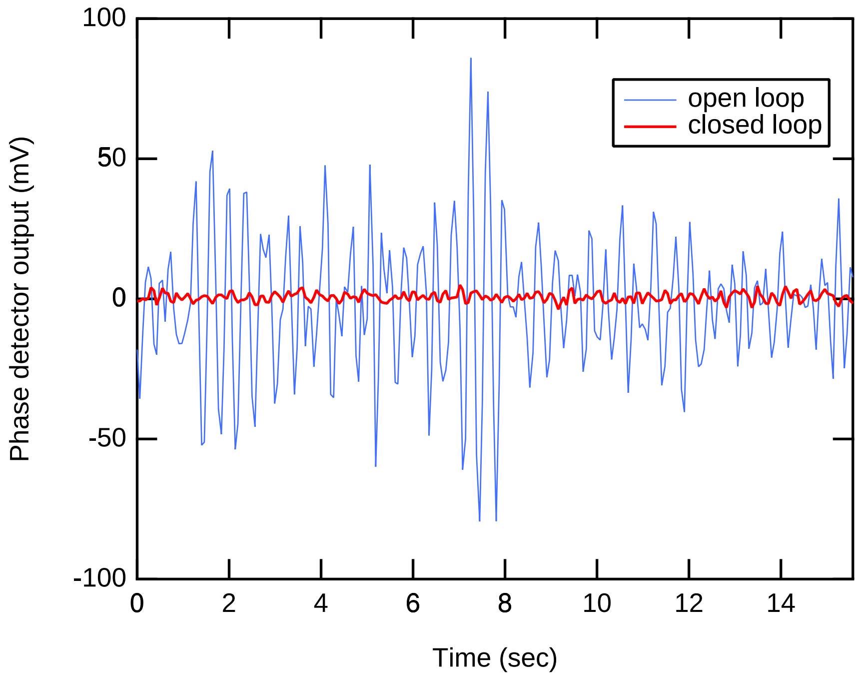

Active control of a 3 Hz resonant inverted pendulum

Balanced sensing and actuation

double resonator

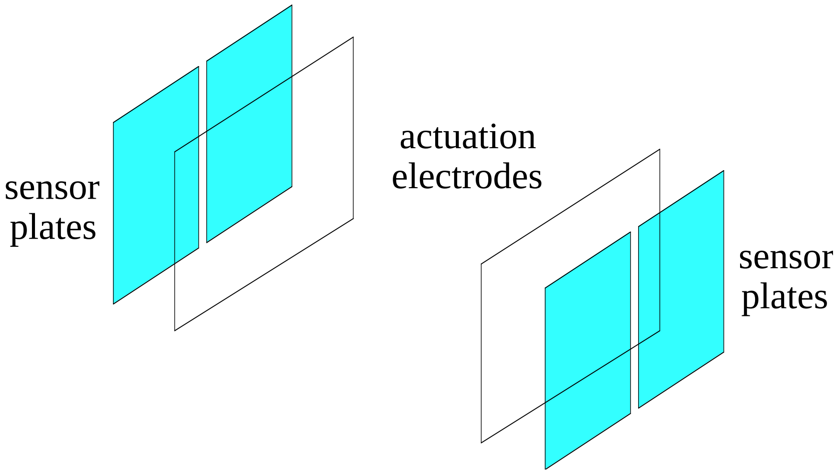

bridge

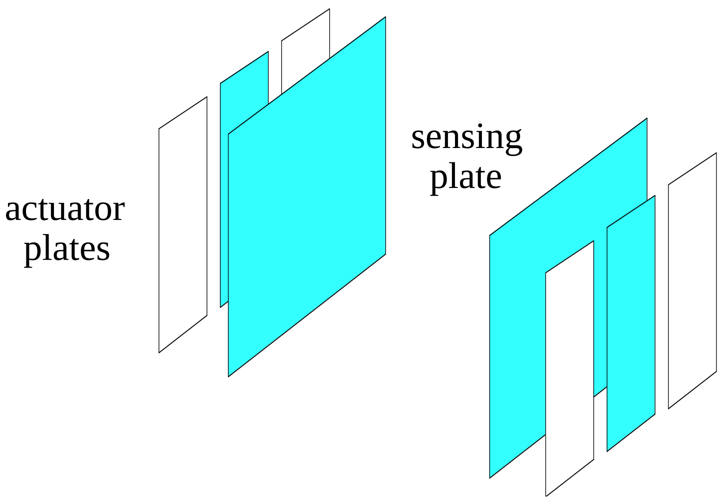

SAS-SUS Inertial Damping

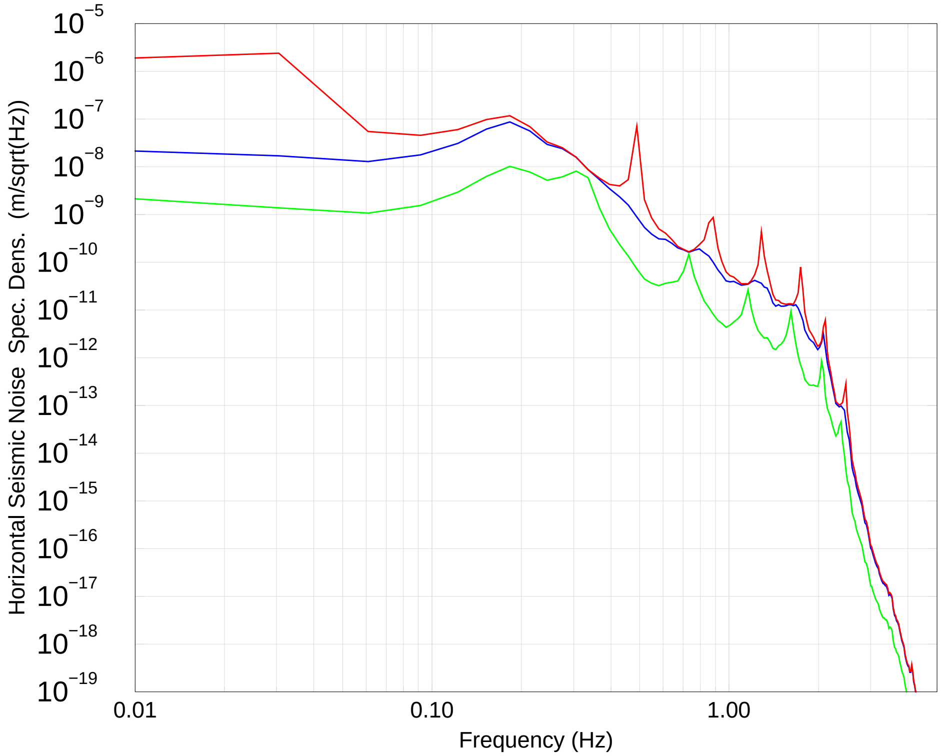

Horizontal Seismic Noise Spectral Densities

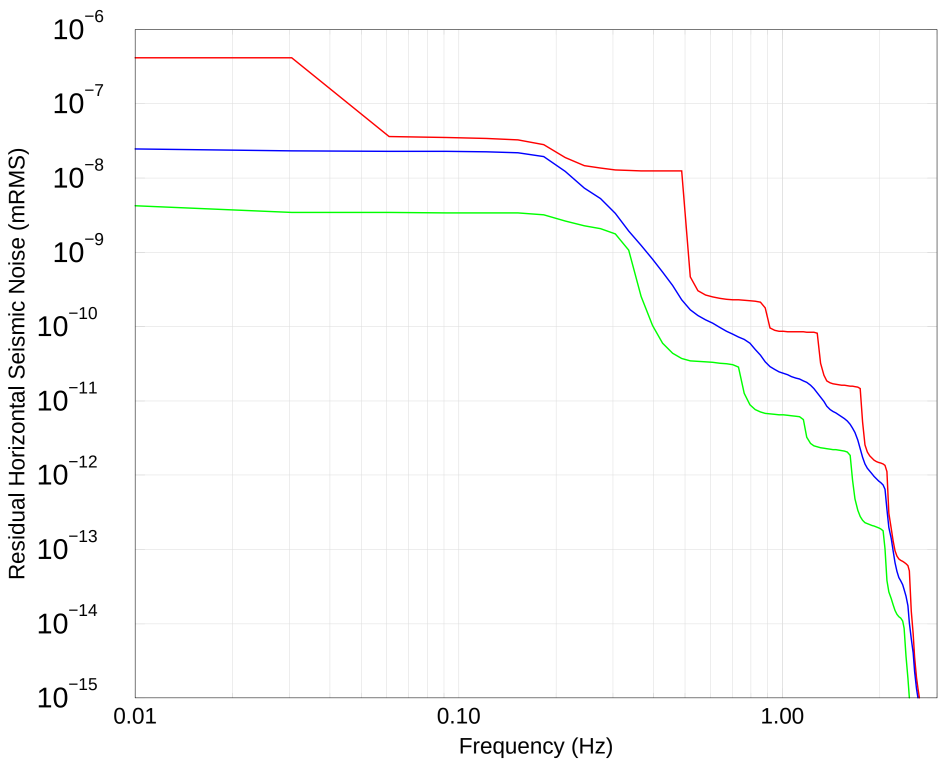

Horizontal Seismic RMS Residual Displacement

IP Inertial Damping , Open Loop Transfer Function

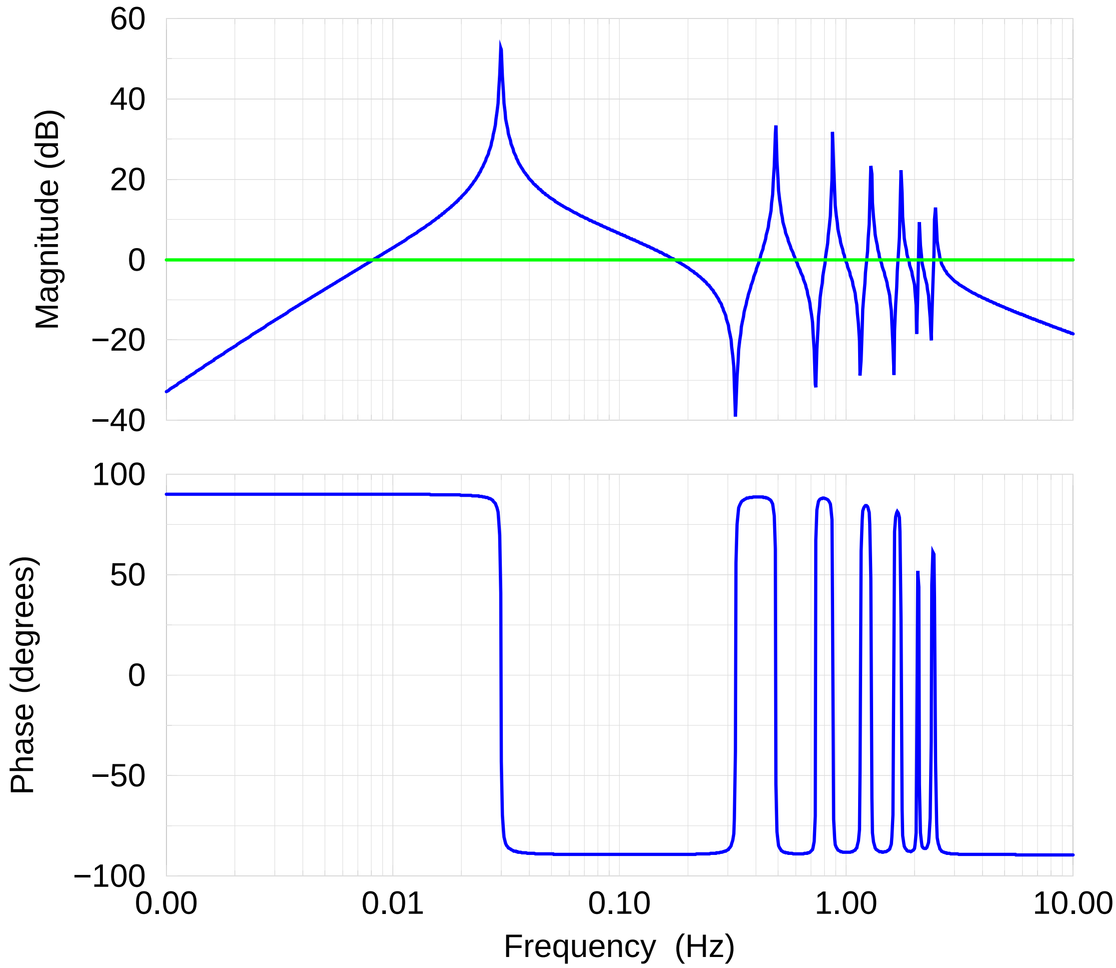

SAS-SUS Global Control Simplified Model (GEO Code)

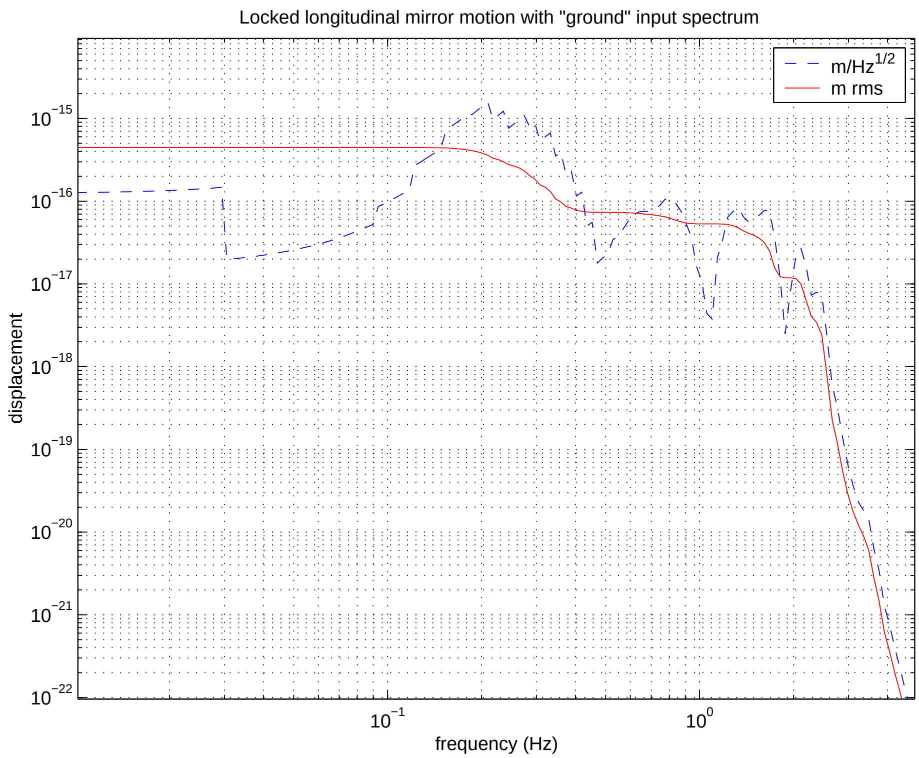

Global Control Spectral Density and RMS Res. Displ.

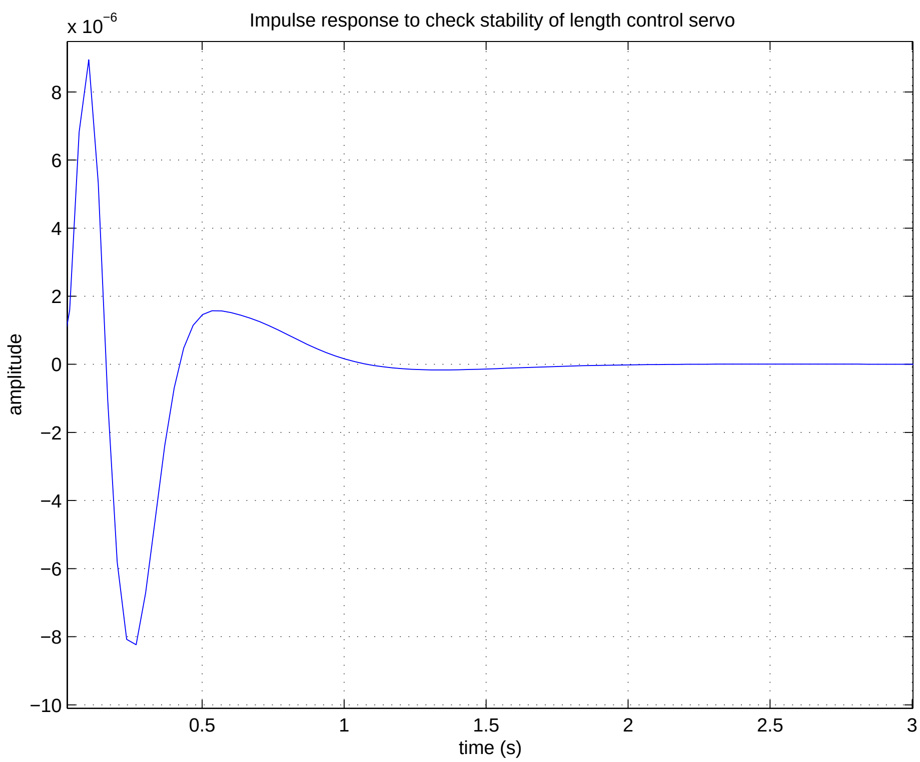

Global Control Impulse Response

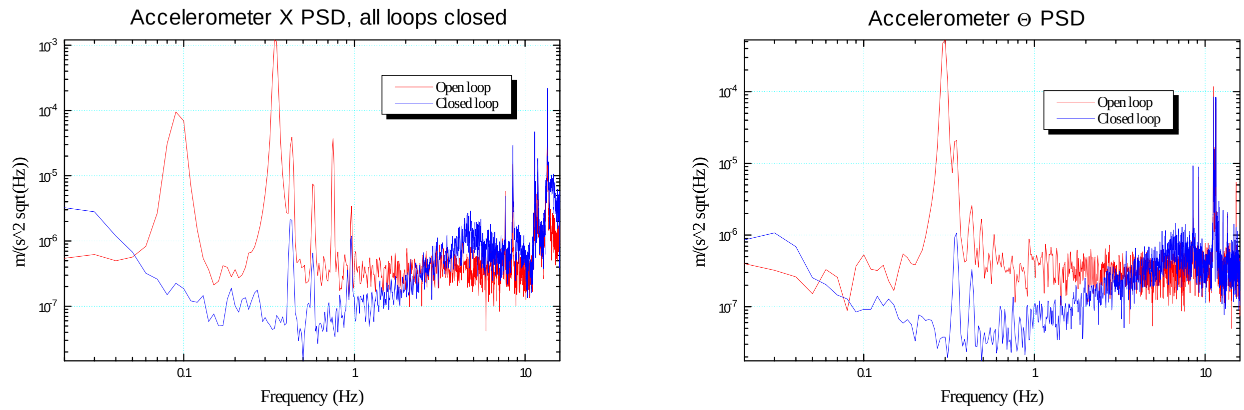

Figure 9: Spectra of the virtual accelerometers X and Θ with the damping ON and OFF.

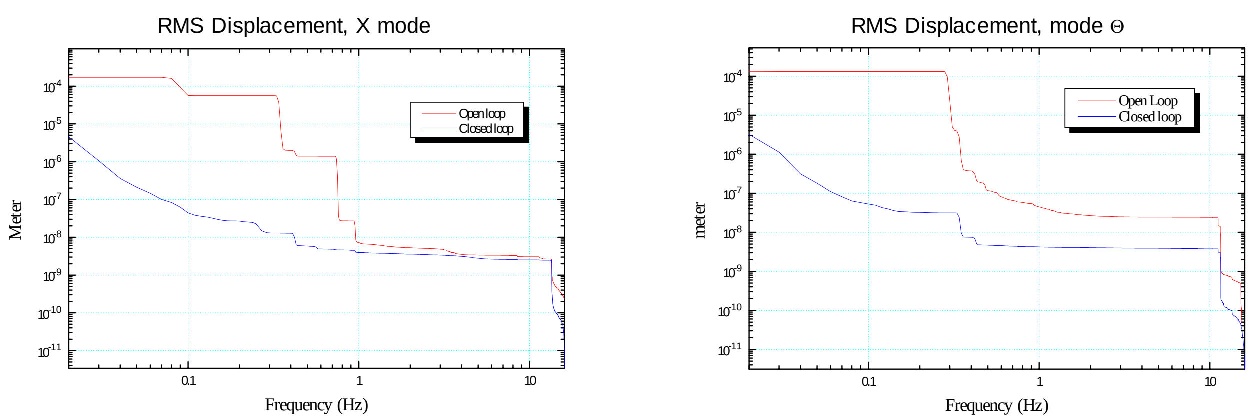

Figure 10: RMS motion of the IP top table, calculated from the spectra of fig. 9. The translational RMS motion at 100 mHz is reduced from ~ 70 μm (damping OFF) to ~ 50 nm (damping ON).

TAMA SAS

Open loop transfer function for inertial damping

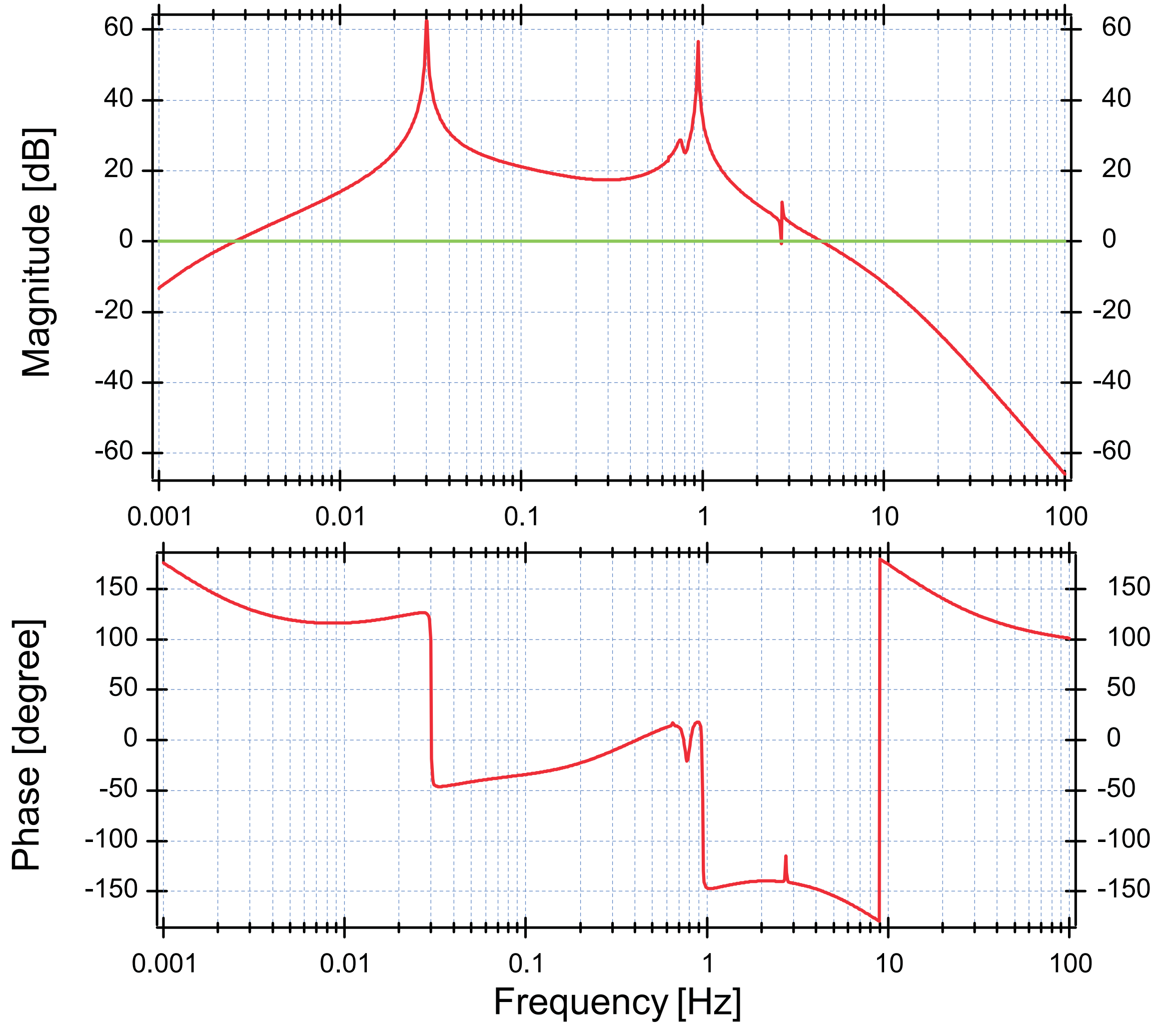

TAMA SAS

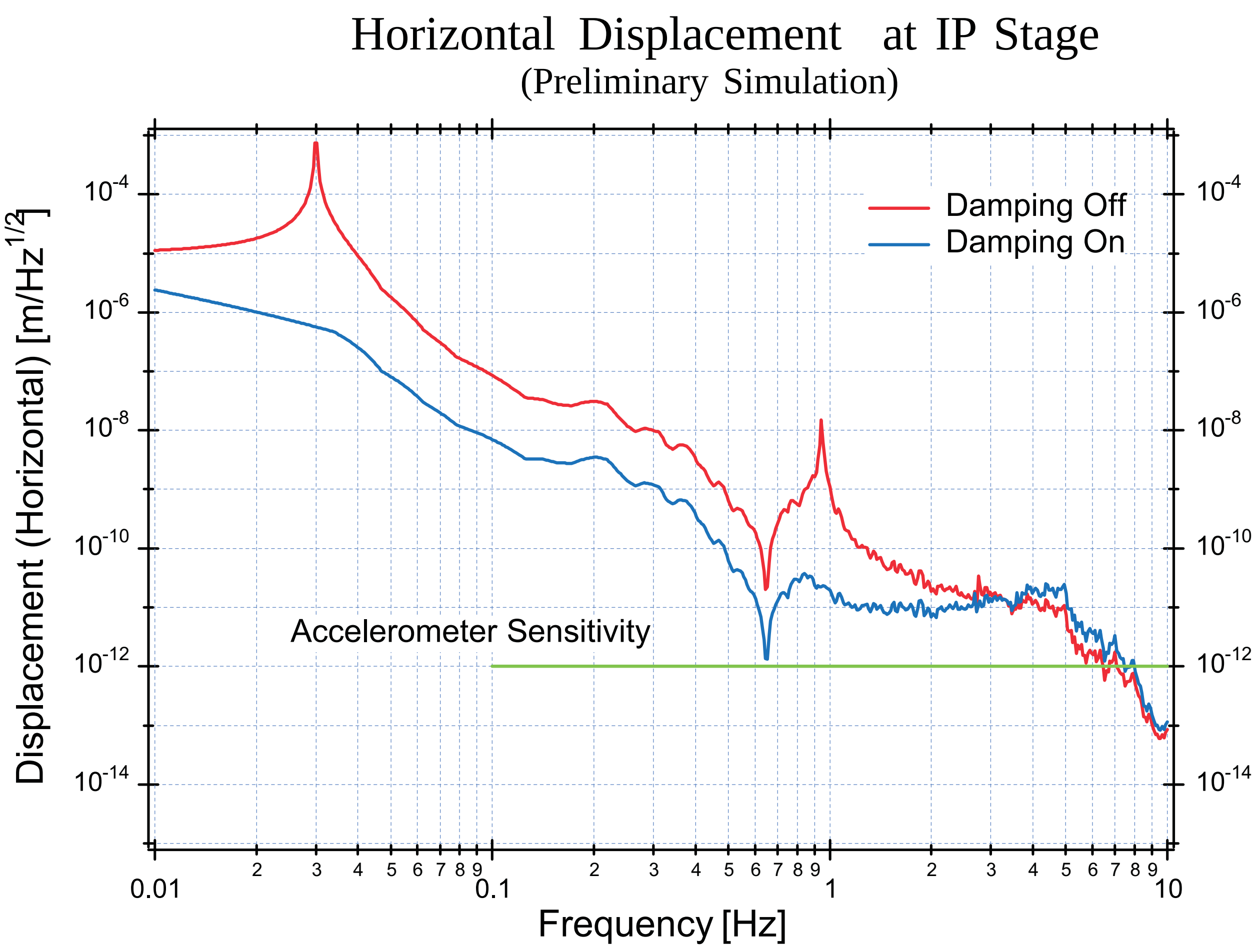

Akiteru Takamori

TAMA SAS

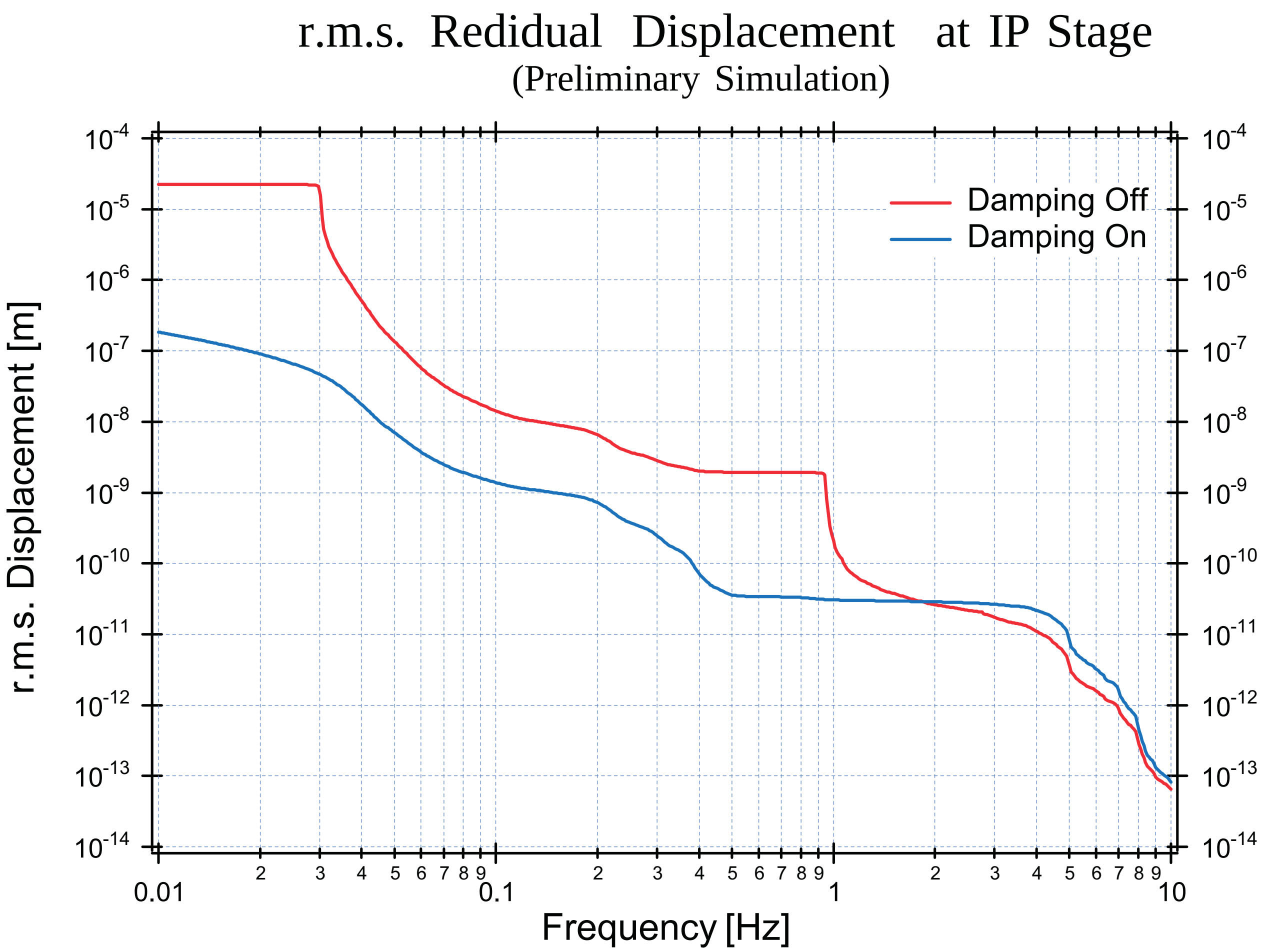

Akiteru Takamori

TAMA SAS

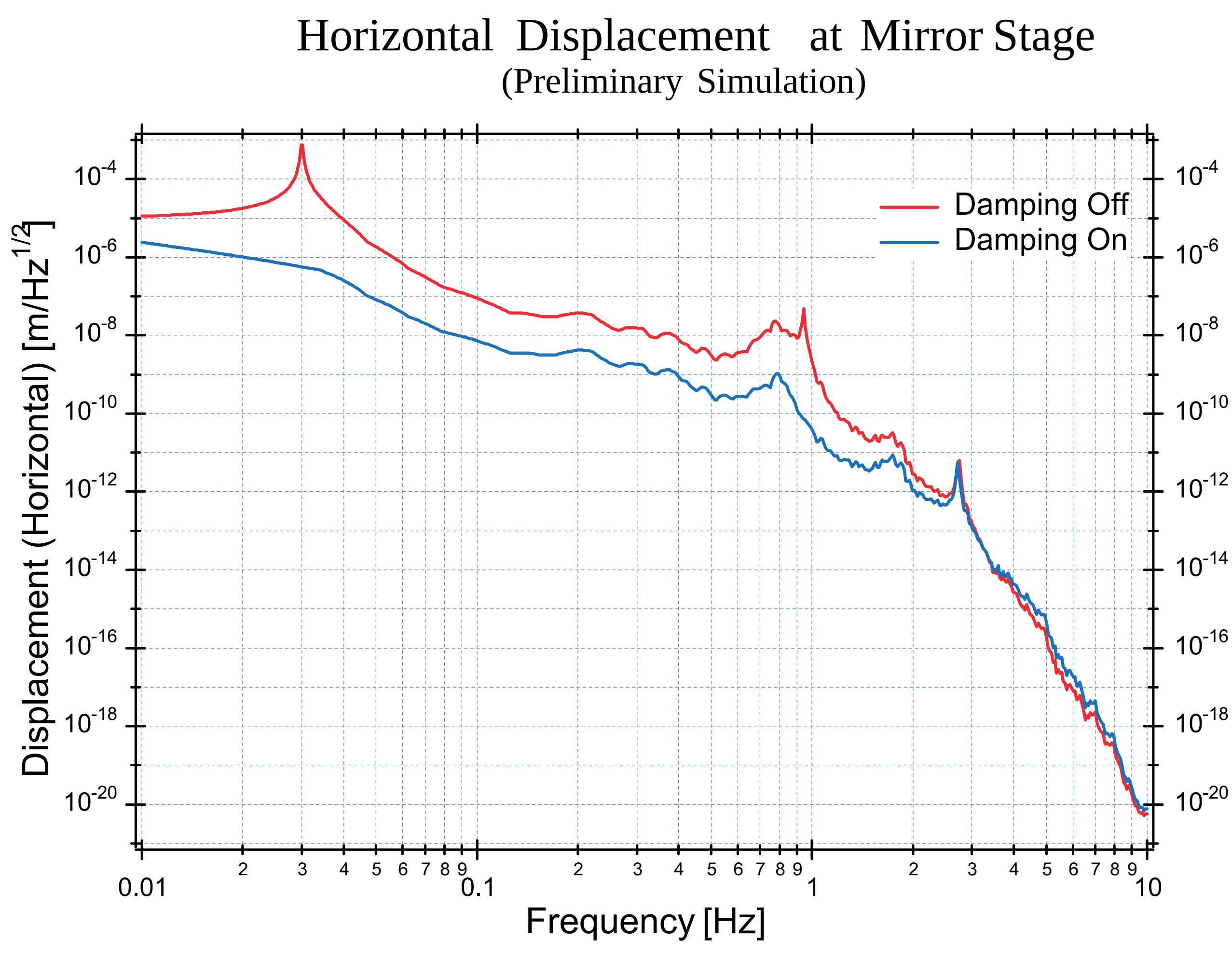
Horizontal Displacement at Mirror Stage
(Preliminary Simulation)
Damping Off
Damping On
Displacement (Horizontal) [m/Hz^1/2]
Frequency [Hz]
0.01
0.1
1
10
10^-4
10^-6
10^-8
10^-10
10^-12
10^-14
10^-16
10^-18
10^-20

TAMA SAS

r.m.s. Redidual Displacement at Mirror Stage

(Preliminary Simulation)

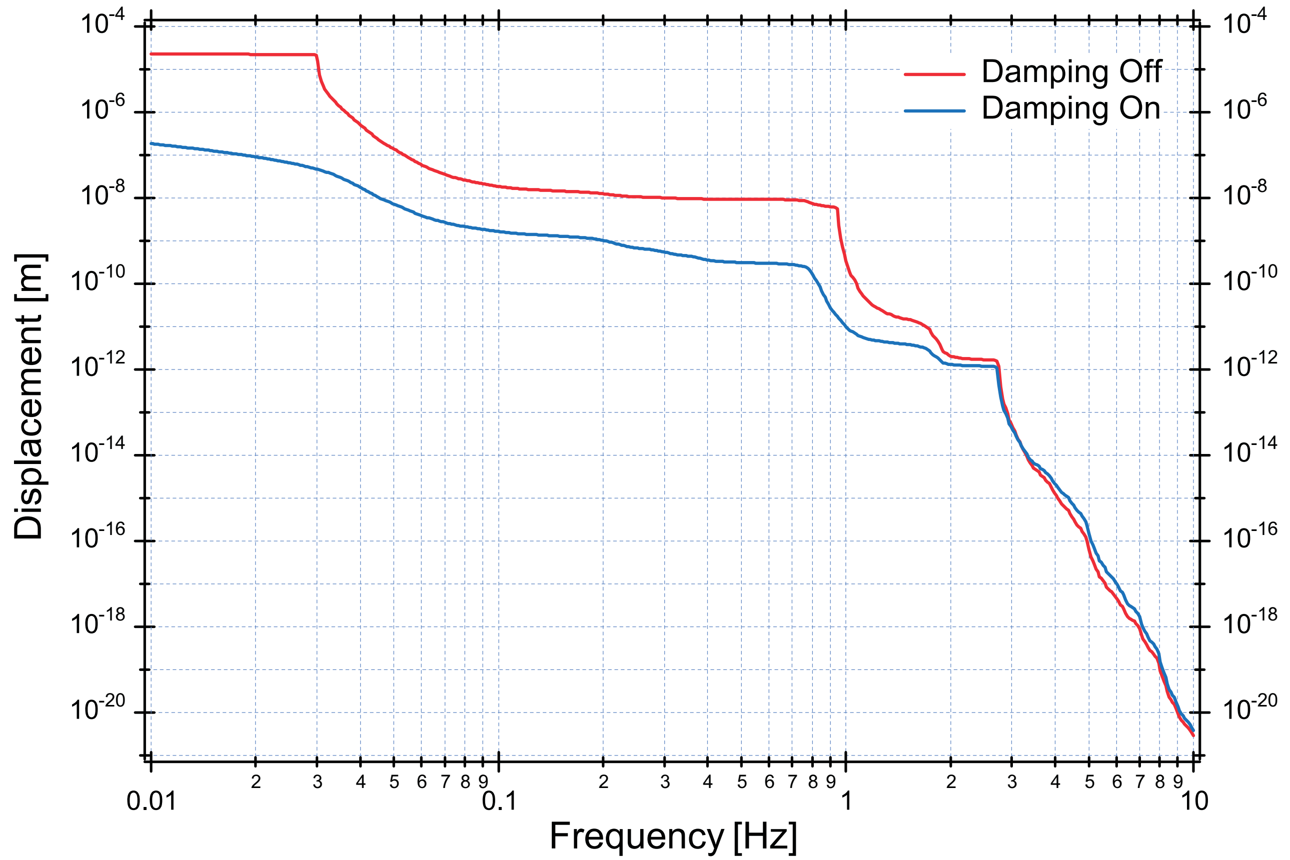

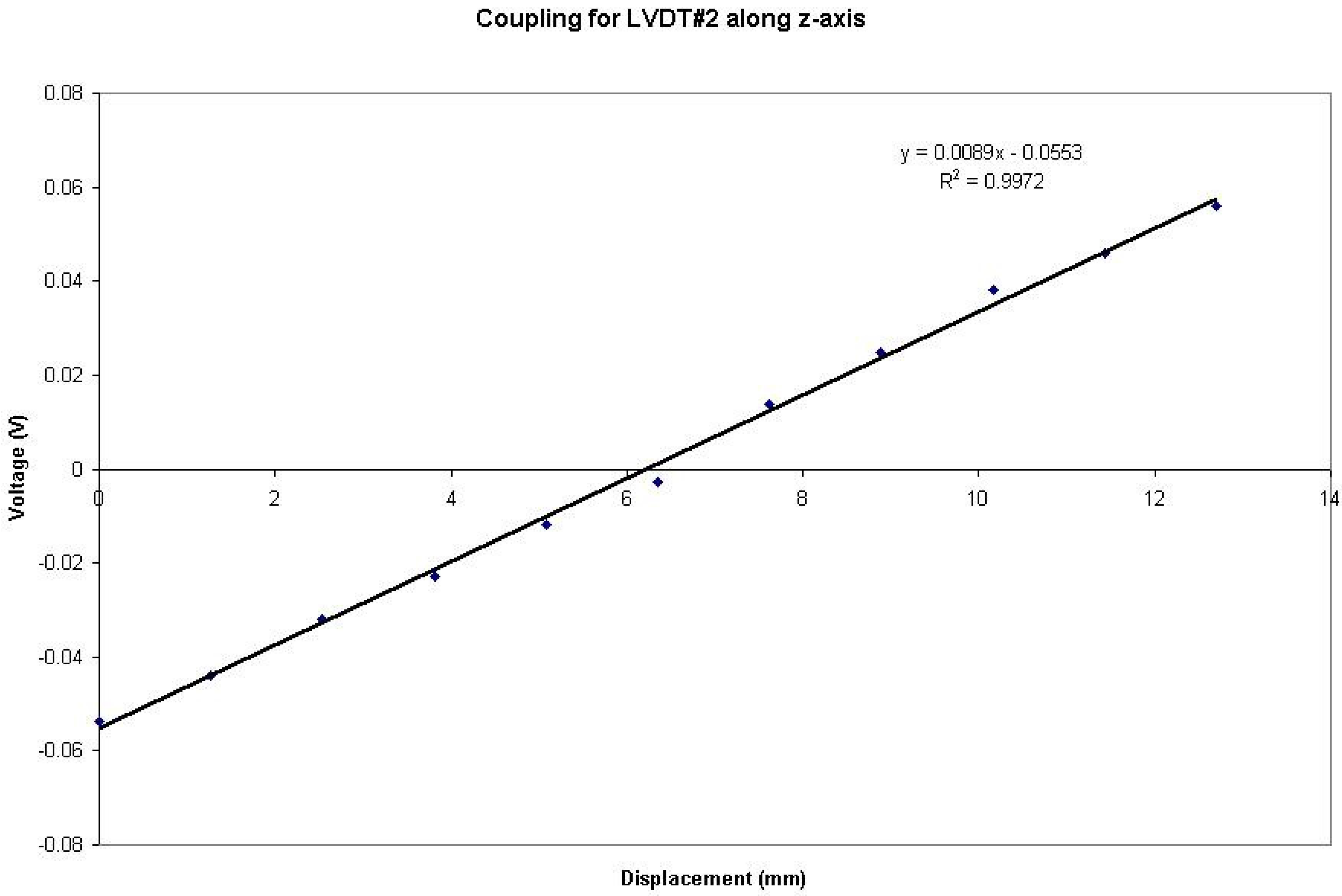

Coupling for LVDT#2 along z-axis
y = 0.0089x - 0.0553
R2 = 0.9972
0.08
0.06
0.04
0.02
0
-0.02
-0.04
-0.06
-0.08
0
2
4
6
8
10
12
14
Voltage (V)
Displacement (mm)

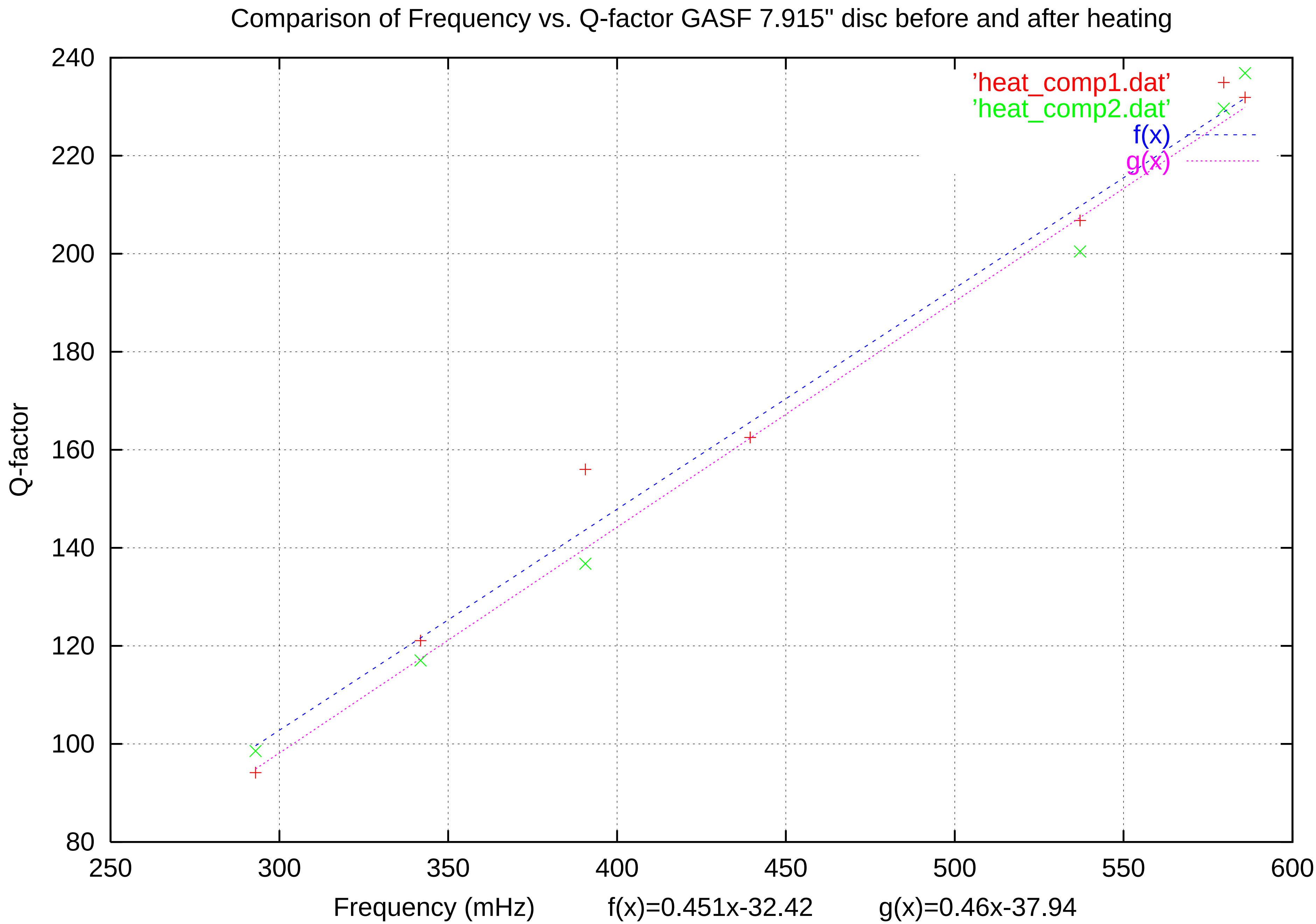

Comparison of Frequency vs. Q-factor GASF 7.915" disc before and after heating
'heat_comp1.dat'
'heat_comp2.dat'
f(x)
g(x)
Q-factor
240
220
200
180
160
140
120
100
80
250
300
350
400
450
500
550
600
Frequency (mHz)
f(x)=0.451x-32.42
g(x)=0.46x-37.94

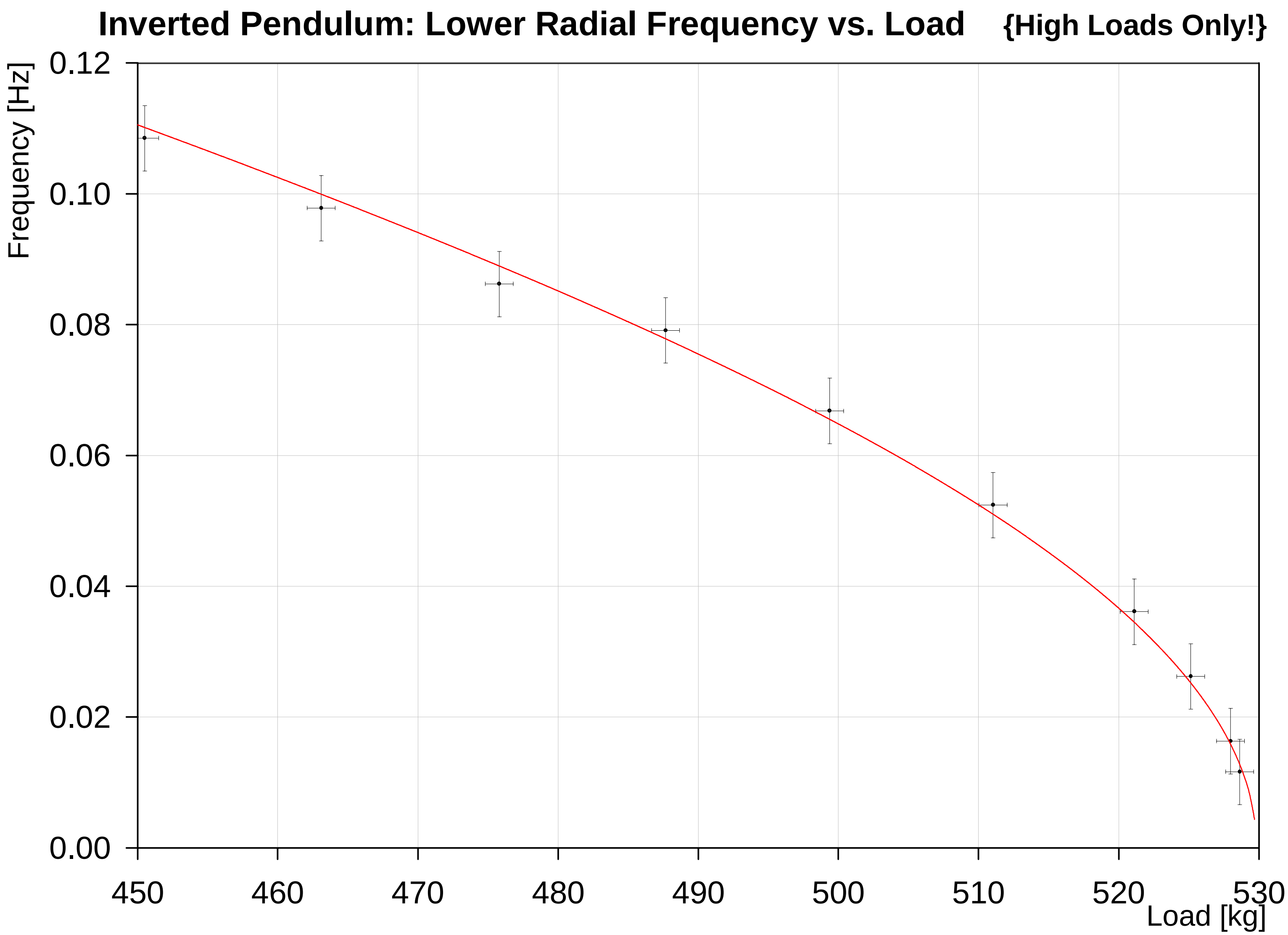
Inverted Pendulum: Lower Radial Frequency vs. Load {High Loads Only!}
Frequency [Hz]
0.12
0.10
0.08
0.06
0.04
0.02
0.00
450
460
470
480
490
500
510
520
530
Load [kg]

GAS Filter : Current Work

"Link-less" GASF

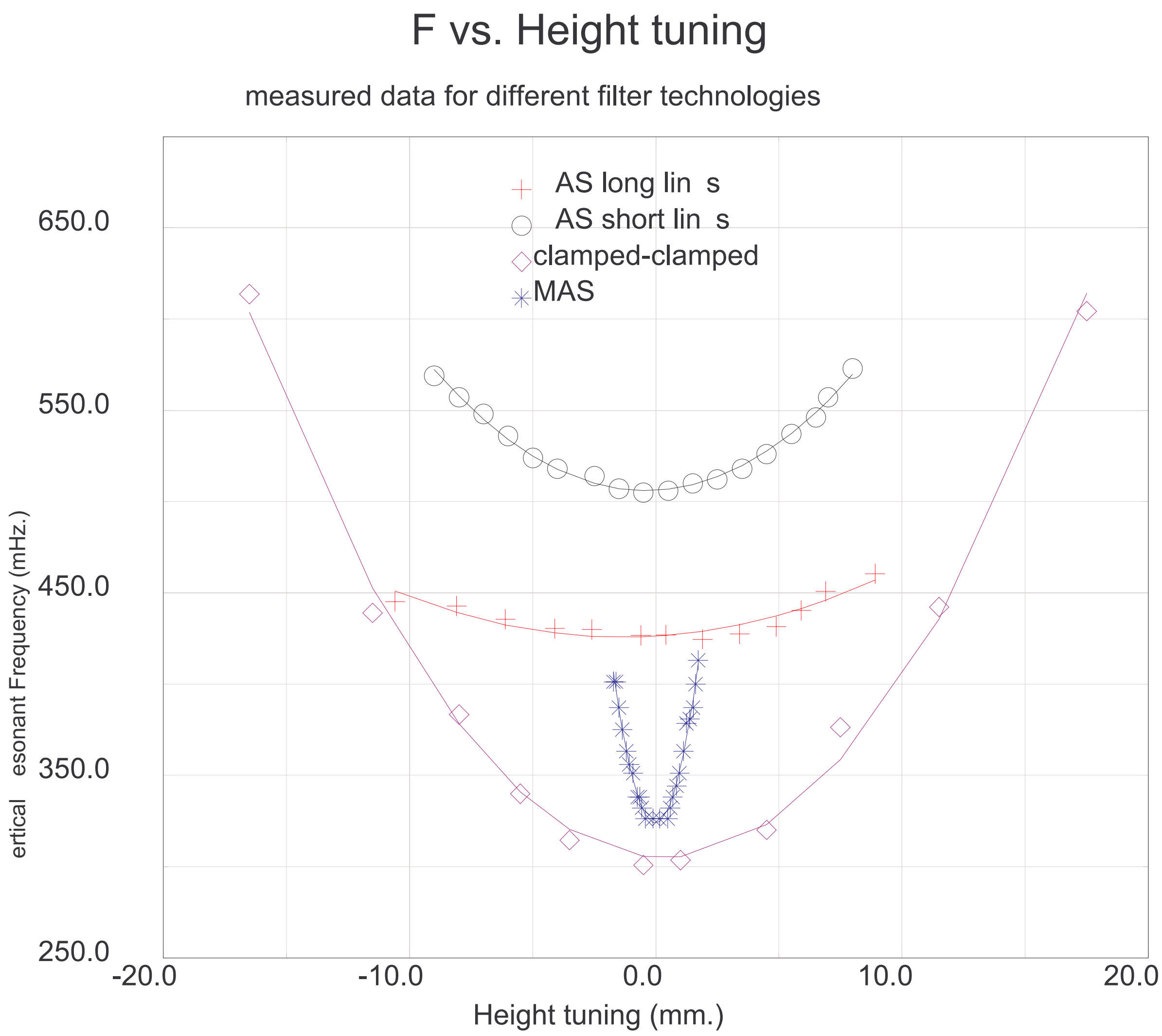

IP Inertial Damping , Open and Closed Loop Spec. Dens

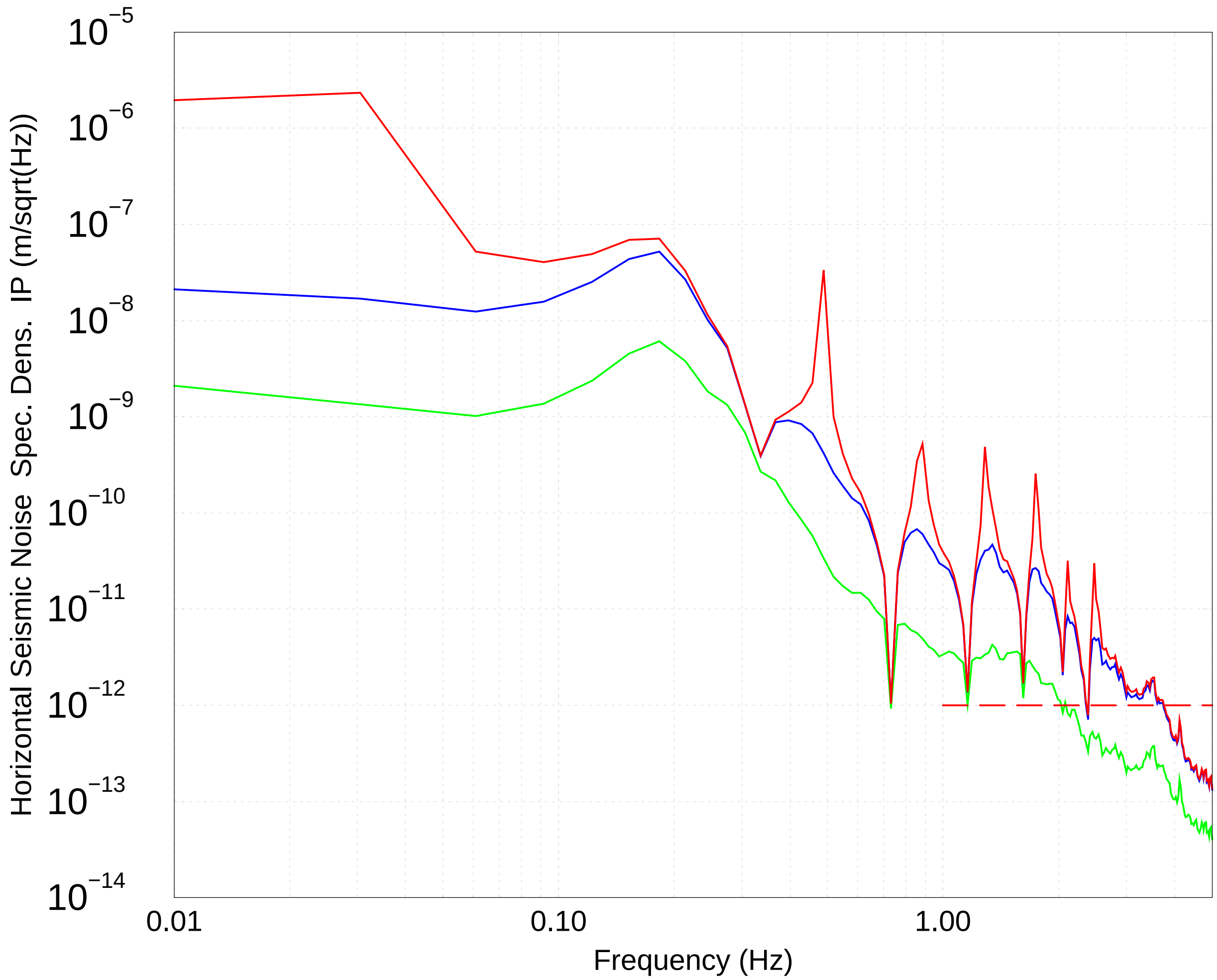

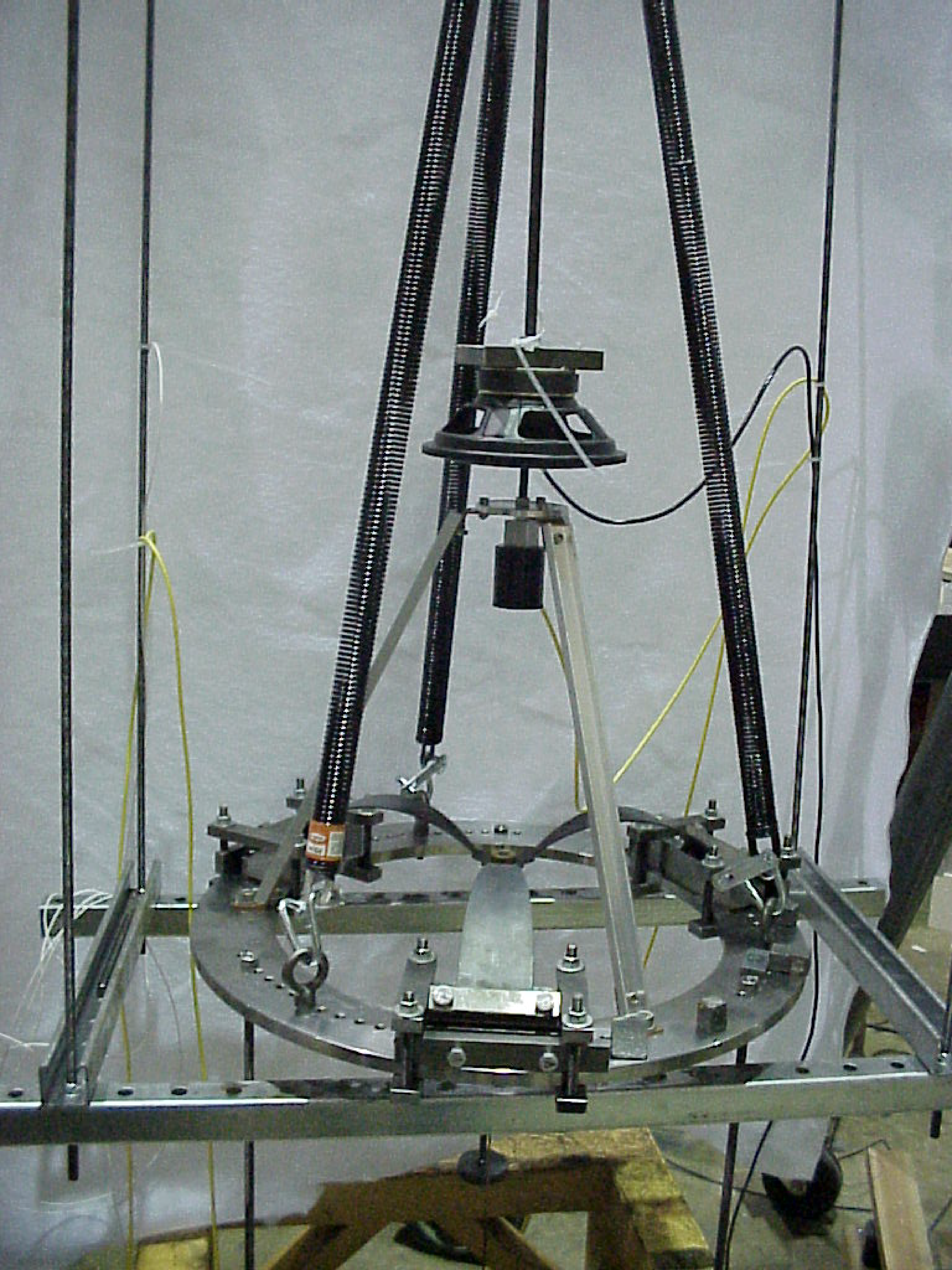

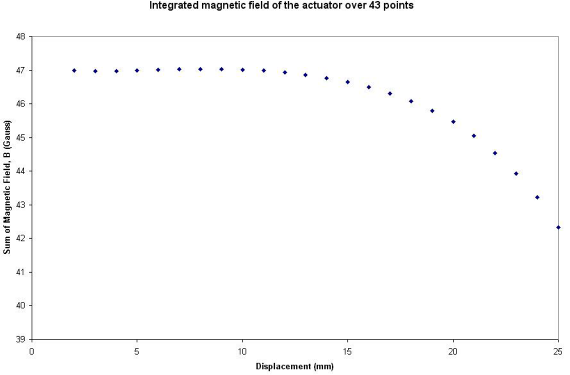

Integrated magnetic field of the actuator over 43 points
Sum of Magnetic Field, B (Gauss)
Displacement (mm)
48
47
46
45
44
43
42
41
40
39
0
5
10
15
20
25